

# SPREAD SPECTRUM FOR A HIGH FREQUENCY DISPERSED RADIO ALARM SCHEME

*David G. M. Cruickshank*

A thesis submitted for the degree of

Doctor of Philosophy

University of Edinburgh

1992



---

# Abstract

---

Alarm schemes for the elderly that are currently available are expensive. The vast majority of these schemes use a portable trigger worn by the client to transmit to a receiver unit within the client's home. This receiver unit then calls for help through the public telephone network. A large proportion of the overall cost of this type of scheme is the cost of providing each client with a receiver unit and a modem.

In this thesis we look at the possibility of transmitting a high frequency alarm signal directly to a service centre from a portable transmitter worn by the client. This method should be much cheaper than a conventional telephone based system, as a receiver and modem for each client is not required. To obtain the required range, we sacrifice the speech link between the client and the service centre and use spread spectrum techniques to reduce the equivalent noise bandwidth of the system. There is a channel reserved exclusively for elderly alarm schemes, this channel in the high frequency radio band. In the high frequency radio band, the background noise is often dominated by the man-made components and is therefore impulsive. The distribution of the impulsive noise in these channels is non-stationary and unknown to the system designer. An analysis of the performance of a direct sequence spread spectrum system using matched filter reception is developed. This analysis concentrates on providing a guaranteed minimum performance from a limited precision digital matched filter, regardless of the noise distribution. The performance of a non-linear clipping device preceding the matched filter is analysed and is shown to improve performance in impulsive noise

Finally, we study the design of a practical alarm scheme based on direct sequence spread spectrum.

---

## **Declaration of originality**

---

This thesis and the work reported herein was composed and originated entirely by the author except where clearly acknowledged.

David G. M. Cruickshank

---

# Contents

---

Abstract . . . . .	ii
Declaration of originality . . . . .	iii
Acknowledgements . . . . .	viii
Abbreviations . . . . .	ix
1. Introduction . . . . .	1
1.1 Organisation of this thesis . . . . .	3
2. Background . . . . .	5
2.1 Alarm systems for the elderly and infirm . . . . .	5
2.1.1 The clients . . . . .	6
2.1.2 Requirements for a successful alarm scheme . . . . .	7
2.2 Spread spectrum communications . . . . .	9
2.2.1 Direct sequence spread spectrum . . . . .	10
2.2.2 The advantages of spread spectrum in this application . . . . .	13
2.2.3 Disadvantages of spread spectrum in this application . . . . .	15
3. Digital matched filters in unknown interference . . . . .	16
3.1 Guaranteed minimum performance digital matched filters . . . . .	16
3.1.1 Binary quantisation . . . . .	17
3.1.2 Dither . . . . .	18

## CONTENTS

3.1.3 Multilevel quantisation . . . . .	25
3.1.4 Lower bound on performance with four quantisation levels . . . . .	28
3.2 Simulation results and discussion . . . . .	34
3.2.1 Binary quantisation . . . . .	34
3.2.2 Four-level quantisation . . . . .	37
3.3 Chapter summary . . . . .	40
<b>4. Extension of previous work . . . . .</b>	<b>41</b>
4.1 Extension of Cahn's work to larger numbers of quantisation levels . . . . .	41
4.1.1 Binary quantisation using the multi-level technique . . . . .	41
4.1.2 Six and eight level quantisation using the multi-level technique . . . . .	47
4.2 Linear integer quantisation weights . . . . .	56
4.3 Improvements to Cahn's DMF . . . . .	60
4.4 Chapter summary . . . . .	64
<b>5. Impulsive noise and the clip to zero algorithm . . . . .</b>	<b>66</b>
5.1 Introduction to impulsive noise . . . . .	66
5.2 Impulsive noise models . . . . .	67
5.3 The effect of impulsive noise on conventional systems . . . . .	72
5.4 The effect of impulsive noise on direct sequence spread spectrum systems . . . . .	74
5.5 Improving the performance of direct sequence spread spectrum systems in impulsive noise . . . . .	76
5.5.1 The clip to zero algorithm for analogue matched filters in Gaussian noise . . . . .	78
5.5.2 The clip to zero algorithm in $\epsilon$ -mixture noise . . . . .	83

## CONTENTS

5.5.3 Using the clip to zero algorithm . . . . .	85
5.6 Combining guaranteed minimum performance digital matched filters with the clip to zero algorithm . . . . .	87
5.7 Chapter summary . . . . .	92
<b>6. System Design . . . . .</b>	<b>93</b>
6.1 Preliminary assumptions and decisions . . . . .	93
6.1.1 Transmission format . . . . .	94
6.2 Multiple systems . . . . .	99
6.3 A single system . . . . .	102
6.4 Transmitter design . . . . .	102
6.4.1 The transmitted signal . . . . .	103
6.4.2 Transmitter operation . . . . .	105
6.4.3 Design and physical construction . . . . .	107
6.5 Receiver design . . . . .	108
6.5.1 Demodulation . . . . .	108
6.5.2 Despreading . . . . .	115
6.5.3 Synchronisation . . . . .	118
6.5.4 Error correction . . . . .	119
6.5.5 Appropriate action . . . . .	119
6.6 Personnel . . . . .	123
6.7 Range . . . . .	124
6.8 Chapter summary . . . . .	126
<b>7. Conclusions . . . . .</b>	<b>127</b>
7.1 Limited precision matched filters . . . . .	127
7.2 The clip to zero algorithm . . . . .	128

*CONTENTS*

7.3 The feasibility of a spread spectrum alarm scheme . . . . .	128
7.4 Limitations of this work and suggestions for future work . . . . .	129
<b>Appendix A: Verified m-sequences . . . . .</b>	<b>140</b>
<b>Appendix B: Original publications . . . . .</b>	<b>145</b>
<b>Appendix C: Software . . . . .</b>	<b>160</b>

---

# Acknowledgements

---

I would like to express my gratitude to the following people:-

- My main supervisor, Dr. J. H. Dripps for his enthusiasm throughout this project.
- The Science and Engineering Research Council (SERC) for funding the work.
- Those who read through the manuscript, Dr. D. Renshaw (my second supervisor), Dr J. H Dripps and especially Miss A. Moore who had the dubious honour of having to read it several times.
- Those who have given me advice throughout the project, especially Prof. P. M. Grant, Dr. S. McLaughlin and Dr. D. Renshaw.
- My fellow PhD students who have helped with small contributions to the work and big contributions to the play:- D. Baxter, R. Bedi, C. Callender, S. Churcher C. Cubiss, S. Hovell, D. Hughes, D. Laurenson, N. Lo (great holiday!), J. Martin, A. Moore, S. Mowbray, P. Newson, G. Povey, I. Scott and G. Ushaw

This thesis is dedicated to my parents. Without their continuous support for my education, it would not exist.



---

# Abbreviations

---

ADC	Analogue to Digital Converter
AGC	Automatic Gain Controlled
ASIC	Application Specific Integrated Circuit
BER	Bit Error Rate
BFSK	Binary Frequency Shift Keying
BPSK	Binary Phase Shift Keying
CDMA	Code Division Multiple Access
DMF	Digital Matched Filter
DSSS	Direct Sequence Spread Spectrum
FDMA	Frequency Division Multiple Access
FIFO	First In First Out
HF	High Frequency
LF	Low Frequency
MF	Medium Frequency
OOK	On Off Keying
PDF	Probability Density Function
PLA	Programmable Logic Array
PN	Pseudo Noise
PROM	Programmable Read Only Memory

## *ABBREVIATIONS*

RF	Radio Frequency
RMS	Root Mean Square
SAW	Surface Acoustic Wave
SPW	Signal Processing Worksystem
TDMA	Time Division Multiple Access
VAT	Value Added Tax
VCO	Voltage controlled Oscillator

---

# 1. Introduction

---

Currently available alarm systems for the elderly and infirm have had a mixed reception. They are perceived as a good method of preventing clients from suffering after relatively minor incidents. There have been many reports in the press of people lying alone in their homes for long periods, unable to draw attention to themselves. Alarm systems can prevent this and this is their most positive facet. If the only medical condition that a person suffers from is a tendency to fall then an alarm system may enable them to live in their own home amongst their friends and neighbours. Many elderly people wish to maintain their independence as long as possible and an alarm scheme may be one method of helping them achieve this aim. An alarm may also help increase a person's confidence after an incident such as a fall, even if the alarm is never used.

However, many people have expressed doubts about the social and practical benefits of an alarm scheme. Doubts on the social benefits of an alarm scheme centre on the suspicion that they may be used as a substitute for the type of care that is really required. Government agencies may give people alarms as a substitute for more expensive forms of care such as residential care or visits by social workers. A perceived negative effect of an alarm scheme has been that they may reduce the number of friends and relatives that visit a client, because visits will not be made to check on the well being of the client. Fears of increased isolation of alarm scheme clients are not true according to some survey work and several pieces of evidence suggest that the amount of personal contact an elderly person receives is not reduced by them having an alarm installed.

## *CHAPTER 1: INTRODUCTION*

However, doubt about the practical benefits of some alarm schemes are well substantiated. Many reports reviewing alarm schemes currently in operation reveal practical problems which significantly reduce the effectiveness of the scheme. Some forms of alarm scheme which have been shown to be ineffective are still being installed and many schemes have major design faults. This leads to the suspicion that many alarm systems are poorly designed. This suspicion is fuelled by reports of unreliability, false alarms and large variations in the performance of samples of the same alarm scheme equipment. There is also a distinct lack of technical information on the design of an alarm scheme in either the communications or sociology literature. This study is motivated by an attempt to design an alarm scheme with as few practical problems as possible.

In this thesis we study the design of an alarm scheme from the point of view of a communications system. To reduce the cost of the system, we will look at the design of a system which transmits a call for help directly to a service cent from a portable trigger worn by the client. This direct transmission method will make the new system much cheaper and easier to install than the conventional telephone based system, as there is no requirement to provide and install a modem for each client. In particular we shall attempt to demonstrate that the use of spread spectrum communications techniques may be beneficial to the technical performance of a direct transmission alarm scheme. Spread spectrum techniques were originally developed for use in military communications systems. There are however large contrasts between some of the properties desirable in a military system and the properties required for this application. In particular, the cost of any alarm scheme must be affordable by some of the poorest members of our society. This is as much a parameter in the design of an alarm scheme as any engineering constraint.

**1.1. Organisation of this thesis**

Chapter 2 provides the background to this study. It is split into two distinct parts. The first part is concerned with alarm schemes for the elderly. This section isolates the desirable properties of an alarm scheme, based on the previous experience of operators, clients and sociologists. The second part of this chapter introduces spread spectrum techniques and shows that communications systems based on spread spectrum techniques have some desirable properties in the context of an alarm scheme.

Chapters 3 and 4 study the digital matched filter necessary in the type of spread spectrum system envisaged for an alarm scheme. Chapter 3 draws heavily on the work of C. R. Cahn to show that it is possible to design a digital matched filter with a limited number of quantisation levels that has a guaranteed minimum performance regardless of the input noise distribution. The number of quantisation levels required to produce reasonable performance is small. Chapter 4 aims to extend and improve the work in chapter 3 to develop a practical digital matched filter with a good guaranteed minimum performance regardless of the input noise distribution.

Chapter 5 looks at the type of noise that occurs in the HF radio bands. The effect that this noise has on conventional systems is compared with the effect we expect it to have on a spread spectrum system. A method of improving the performance of the matched filters in HF noise is developed.

Chapter 6 examines the design of an alarm system based on spread spectrum techniques. This chapter employs techniques used in many other communications systems currently in use, but as yet not found in alarm schemes. It also highlights some of the problems of trying to design a communications system purely on paper. Chapter 7 draws some conclusions about the potential success of a high frequency radio alarm scheme based on spread spectrum.

## *CHAPTER 1: INTRODUCTION*

There are three appendices at the back of this thesis. Appendix A contains lists of verified m-sequences. The properties and the use of m-sequences are discussed in Chapter 5. Appendix B contains some of the original publications arising from the work reported here. Finally, appendix C contains some of the software used to obtain the simulation results included in this thesis.

---

## **2. Background**

---

This chapter is split into two distinct parts. Part 1 introduces alarm systems for the elderly and infirm. It contains the definition of the problem we are trying to solve, extracting from the sociology literature the desirable properties of an alarm scheme, and the current levels of technology being used. Part 2 introduces the main technique which we are going to use in the development of the alarm scheme, spread spectrum. We define the basic properties of spread spectrum systems and show that these properties are useful in the context of an elderly alarm scheme.

### **2.1. Alarm systems for the elderly and infirm**

Alarm systems for the elderly and infirm have been around for some considerable time. Early systems were very simple such as a light in the window or a siren, operated by mechanical switch. Such systems had severe limitations, they advertised the vulnerability of the person to everyone, not just those with good intentions. They also relied on someone seeing or hearing the alarm signal and they required operation of a hard-wired switch, which could prove to be out of reach in an emergency. Hard-wired systems using pull cords to alert a warden in sheltered housing are still being installed, despite the problem of activating the alarm. Two major problems of hard wired alarm systems are availability and installation costs. Due to the wiring requirement, this type of system can only be installed in very localised areas, such as a sheltered housing scheme or a home for the elderly. Many elderly people wish to stay in their own homes as long

## *CHAPTER 2: BACKGROUND*

as possible, excluding them from the benefits of this type of alarm scheme. The costs of a hard-wired system can also be extremely high. The installation of a new scheme of this type in Glasgow is estimated to cost £14M for 30,000 homes or £467 per house. This scheme is particularly comprehensive, but few local authorities would be prepared to spend this amount of money on an alarm scheme.

In more recent times, telephone based alarm schemes have been used. These systems use portable radio triggers worn by the client, which trigger an auto-dial modem to call for help. The advantages of this type of scheme are that it is available to all households, and that it does not advertise the vulnerability of the client. However, it does have several disadvantages. The system is subject to the reliability of the public telephone network and reliability can be further compromised by accidental disconnection e.g. leaving the phone off the hook, or problems with the radio receiver which feeds the telephone modem. The main drawback for telephone based alarm systems is their cost. Such systems are available from both the public and the private sector. In a survey of private sector systems in 1989, the average cost was around £200 + VAT for a basic modem and one trigger [1]. This does not include monitoring, nor the cost of installing a phone line if one does not already exist.

There are a few direct radio link systems currently available, but they are very expensive, one included in the 1989 survey cost £775 + VAT.

### **2.1.1. The clients**

These alarms may be used by a large variety of people who are perceived to be at risk of requiring medical help with no-one available to obtain it for them. As well as the elderly who are prone to falls and dizzy spells [2-5] etc., they may be given to people recovering from major surgery such as amputations. Connected to the correct sensing



## *CHAPTER 2: BACKGROUND*

equipment, it may be possible to detect other ailments, such as epilepsy or chronic asthma. This group of clients is growing in number, as the vast majority of clients are elderly and the elderly population is increasing in Britain and in Europe [6]. However there are some groups which should not be given client operated alarms. Mentally ill clients are likely to cause a large number of false alarms which may, in extreme cases, compromise the system. Automatic triggers may be provided for such clients if a suitable sensing device exists. Sadly, the mass issuing of alarms to the elderly and people at risk of sudden fatal conditions is not likely to prevent many deaths. Surveys have shown that the vast majority of people in this group would die before help arrived [7].

### **2.1.2. Requirements for a successful alarm scheme**

To operate a successful alarm scheme there are two important aspects which must be implemented, the organisation and the technology. This thesis shall concentrate on the technological aspect, but many social workers have expressed the feeling that the organisational aspect is more important [8].

In the organisation of a good alarm scheme, there are three distinct phases.

The first phase is the identification of the client and the installation of the alarm. The client should belong to one of the groups mentioned in section 1.2, but another important criterion is that the client should desire the alarm. Uncooperative clients who accept the alarm reluctantly are likely not to be wearing the alarm when they need it [9]. The designers and installers of the alarm can help in this respect by making it as unobtrusive and convenient for the user as possible.

The second phase of the organisation is the maintenance of the alarm scheme and monitoring. Regular checks should be made to make sure that the alarm is working, and

## *CHAPTER 2: BACKGROUND*

the client is satisfied with the scheme. Often this will involve visiting the client's home. Maintenance of records is a very important part of this procedure, knowing who has an alarm and where they are living. A record which provides the wrong address for an alarm could have disastrous consequences. Monitoring of an alarm scheme should be continuous, 24 hours a day, 7 days a week. Although most incidents happen at certain times of the day, one of the important functions of an alarm is to provide peace of mind for the client. Ideally, monitoring should be done by specialist trained personnel who understand the scheme. However, systems have been operated successfully without this costly provision.

The third phase of an alarm scheme is the answering of distress calls. This may be done by a variety of methods. In some schemes, the client may be asked to nominate a number of friends or neighbours who will be telephoned in the event of an alarm call. This list can be supplemented by asking the friends and neighbours of one client to be helpers for other clients in the scheme. This type of scheme has proven to be effective and saves money [8, 10]. In some cases local police have agreed to answer alarm calls if the list of helpers for a particular client is exhausted. The maintenance of good records is vitally important in this type of scheme. Other schemes use wardens to answer distress calls, but this is more expensive and difficult in a scheme covering a wide area.

The important attributes of the technology (ie. the hardware) used in an alarm scheme are described below, with particular reference to one way (simplex) radio systems.

The technology must be extremely reliable, both in transmitting alarm signals and preventing false alarms. The serious consequences of failing to transmit an alarm signal correctly are obvious. Perhaps less obvious are the consequences of too many false alarms. This can lead to complacency by the operating staff and the disturbance of the clients and seriously undermines confidence in the system. It uses more human resources than strictly necessary and therefore increases the cost of the system. The technology

must be cheap. The market for this type of system is likely to be local authorities, old peoples homes, hospitals or the clients themselves. None of these groups is likely to be particularly affluent. In a one way radio system, this means cheap transmitters, as there are many transmitters to each receiver. The transmitters should be light, convenient, easy to maintain (eg. long battery life) and as unobtrusive as possible for the client. The receiver should be easy to operate and extremely reliable under all operating conditions. These conditions include extremes of temperature, under interference from other equipment and adverse transmission characteristics. Equipment for use in an alarm scheme should incorporate high reliability techniques, such as battery backup and redundancy in crucial components. These attributes are in addition to the regulatory requirements and the relevant standards (see [11, 12] for example).

## 2.2. Spread spectrum communications

The principles of spread spectrum communication were first expressed in Shannon's equation for channel capacity [13] :-

$$C = W \log_2 \left( 1 + \frac{S}{N} \right) \quad (2.1)$$

where  $C$  is the channel capacity in bits per second,  $W$  is the bandwidth in Hertz,  $N$  is the noise power and  $S$  is the signal power. From the equation we can see that for a fixed capacity, the signal to noise ratio required drops as the bandwidth increases.

The definition of a spread spectrum system is a system that uses a bandwidth far in excess of the minimum bandwidth required to transmit the information. The definition of a spread spectrum system is often restricted to systems that use some function other than the information being sent to determine the transmitted signal. This excludes several formats from being considered as spread spectrum systems, eg. wide-band FM. A spread

spectrum system typically has a spreading process at the transmitter, which widens the bandwidth of the data to be transmitted and a de-spreading process at the receiver, which collapses the received signal to the original data bandwidth. At the receiver, the collapsing of the signal to the bandwidth of the data rejects most of the noise in the received signal. This noise rejection is known as the process gain and is given by

$$\text{process gain} = \frac{\text{transmission bandwidth}}{\text{data bandwidth}} \quad (2.2)$$

It is worth noting at this point that spread spectrum transmission does not provide increased signal to noise ratio for systems operating in thermal noise, as the noise power in this case is proportional to the bandwidth used to transmit the signal. More details of various spread spectrum systems can be found in [14-22]. However, we shall confine ourselves to a discussion of the type of spread spectrum system that is to be employed here, ie. direct sequence spread spectrum.

### 2.2.1. Direct sequence spread spectrum

Direct sequence is one method of creating and demodulating spread signals. Direct sequence spread spectrum (DSSS) signals are created by multiplying the data to be transmitted by a sequence with a much higher bit rate (see fig. 2.1). The sequence is often referred to as a pseudo-noise (PN) sequence because it does not contain any useful information and is essentially a randomly selected code. Each bit of this sequence is known as a chip and the bit rate of the sequence as the chip rate to avoid confusion with the data rate of the information being transmitted. This signal, which now has a higher bandwidth than the data, is modulated and transmitted. At the receiver the signal is demodulated and then multiplied by a reference copy of the PN sequence (fig. 2.2). If

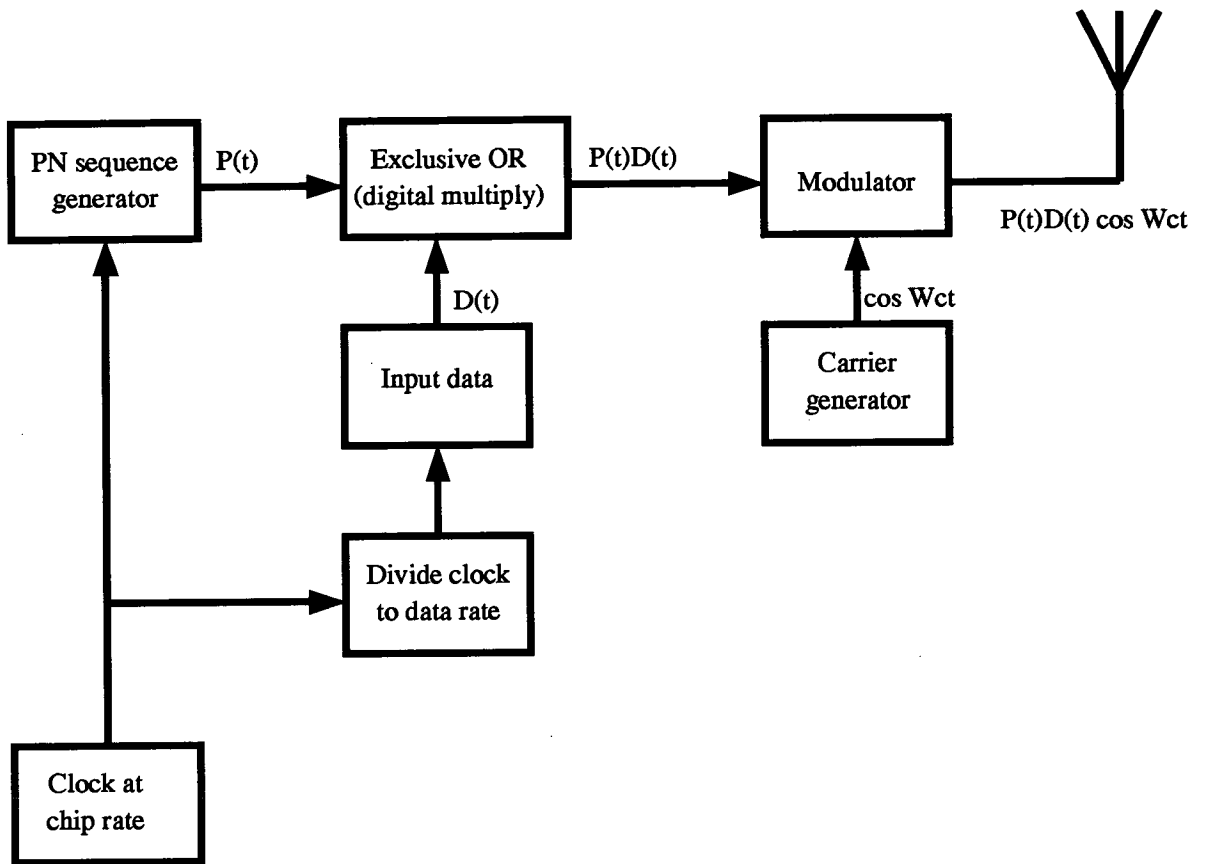


Fig. 2.1: Block diagram of a direct sequence spread spectrum transmitter

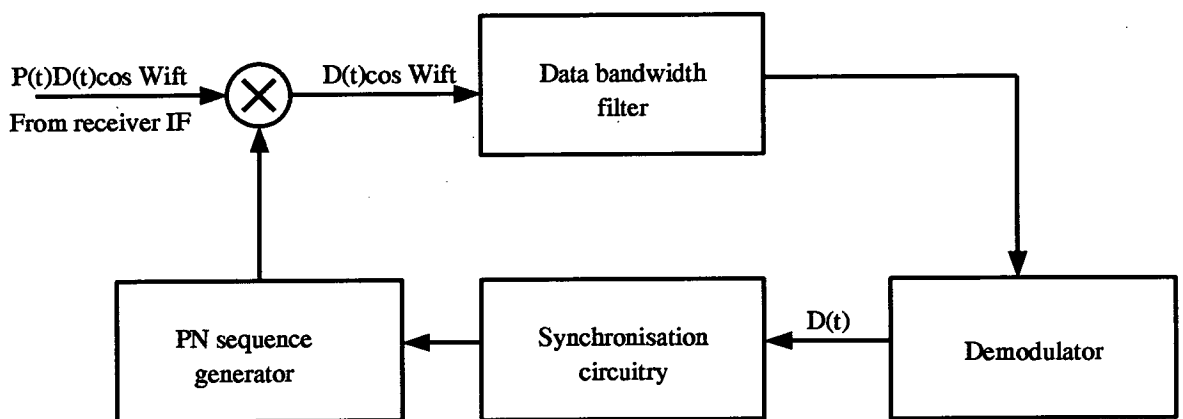


Fig. 2.2: Block diagram of a direct sequence spread spectrum receiver

the reference PN sequence is synchronised with the transmitter sequence, this restores the data to its original bandwidth and enables it to be passed through a filter set to the bandwidth of the data signal [14]. This type of system relies on being able to synchronise the reference PN code with the incoming code. This is a difficult and time consuming task, and in the alarm scheme case almost certainly too time consuming (see [14, 23] ). Therefore, we employ a different type of direct sequence spread spectrum receiver using a matched filter. The parallel nature of the matched filter device means that there is no synchronisation time, and provided that the peaks which come out of the matched filter can be detected, the performance of the matched filter circuit is the same as the circuitry in fig. 2.1. In military systems, the matched filtering is done by a surface acoustic wave (SAW) matched filter [24] as shown in fig. 2.3.

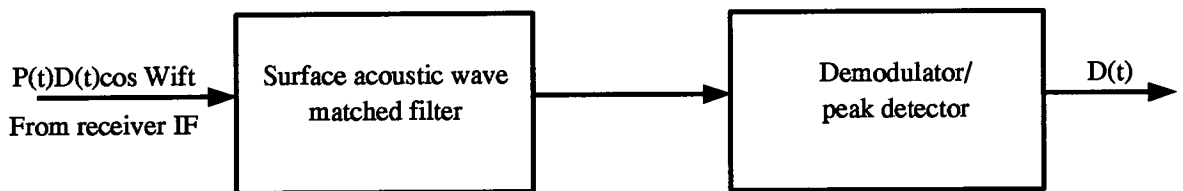


Fig. 2.3: Block diagram of a direct sequence spread spectrum receiver using a SAW matched filter.

However, because of the velocity of the waves in a SAW devices (see [25, 26, 21] ), the maximum total delay available is about  $1 \mu s$ . This means that the minimum data rate in a spread spectrum system using these devices is about 1 Mb/s. This is far higher than the data rate required in an alarm system. Therefore, we are forced to use the receiver circuitry in fig. 2.4, where the matched filtering operation is done by a baseband digital matched filter (DMF). The performance of these DMFs is one of the major topics in this thesis and will be discussed in detail in chapters 3-5.

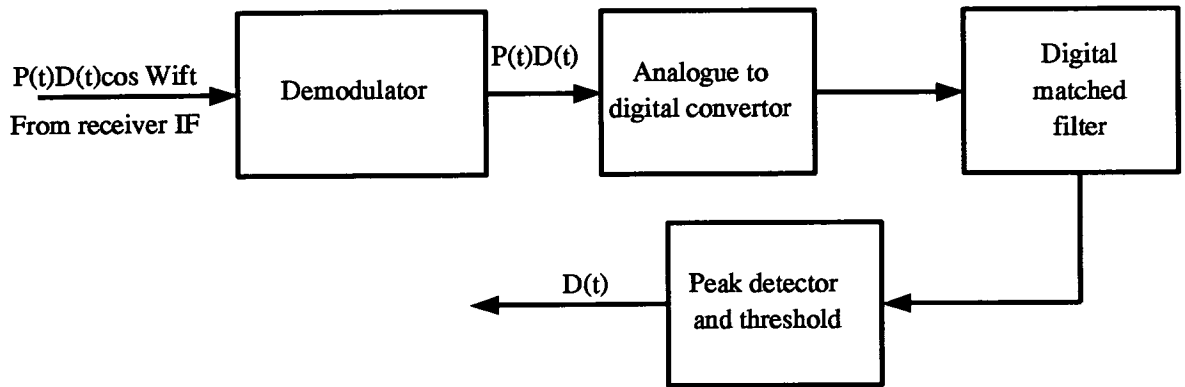


Fig. 2.4: Block diagram of a direct sequence spread spectrum receiver using a digital matched filter.

### 2.2.2. The advantages of spread spectrum in this application

There are several reasons why spread spectrum transmission may have advantages over conventional transmission in this application.

The channels being used for elderly alarms are often subject to stray narrow-band interference from adjacent channels used for citizen band radio and RF remote control units such as garage door openers. For example, one of the bands adjacent to the 27.450 MHz frequency is reserved for model aircraft controllers [27]. Spread spectrum transmission enables much of this noise to be rejected, as when the received narrow-band interferer is multiplied by the reference PN code it is spread over a wide bandwidth and thus most is rejected by the data bandwidth filter (fig. 2.5).

It is possible to operate two or more spread spectrum systems in the same channel providing that different PN codes are used. This is because a code which is not matched to the one in the receiver is rejected in a similar manner to narrow-band interference.

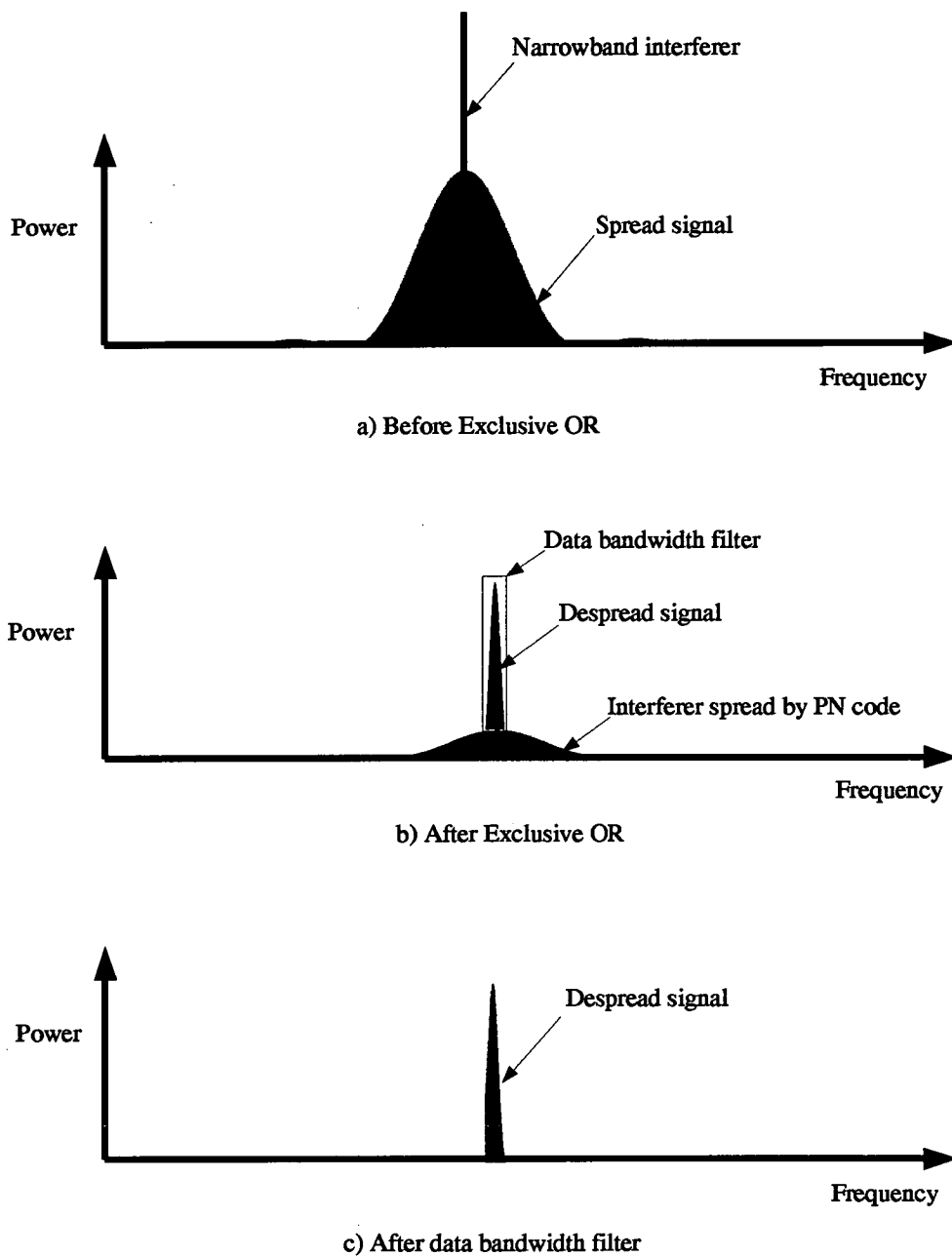


Fig. 2.5: Rejection of narrowband interference by a direct sequence spread spectrum system.



## *CHAPTER 2: BACKGROUND*

This property is known as code division multiple access (CDMA). Currently there is much debate as to whether or not this method of separating transmissions is more efficient than the more common frequency division multiple access (FDMA) or time division multiple access (TDMA) [28-33]. In an elderly alarm scheme however, it may be a convenient property for separating different schemes in the same area or operating a cell type structure for adjoining schemes. Spectral efficiency, the number of channels per unit bandwidth, may be less important.

If conventional techniques were used to transmit an alarm signal at the minimum rate of around 1 bit/s, it would require very accurate frequency references at the receiver and very narrow band filters to obtain the optimal signal to noise ratio. Due to the wider bandwidth of spread spectrum signals, this is less of a problem.

The noise prevailing in the channel under consideration is impulsive (see chapter 5). It has already been shown that spread spectrum systems have good performance in this type of interference. This will be discussed in detail in chapter 5.

### **2.2.3. Disadvantages of spread spectrum in this application**

The only disadvantage of spread spectrum in this application is an increase in complexity of the hardware and the system design. The increase in hardware complexity is mostly at the receiver. If the spread spectrum system can be made to transmit from the client direct to a remote receiver, there will be many transmitters for one receiver and the cost due to this increase in complexity should be small for each client. This cost will be more than recouped from the substantial saving made by not having to provide each client with a receiver and telephone modem.

---

## **3. Digital matched filters in unknown interference**

---

In the next three chapters, we develop digital matched filters for use in direct sequence matched filter receivers of the type shown in chapter 2. They must have a guaranteed minimum performance. When designing systems of this type, we have to be able to quote a usable range, within which the system must work extremely reliably regardless of adverse circumstances within the transmission channel. In the case of the alarm scheme channel, one of the potentially adverse circumstances is the distribution of the interference. There will be more discussion of the interference distributions likely to be encountered by this system in chapter 5, but one of the most important features of this channel is that the interference present in it is likely to be dominated by man-made interference. Its distribution is therefore unknown.

In this chapter, we examine previous work into digital matched filters with a guaranteed minimum performance in interference with an unknown distribution.

### **3.1. Guaranteed minimum performance digital matched filters**

In his 1971 papers [34, 35] C. R. Cahn outlined a method for designing digital matched filters (DMFs) with guaranteed minimum performance in unknown interference.

This section is an interpretation of Cahn's work.

### 3.1.1. Binary quantisation

A binary quantisation scheme tries to establish the polarity of a transmitted signal  $S$  from a received signal plus noise  $S + N$ . Assuming each chip is independent, and the probability of error in one chip is  $P$ , then the output signal to noise ratio for a matched filter of length  $K$  is given by [36] :-

$$\frac{S}{N} = K \frac{(1 - 2P)^2}{4P(1 - P)} \quad (3.1)$$

As  $P$  tends to 0.5, as it will in a spread spectrum system with  $S \ll N$

$$\frac{S}{N} = K(1 - 2P)^2 \quad (3.2)$$

One of the problems of binary quantisation is the complete suppression effect. This occurs when the the noise is greater than the signal for all samples, as it would be for a spread spectrum system with  $S \ll N$  and square wave interference. In this case,  $P = 0.5$ . Thus, from equation 3.2, the signal to noise ratio at the output of the DMF is 0. The following analysis tries to establish a lower bound for the signal to noise ratio with a specified bound on the noise power. It will avoid the complete suppression effect and provide a guaranteed minimum performance. The cost of this is slightly reduced performance for Gaussian noise.

3.1.2. Dither

The method used to avoid the complete suppression effect is to add a dither voltage  $\beta$  to the input signal before the polarity quantiser as shown in fig. 3.1.

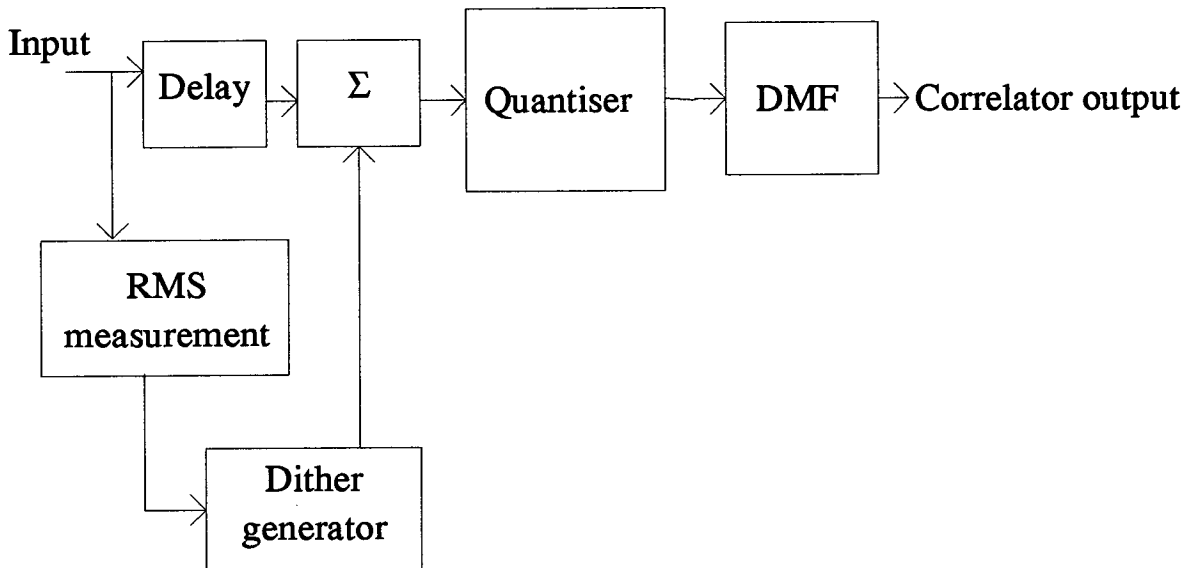


Fig. 3.1: DMF with dither voltage on input.

The dither at each sample is chosen from a PDF  $g(\beta)$ . The object is to find the  $g(\beta)$  that minimises the probability of quantising to the incorrect polarity when the noise interference distribution is worst case. For a particular  $\beta$ , the probability of error is 0.5 times the probability that the modulus of  $n - \beta$  is greater than the signal, where  $n$  is the noise sample. If we normalise the signal to 1 then the probability of an error for a single sample is:-

$$P_{\text{sample error}} = \frac{1}{2} - \frac{1}{2} P(-1 < n - \beta < 1) \quad (3.3)$$

The average probability of error is then given by integrating over  $\beta$ .

$$P = \frac{1}{2} - \frac{1}{2} \int_{-\infty}^{\infty} \int_{-1+\beta}^{1+\beta} g(\beta) p(n) dn d\beta \quad (3.4)$$

If the worst case noise probability density is known, then the probability of error,  $P$ , is minimised by setting  $\beta$  so that:-

$$\int_{-1+\beta}^{1+\beta} p(n)dn = \text{maximum} \quad (3.5)$$

By reversing the order of integration, equation 3.4 may be re-written as:-

$$P = \frac{1}{2} - \frac{1}{2} \int_{-\infty}^{\infty} \int_{-1+n}^{1+n} g(\beta) p(n) d\beta dn \quad (3.6)$$

Since the noise voltage  $\gg 1$ , we can assume that  $g(\beta)$  is essentially constant over a region of width 2. Therefore:-

$$P = \frac{1}{2} - \int_{-\infty}^{\infty} p(n)g(n)dn \quad (3.7)$$

A solution is sought which maximises  $P$  with respect to  $p(n)$  (the noise PDF, outwith the system designer's control), and minimises  $P$  with respect to  $g(n)$  (the dither PDF, controlled by the designer). The constraints are that  $p(n)$  and  $g(n)$  are both PDFs and that the noise PDF has variance  $\sigma^2$ , ie.:-

$$\int_{-\infty}^{\infty} g(n) dn = 1 \quad (3.8)$$

$$\int_{-\infty}^{\infty} p(n) dn = 1 \quad (3.9)$$

$$\int_{-\infty}^{\infty} n^2 p(n) dn = \sigma^2 \quad (3.10)$$

Using Lagrangian multipliers [37] for the constraint equation 3.8:-

$$d \left[ \frac{1}{2} - \int_{-\infty}^{\infty} p(n)g(n)dn + \lambda_1 \left( \int_{-\infty}^{\infty} g(n)dn - 1 \right) \right] = 0 \quad (3.11)$$

$$\rightarrow d \left[ \frac{1}{2} - \int_{-\infty}^{\infty} g(n)[p(n) - \lambda_1]dn - \lambda_1 \right] = 0 \quad (3.12)$$

$g(n) = 0$  contradicts equation 3.8, hence:-

$$p(n) - \lambda_1 = 0 \quad (3.13)$$

Using Lagrangian multipliers for the constraint equations 3.9 and 3.10:-

$$d \left[ \frac{1}{2} - \left[ \int_{-\infty}^{\infty} p(n)g(n)dn \right] + \lambda_2 \left[ \int_{-\infty}^{\infty} p(n)dn - 1 \right] + \lambda_3 \left[ \int_{-\infty}^{\infty} n^2 p(n)dn - \sigma^2 \right] \right] = 0 \quad (3.14)$$

$$\rightarrow d \left[ \int_{-\infty}^{\infty} p(n)g(n)dn - \lambda_2 \int_{-\infty}^{\infty} p(n)dn - \lambda_3 \int_{-\infty}^{\infty} n^2 p(n)dn \right] = 0 \quad (3.15)$$

$$\rightarrow d \left[ \int_{-\infty}^{\infty} p(n)[g(n) - \lambda_2 - \lambda_3 n^2] dn = 0 \right] \quad (3.16)$$

$p(n) = 0$  contradicts equations 3.9 and 3.10, hence:-

$$g(n) - \lambda_2 - \lambda_3 n^2 = 0 \quad (3.17)$$

From equation 3.13,

$$p(n) = \lambda_1 \quad (3.18)$$

Applying equation 3.9, and assuming that  $p(n)$  only exists over a limited range  $[a, -a]$  and is zero elsewhere (from equations 3.18 and 3.9, this is reasonable) yields:-

$$\int_{-a}^a \lambda_1 dn = 1 \quad (3.19)$$

$$\rightarrow 2\lambda_1 a = 1 \quad (3.20)$$

$$\rightarrow a = \frac{1}{2\lambda_1} \quad (3.21)$$

Applying equation 3.10,

$$\int_{-a}^a n^2 p(n) dn = \sigma^2 \quad (3.22)$$

$$\rightarrow 2\lambda_1 \frac{a^3}{3} = \sigma^2 \quad (3.23)$$

Applying equation 3.21,

$$p(n) = \frac{1}{2\sqrt{3}\sigma} \quad [-\sqrt{3}\sigma, \sqrt{3}\sigma] \quad (3.24)$$

$g(n)$  should have the same range as  $p(n)$

$$g(n) = 0, \quad n = \pm\sqrt{3}\sigma \quad (3.25)$$

re-writing equation 3.17 in the form

$$g(n) = \lambda_4[1 - \lambda_5 n^2] \quad (3.26)$$

$$\rightarrow \lambda_5 = \frac{1}{3\sigma^2} \quad (3.27)$$

$$\rightarrow g(n) = \lambda_4 \left[ 1 - \frac{n^2}{3\sigma^2} \right] \quad (3.28)$$

Applying equation 3.8:-

$$\int_{-\sqrt{3}\sigma}^{\sqrt{3}\sigma} g(n) dn = 1 \quad (3.29)$$



$$\rightarrow \int_{-\sqrt{3}\sigma}^{\sqrt{3}\sigma} \lambda_4 \left[ 1 - \frac{n^2}{3\sigma^2} \right] dn = 1 \quad (3.30)$$

$$\rightarrow \lambda_4 \left[ n - \frac{n^3}{9\sigma^2} \right]_{-\sqrt{3}\sigma}^{\sqrt{3}\sigma} = 1 \quad (3.31)$$

$$\rightarrow \lambda_4 \left( 2\sqrt{3}\sigma - 6\sqrt{3} \frac{\sigma^3}{9\sigma^2} \right) = 1 \quad (3.32)$$

$$\rightarrow \lambda_4 = \frac{\sqrt{3}}{4\sigma} \quad (3.33)$$

This implies the solution:-

$$g(\beta) = \frac{\sqrt{3}}{4\sigma} \left( 1 - \frac{\beta^2}{3\sigma^2} \right) \quad -\sqrt{3}\sigma < \beta < \sqrt{3}\sigma \quad (3.34)$$

$$g(\beta) = 0 \quad \text{elsewhere} \quad (3.35)$$

Note that this solution avoids the complete suppression effect. Substituting this solution into (3.7) we obtain:-

$$P = \frac{1}{2} - \frac{\sqrt{3}}{4\sigma} \int_{-\sqrt{3}\sigma}^{\sqrt{3}\sigma} \left( 1 - \frac{n^2}{3\sigma^2} \right) p(n) dn \quad (3.36)$$

$$\rightarrow P = \frac{1}{2} - \frac{\sqrt{3}}{4\sigma} \left(1 - \frac{1}{3}\right) \quad (3.37)$$

$$\rightarrow P = \frac{1}{2} - \frac{1}{2\sqrt{3}\sigma} \quad (3.38)$$

In an analogue system, the signal to noise ratio may be defined as:-

$$\left(\frac{S}{N}\right)_{analogue} = \frac{K}{\sigma^2} \quad (3.39)$$

Hence, from equations 3.2, 3.38 and 3.39:-

$$\left(\frac{S}{N}\right)_{binary\ worst\ case} = K(1 - 2P)^2 = \frac{K}{3\sigma^2} = \frac{1}{3} \left(\frac{S}{N}\right)_{analogue} \quad (3.40)$$

Thus the worst case performance of a binary quantisation system, using dither with a PDF as described in (3.34) and (3.35) is 4.8 dB below that of an analogue filter. To simulate this worst case condition, we are required to know the worst case interference. From equation 3.40, we know that summation over a sequence of length  $K$  gives:-

$$\left(\frac{S}{N}\right)_{binary} = \frac{K}{3\sigma_K^2} \quad (3.41)$$

where

$$\sigma_K^2 = \text{average interference power in each of } K \text{ samples} \quad (3.42)$$

Consider averaging over  $n$  sets of  $K$  samples, where  $n$  is an integer for simplicity.

$$\left(\frac{S}{N}\right)_{binary} = \frac{K}{3n} \sum_{i=1}^n \frac{1}{(\sigma_K^{(i)})^2} \quad (3.43)$$

If the root mean square (RMS) interference is  $\sigma$ , it follows that:-

$$\sum_{i=1}^n (\sigma_K^{(i)})^2 = n\sigma^2 \quad (3.44)$$

We have to minimise (3.43) subject to (3.44), which means maximising

$$\sum_{i=1}^n (\sigma_K^{(i)})^2 \quad (3.45)$$

subject to (3.44). This gives the solution:-

$$(\sigma_K^{(i)})^2 = \sigma^2 \quad \text{for all } i \quad (3.46)$$

Thus square wave interference is the worst case interference for binary quantisation with a dither PDF as given in equations 3.34 and 3.35, and results in performance described by equation 3.40.

### 3.1.3. Multilevel quantisation

We can now extend the minimax design criterion to multilevel quantisation, using a similar structure to fig 3.1, but with some subtle differences. Fig. 3.2 shows a block diagram of a multi-level system. The main differences are that the delay has been excluded and that the dither function has been modified. In the simulations to follow, the noise statistics are assumed to be stationary and the RMS measurement perfect. Thus the delay will have no effect. The dither function has been modified in two ways. First, it is no longer added to the signal, but instead it is used to change thresholds. Secondly, the dither function is constrained to be made up of a series of uniform distributions. The effect of this constraint will be discussed in the next chapter. The dither function will be

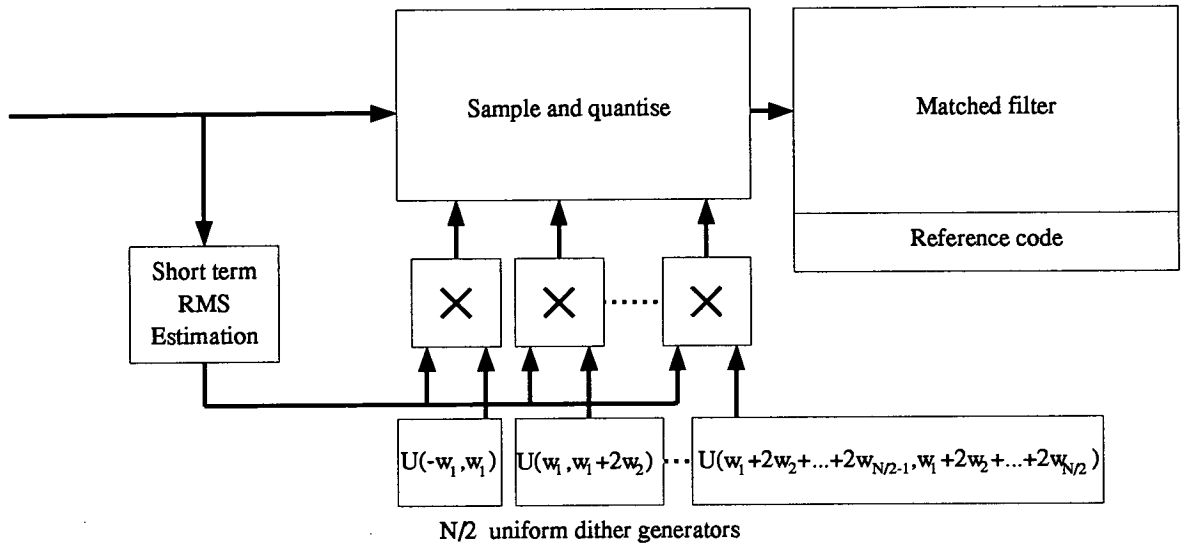


Fig. 3.2: Multi-level DMF structure.

used to assign each sample of received signal plus interference to one of  $Q$  levels. We define the reception probabilities  $p(q/r)$ , the probability of a received amplitude  $r$  being quantised to level  $q$ . Each received signal  $r$  must be quantised to one of the  $Q$  levels, thus:-

$$\sum_{q=1}^Q p(q/r) = 1 \tag{3.47}$$

If the signal has the value  $s$  at the receiver, the overall quantisation probabilities are given by:-

$$p(q/s) = \int p(q/r)p(r-s)dr \tag{3.48}$$

Expanding  $p(r-s)$  using a Taylor series and assuming  $s \ll r$  as it will be in the case of the noise being much greater than the signal:-

$$p(q/s) = \int p(q/r)p(r)dr - s \int p(q/r)p'(r)dr \quad (3.49)$$

$p'(r)$  denotes  $1 - p(r)$ . Therefore:-

$$p(q/s) = p_q - s \int p(q/r)p'(r)dr \quad (3.50)$$

where  $p_q$  denotes  $\int p(q/r)p(r)dr$ .  $s = \pm 1$  for transmitting binary digits, thus:-

$$p(q/\pm 1) = p_q \pm \left\{ - \int p(q/r)p'(r)dr \right\} \quad (3.51)$$

$$p(q/\pm 1) = p_q \pm \varepsilon_q \quad (3.52)$$

where  $\varepsilon_q$  denotes  $-\int p(q/r)p'(r)dr$ . If we assign a weight  $\gamma$  to each level  $q$ , the correlation output  $v$  becomes:-

$$v = \sum_{i=1}^K s_i \gamma_{q_i} \quad (3.53)$$

$q_i$  is the level assigned to the  $i$ th sample.

$$E(v) = K \sum_{all\ q} \varepsilon_q \gamma_q \quad (3.54)$$

$$E(v^2) = K \sum_{all\ q} p_q \gamma_q^2 \quad (3.55)$$

Defining output signal to noise ratio as:-

$$\left( \frac{S}{N} \right)_{output} = \frac{(E(v))^2}{E(v^2)} \quad (3.56)$$

From (3.54), (3.55) and (3.56):-

$$\left(\frac{S}{N}\right)_{output} = K \frac{\left(\sum_{all\ q} \varepsilon_q \gamma_q\right)^2}{\sum_{all\ q} p_q \gamma_q^2} \leq K \sum_{all\ q} \varepsilon_q^2 / p_q \quad (3.57)$$

This is maximised when:-

$$\gamma_q = \varepsilon_q / p_q \quad (3.58)$$

and the right hand term in equation 3.57 becomes an equality. If we find values:-

$$\varepsilon_q = \varepsilon_q^* \quad (3.59)$$

$$p_q = p_q^* \quad (3.60)$$

that minimise this S/N ratio, we can apply the arguments used by Stiglitz [38] to say that:-

$$\left(\frac{S}{N}\right)_{output} \geq K \sum_{all\ q} \varepsilon_q^{*2} / p_q^* \quad (3.61)$$

if we use the weights:-

$$\gamma_q^* = \varepsilon_q^* / p_q^* \quad (3.62)$$

### 3.1.4. Lower bound on performance with four quantisation levels

Using the equations 3.61 and 3.62 above, we can set about designing a system, based on the circuit in fig. 3.2, which maximises the worst case output S/N ratio.

Assuming symmetry around zero, (see equation 3.51).

$$p_1 = p_{-1} \quad (3.63)$$

$$p_2 = p_{-2} \quad (3.64)$$

and

$$\varepsilon_1 = \varepsilon_{-1} \quad (3.65)$$

$$\varepsilon_2 = \varepsilon_{-2} \quad (3.66)$$

From equation 3.61 the output S/N is given by:-

$$\left(\frac{S}{N}\right)_{output} \geq 2K \left( \frac{\varepsilon_1^2}{p_1} + \frac{\varepsilon_2^2}{p_2} \right) \quad (3.67)$$

We assume a uniform distribution of the thresholds over four regions (see fig. 3.3). Thus, the probability density of the location of the thresholds is given by:-

$$p(1:2) = p(-2:-1) = \frac{1}{2w_2} \quad (3.68)$$

$$p(-1:1) = \frac{1}{2w_1} \quad (3.69)$$

where  $p(1:2)$  denotes the probability density of the threshold between region 2 and 1.  $\varepsilon_1$  is the probability that the signal content will displace the input sample into region 1. If the interference value  $n$  lies anywhere in the region:-

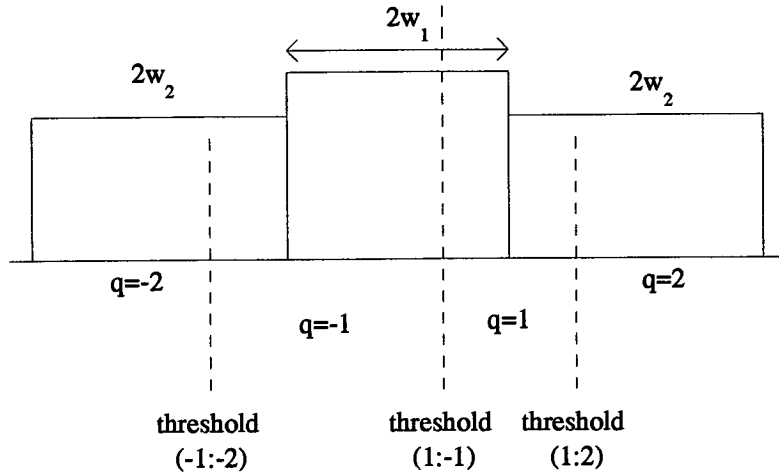


Fig. 3.3: Probability densities using four level quantisation with uniform dither functions.

$$-w_1 < n < w_1 \tag{3.70}$$

then with a signal of magnitude 1 and the above threshold probability densities:-

$$\epsilon_1 = \frac{1}{2w_1} \tag{3.71}$$

which is the probability of crossing from region -1 to 1. The worst case interference in this case is to utilise  $n = 0$ , which takes no power, with probability  $p_0$ . If the interference lies in the range

$$w_1 < n < w_1 + 2w_2 \tag{3.72}$$

then:-

$$\epsilon_1 = -\frac{1}{2w_2} \tag{3.73}$$



$$\varepsilon_2 = \frac{1}{2w_2} \quad (3.74)$$

The contribution to  $\varepsilon_1$  is negative, as in this region the sample can only be displaced out of region 1. In this range, the worst case strategy is to set  $n = A$ , since the average value of  $n$  sets the transition probabilities and the power is minimised for a constant value. The probability of  $n = A$ ,  $pA$ , is still to be determined. Finally, in the region:-

$$n \geq w_1 + 2w_2 \quad (3.75)$$

the signal has no effect, so there is no contribution to any of the  $\varepsilon$  values. The minimum interference power causing this is given by:-

$$n = w_1 + 2w_2 \quad (3.76)$$

To calculate the overall value of  $\varepsilon_1$ , the values of  $\varepsilon_1$  given in equations 3.71 and 3.73 are summed, weighted by the probability of the sample lying in the relevant range. Note that as long as

$$w_1 + 2w_2 < \sigma \quad (3.77)$$

the complete suppression effect is avoided. We now have the general form of the worst case interference distribution. It is:-

$$n = 0 \quad \text{with probability } p_0 \quad (3.78)$$

$$n = A, -A \quad \text{each with probability } pA \quad (3.79)$$

$$n = w_1 + 2w_2, -(w_1 + 2w_2) \quad \text{each with probability } 0.5(1 - p_0 - 2pA) \quad (3.80)$$

### CHAPTER 3: DIGITAL MATCHED FILTERS IN UNKNOWN INTERFERENCE

If  $p_0$  and  $p_A$  are taken as parameters to be optimised to find the worst case interference,  $A$  may be computed by solving the noise power equation:-

$$2A^2 p_A + 2(w_1 + 2w_2)^2 0.5(1 - p_0 - 2p_A) = \sigma^2 \quad (3.81)$$

with the constraints for valid probabilities:-

$$w_1 < A < w_1 + 2w_2 \quad (3.82)$$

$$0.5(1 - p_0 - 2p_A) \geq 0 \quad (3.83)$$

For any given value of the  $w$  parameters, chosen by the designer, the interference parameters  $p_0$  and  $p_A$  are varied over their full range and the minimum value is the worst case. This is repeated for all values of the  $w$  parameters, and the best  $w$  parameters are chosen. A computer search algorithm produces the plot shown in fig. 3.4, where the best  $w$  parameters are:-

$$w_1 = 0.61\sigma \quad (3.84)$$

$$w_2 = 0.92\sigma \quad (3.85)$$

which gives an output S/N ratio of (see equation 3.67):-

$$\left(\frac{S}{N}\right) = 0.59K/\sigma^2 \quad (3.86)$$

which is 2.3dB less than the analogue case given in equation 3.39. The worst case noise parameters are:-

$$p_0 = 0.38 \quad (3.87)$$

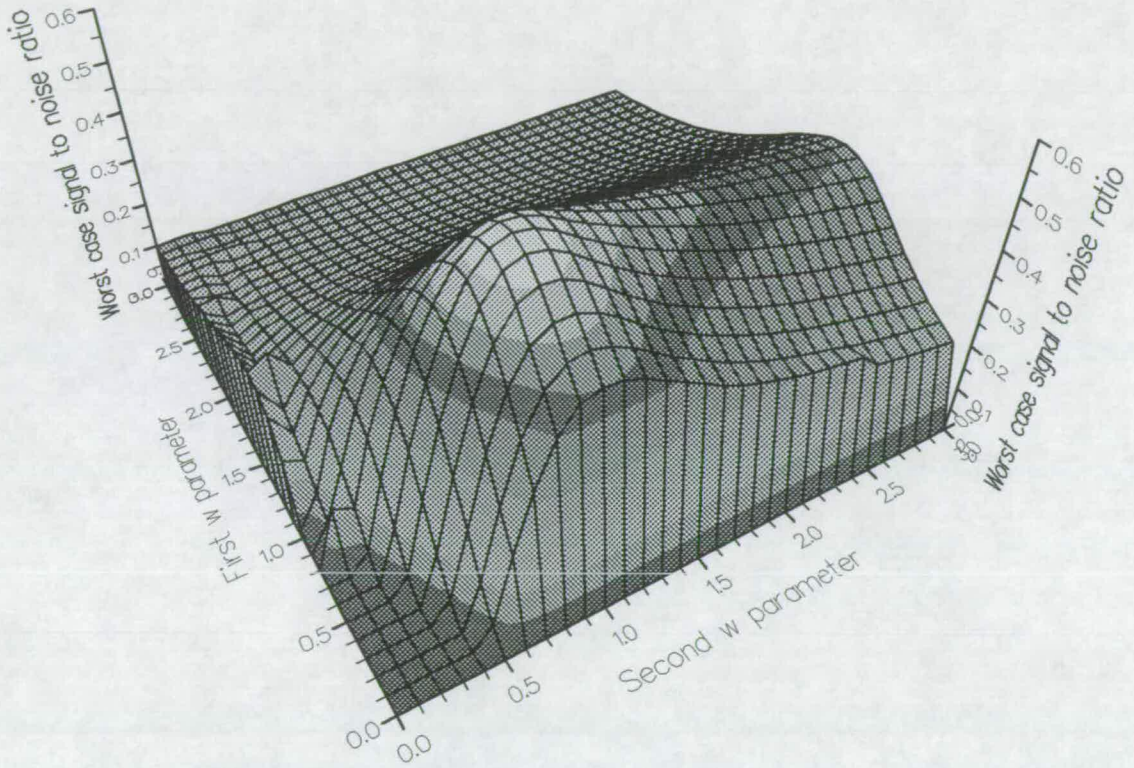


Fig. 3.4: Worst case signal to noise ratio vs the  $w$  parameters.  
 The first  $w$  parameter is  $w_1/\sigma$  and the second  $w$  parameter is  $w_2/\sigma$ .

$$A = 0.98, pA = 0.27 \tag{3.88}$$

Quantisation is done using two uniformly distributed random variables,  $\beta_1$  and  $\beta_2$  such that:-

$$-0.61\sigma < \beta_1 < 0.61\sigma \tag{3.89}$$

$$0.61\sigma < \beta < 2.45\sigma \quad (3.90)$$

A received sample is quantised such that:-

$$\text{amplitude} = 1.0; |r| \leq \beta \quad (3.91)$$

$$= 3.85; |r| > \beta \quad (3.92)$$

$$\text{polarity} = \text{sign}(r - \beta) \quad (3.93)$$

### 3.2. Simulation results and discussion

This section contains simulation results for the binary quantisation case and the four level quantisation case. It is interesting to compare these results with those obtained by Cahn.

#### 3.2.1. Binary quantisation

Fig. 3.5 shows simulation results for binary matched filters of the type discussed in sections 3.1.1 and 3.1.2. For the purposes of simulation,  $g(\beta)$  in equation 3.34 was approximated by the function:-

$$g(\beta) = \frac{\pi}{4\sqrt{3}\sigma} \cos\left(\frac{\pi\beta}{2\sqrt{3}\sigma}\right) \quad (3.94)$$

This enables us to define a random variable  $\beta$  with this distribution from a uniformly

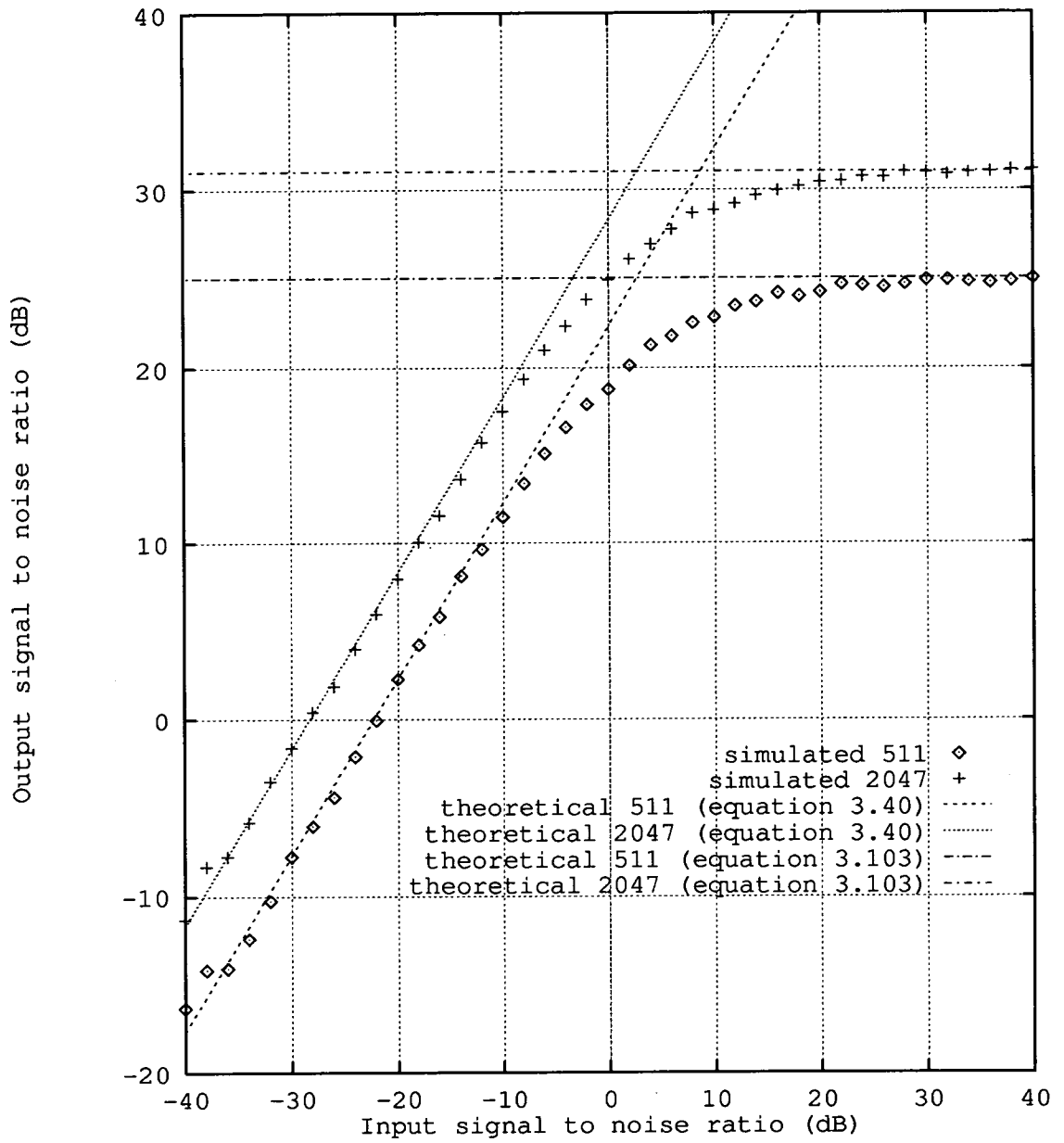


Fig. 3.5: Simulation results for Cahn's binary digital matched filter.

distributed random variable using the transformation (see [39] , chapter 7):-

$$\beta = \frac{2\sqrt{3}\sigma}{\pi} \sin^{-1}(2\beta_{uniform} - 1) \quad (3.95)$$

$\beta_{uniform}$  is a uniformly distributed random variable between 0 and 1. The simulation assumes that the short term RMS estimation in fig 3.1 is perfectly accurate and that there are no problems with synchronisation of the received signal and the reference. Results are given for a matched filter with 511 and 2047 taps. Each point on the simulation result graphs is the result of 2000 independent trials.

The graphs in fig 3.5 show a good correlation with equation 3.40 for the important region for a communications system (0-20 dB output signal to noise ratio). The match with the theory is closer than in Cahn's simulation results because of the assumption that the power measuring device is perfect. At high input signal to noise ratios, the output saturates. This saturation level can be predicted. If the input signal to noise ratio is high enough to consider the noise as negligible, then it is the autocorrelation noise which dominates. Thus:-

$$E(v) = K. P(\text{dither does not influence decision}) \quad (3.96)$$

$$P(\text{dither does not influence decision}) = \int_{-1}^1 g(\beta) \quad (3.97)$$

$$\int_{-1}^1 \frac{\pi}{4\sqrt{3}\sigma} \cos\left(\frac{\pi\beta}{2\sqrt{3}\sigma}\right) \quad (3.98)$$

$$= 0.7876 \quad (3.99)$$

Thus:-

$$E(v) = 0.7876K \quad (3.100)$$

$$E(v^2)_{\text{with uncorrelated signal}} = \text{var}(\text{uncorrelated signal}) \quad (3.101)$$

$$= K \quad (\text{assuming independent samples so } \sum \text{var} = \text{var } \sum) \quad (3.102)$$

Thus as  $S/N$  at the input gets bigger, the output  $S/N$  tends to:-

$$\frac{S}{N_{\text{output}}} = \frac{(0.7876K)^2}{K} \quad (3.103)$$

Graphs of this equation are shown on fig. 3.5.

### 3.2.2. Four-level quantisation

Fig. 3.6 shows simulation results of four-level matched filters of the type discussed in sections 3.1.3 and 3.1.4. As for the binary case, the simulation assumes that the short term RMS measurement is perfectly accurate and each point on the simulation result graphs is the average of 2000 independent trials. Again, the simulation results in fig. 3.6 show a good correlation with equation 3.86 for the important region of the graph for a communication system. The simulation results are again closer to the theoretical predictions than the results in Cahn's paper because of the assumed perfection of the power measuring device. As before, the output signal to noise ratio saturates at a level which can be predicted. At high input signal to noise ratio:-

$$E(v) = K \cdot \sum_{\text{all weights}} \sum_{s=\pm 1} (\text{probability of weight}) \cdot (\text{weight}) \cdot (\text{transmitted signal})$$

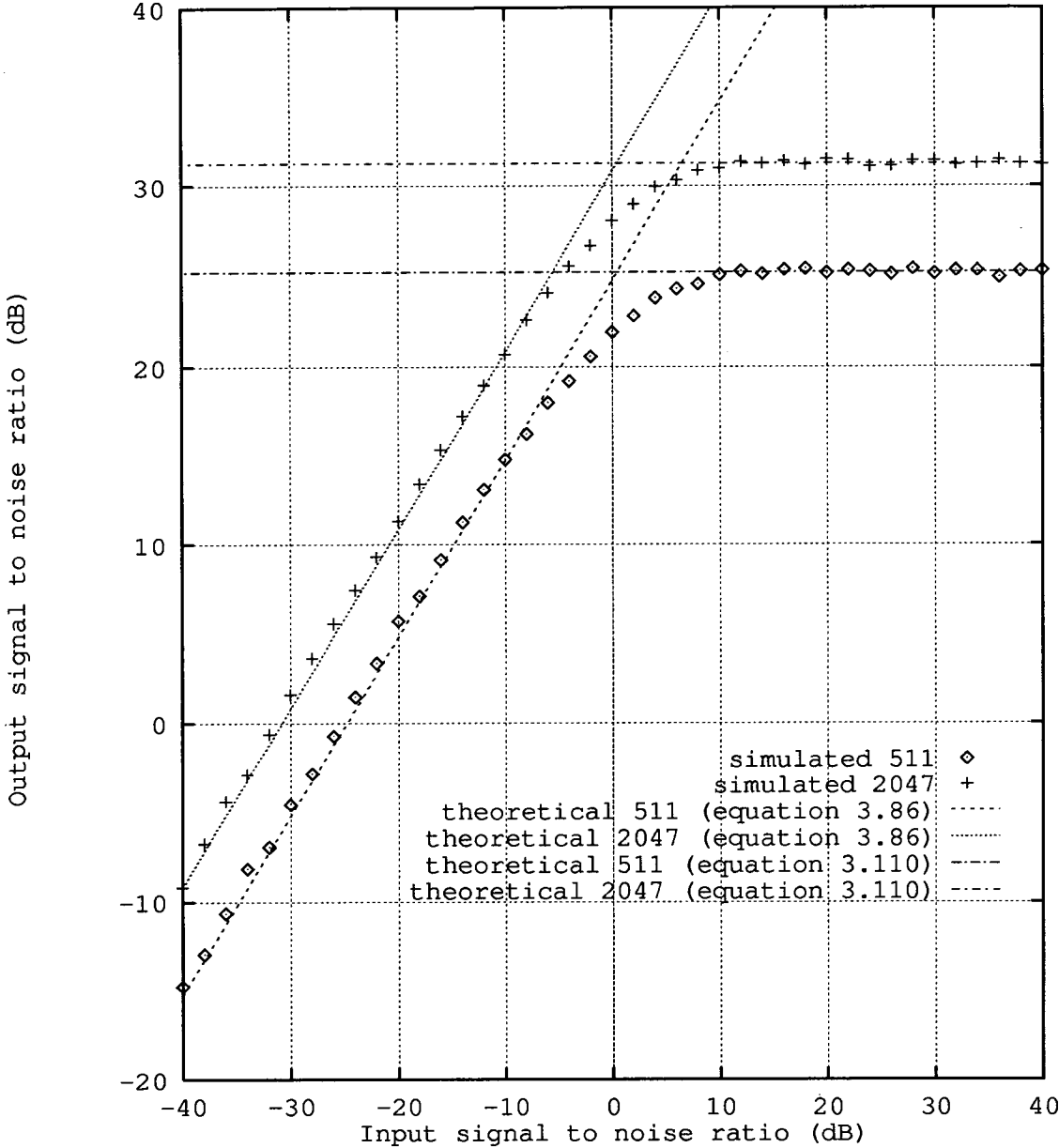


Fig. 3.6: Simulation results for Cahn's four-level digital matched filter.



(3.104)

Substituting in the optimised weights and the probability of the weight calculated from the dither function

$$= K \cdot (2 \cdot (0.4005) \cdot (1) + 2 \cdot (0.0995) \cdot (3.85)) \quad (3.105)$$

$$1.56715K \quad (3.106)$$

Also:-

$$E(v^2) = K \cdot \sum_{\text{all weights}} \sum_{s=\pm 1} (\text{probability of weight}) \cdot (\text{weight}) \cdot (\text{transmitted signal})^2 \quad (3.107)$$

$$= K \cdot \left( 2 \cdot (0.4005) \cdot (1)^2 + 2 \cdot (0.0995) \cdot (3.85)^2 \right) \quad (3.108)$$

$$= 3.75068K \quad (3.109)$$

Thus from equation 3.56:-

$$\frac{S}{N_{\text{output}}} = \frac{(1.56715K)^2}{3.75068K} \quad (3.110)$$

Graphs of this equation are shown on fig. 3.6.

### **3.3. Chapter summary**

In this chapter we have shown that a DMF with a guaranteed minimum performance in any interference distribution can be developed theoretically, and that its performance in simulation matches well with this theoretical prediction. We have shown that a DMF with four quantisation levels has considerably better performance (2.5dB better) than a two level (binary) DMF.

---

## **4. Extension of previous work**

---

In this chapter, we develop Cahn's DMF into a more practical device, improving its performance and making it easy to implement on practical devices.

### **4.1. Extension of Cahn's work to larger numbers of quantisation levels**

In Cahn's original paper, he stated that his multi-level quantisation technique could be extended to any number of levels. However, he did not state results for any more than four quantisation levels. In this section, we shall show that it is difficult to obtain results for more than four quantisation levels using Cahn's technique and try to devise a way round this problem.

#### **4.1.1. Binary quantisation using the multi-level technique**

In the previous chapter, we obtained the result for binary quantisation that the worst case performance was 4.8 dB below the performance of the equivalent analogue matched filter. This was obtained using a significantly different method than the multi-level technique used for obtaining the four level solution. The important difference in the multi-level solution is that the dither function is constrained to be made up of uniform

CHAPTER 4: EXTENSION OF PREVIOUS WORK

distributions. We shall now apply the multi-level technique to binary quantisation. The probability density diagram, equivalent to the one in fig. 3.3 for four-level system, is shown in fig. 4.1.

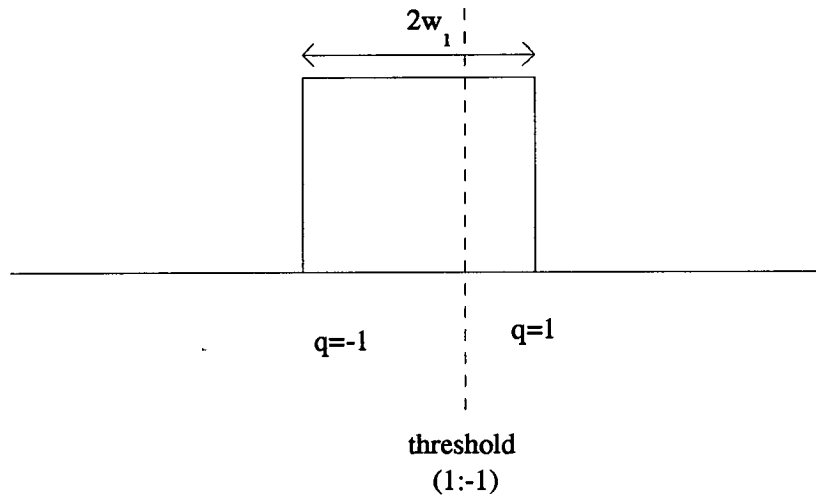


Fig. 4.1: Probability densities for binary quantisation with uniform dither functions.

From this diagram,

$$\varepsilon_1 = \frac{p_0}{2w_1} \quad (4.1)$$

$$p_1 = 0.5 \quad (4.2)$$

The worst case interference distribution is:-

$$n = 0 \text{ with probability } p_0 \quad (4.3)$$

CHAPTER 4: EXTENSION OF PREVIOUS WORK

$$n = w_1, -w_1 \quad \text{each with probability } 0.5(1 - p_0) \quad (4.4)$$

We also have the noise power constraint:-

$$2w_1^2 \cdot 0.5(1 - p_0) = \sigma^2 \quad (4.5)$$

Referring to equation 3.61 and substituting for  $\varepsilon_1$  and  $p_1$ :-

$$\left(\frac{S}{N}\right) = \frac{2K\left(1 - \frac{\sigma^2}{w_1^2}\right)^2}{w_1^2} \quad (4.6)$$

A plot of this equation is shown in fig. 4.2. This equation is easy to optimise analytically with respect to  $w_1$  rather than numerically as is required for the four level case.

Differentiating with respect to  $w_1$  yields:-

$$-\frac{4K}{w_1^3} + \frac{16K\sigma^2}{w_1^5} - \frac{12K\sigma^4}{w_1^7} \quad (4.7)$$

Setting this equal to zero and factorising gives:-

$$w_1 = \pm\sqrt{3}\sigma, \pm\sqrt{-1}\sigma \quad (4.8)$$

$w_1$  is a range and can thus only be a real positive number, therefore:-

$$w_1 = \sqrt{3}\sigma \quad (4.9)$$

is the optimal solution, which yields a signal to noise ratio of

$$\left(\frac{S}{N}\right) = 0.296K/\sigma^2 \quad (4.10)$$

The worst case noise is then given by:-

$$n = 0 \quad \text{with probability } 2/3 \quad (4.11)$$

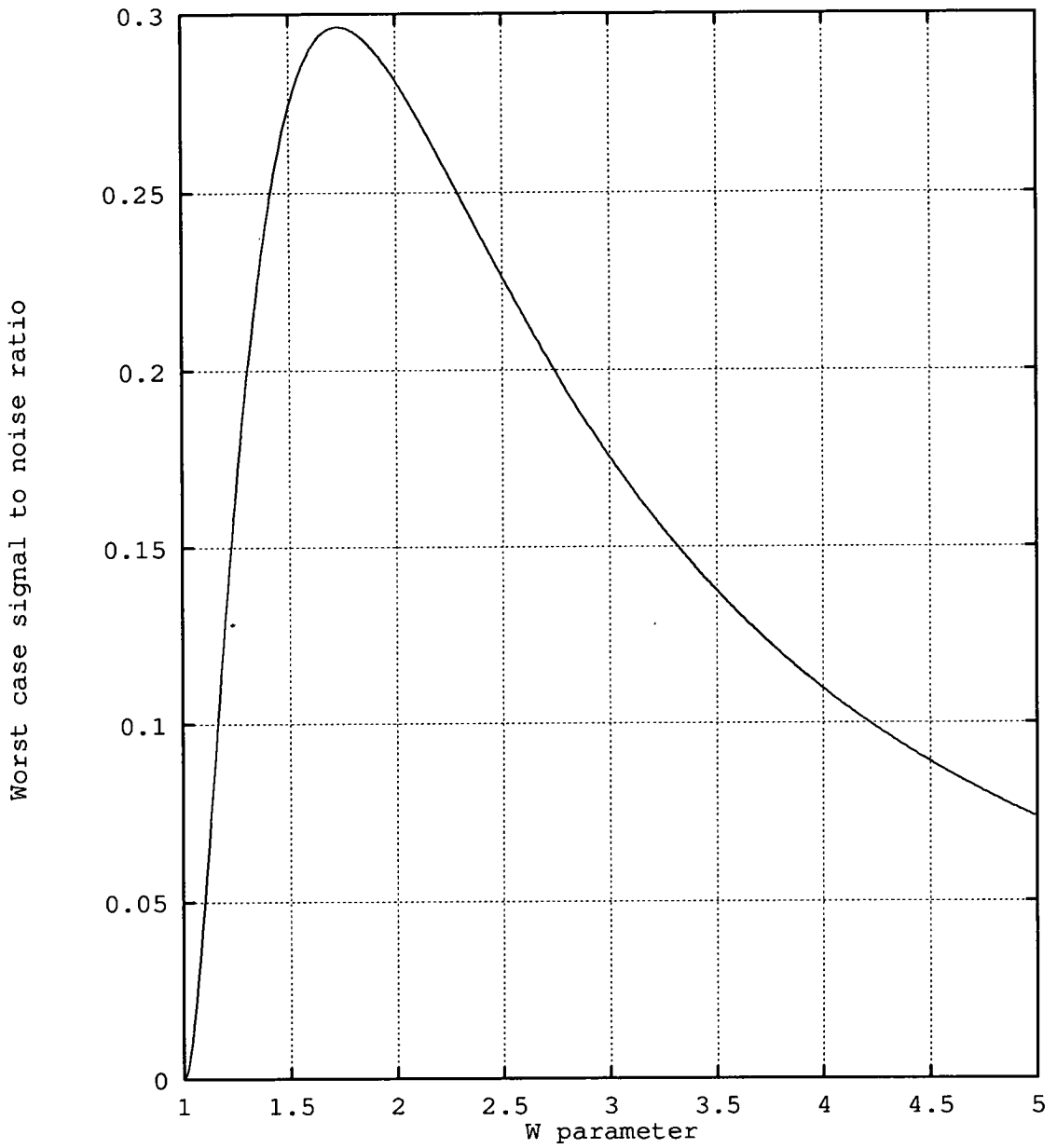


Fig. 4.2: Worst case signal to noise ratio vs the  $w$  parameter.

The  $w$  parameter is  $w_1/\sigma$ .

$$n = \sqrt{3} \quad \text{with probability } 1/3 \quad (4.12)$$

Quantisation is done using a single uniformly distributed random variable,  $\beta$ , where

$$-\sqrt{3}\sigma < \beta < \sqrt{3}\sigma \quad (4.13)$$

A received sample is quantised such that:-

$$\text{amplitude} = 1 \quad (4.14)$$

$$\text{polarity} = \text{sign}(r - \beta) \quad (4.15)$$

The performance of this binary DMF is slightly worse than the one detailed in chapter 3. The loss in signal to noise ratio when compared with the analogue filter is 5.3 dB compared with 4.8 dB for the binary DMF in chapter 3. This suggests that this optimisation process is not the best achievable, in particular the constraint that the dithers are uniformly distributed is a restriction that degrades performance. Other artificial constraints on the dither function produce similar degradations in performance [40]. However, the method used for the binary DMF in chapter 3 does not easily generalise and the extra loss (0.5 dB) is small. Simulation results for the binary DMF optimised using the multi-level technique are given in fig. 4.3. Simulation conditions are the same as those used for fig. 3.6. They show good correlation with the equation 4.10. The saturation levels for these DMFs can be predicted using a similar method to chapter 3. For this DMF at high signal to noise ratio:-

$$P(\text{a single bit correlating}) = \frac{1}{\sqrt{3}} \quad (4.16)$$

Thus from equations 3.94, 3.98 and 3.99,

$$\frac{S}{N_{\text{output}}} = \frac{(0.577K)^2}{K} \quad (4.17)$$

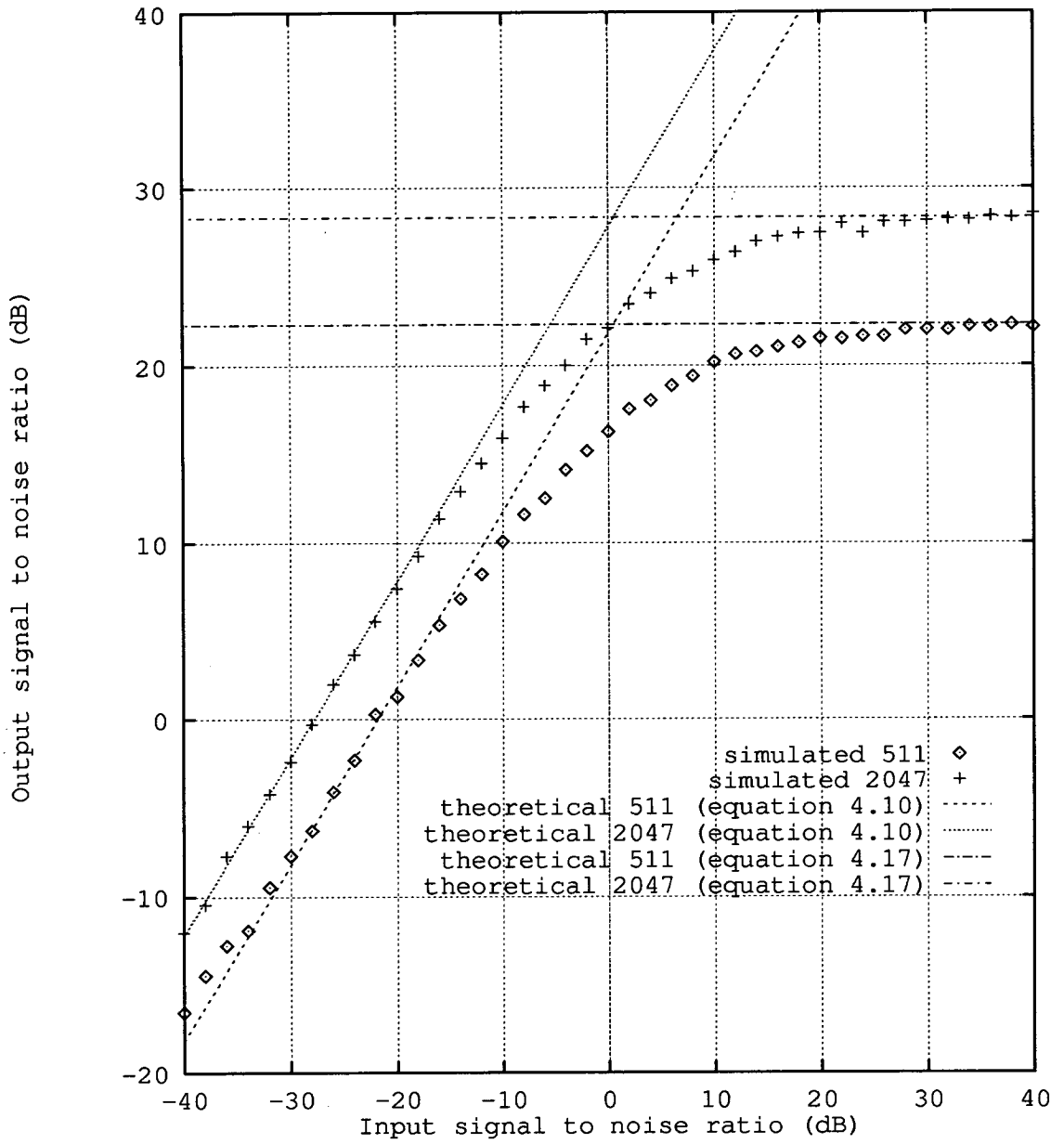


Fig. 4.3: Simulation results for the binary digital matched filter optimised using the multi-level technique.



Graphs of this equation are shown in fig. 4.3.

#### 4.1.2. Six and eight level quantisation using the multi-level technique

We now attempt to obtain solutions for six and eight level quantisation using the multi-level technique described in the previous chapter. This is a little more difficult than it first might seem.

In the binary case, there are two variables to optimise with respect to ( $p_0$  and  $w_1$ ) and one constraint equation (the noise power constraint, equation 4.5). This leaves the optimisation with respect to one variable ( $w_1$ ). We shall term this as an optimisation process of order 1. In the four level case, there are five variables to optimise with respect to ( $p_0$ ,  $p_A$ ,  $A$ ,  $w_1$  and  $w_2$ ) and one constraint equation (the power constraint, equation 3.81). This leaves the optimisation with respect to four variables ( $p_0$ ,  $p_A$ ,  $w_1$  and  $w_2$ ). This optimisation process is therefore of order four. In fact, the order of the optimisation process is:-

$$O = \frac{3Q}{2} - 2 \quad (4.18)$$

where Q is the number of levels. The number of calculations of the signal to noise ratio functions is:-

$$F(Q) = X^{\frac{3Q}{2} - 2} \quad (4.19)$$

where X is 100 divided by the percentage accuracy in the overall range for each variable the optimisation is with respect to. This means that the length of time taken to do the optimisation on a computer increases extremely rapidly with the number of quantisation

## CHAPTER 4: EXTENSION OF PREVIOUS WORK

levels  $Q$ . This is compounded by the fact that the signal to noise ratio function (equation 3.61) has more terms for larger  $Q$ . In fact, it would take far too long to calculate the optimal solution for six and eight levels using the exhaustive search method used to find the four level solution. However, there is a way round this problem. Examination of figs 3.4 and 4.2 shows that the signal to noise ratio function is a smooth function with respect to the  $w$  parameters and that it has a single global maximum. This means that it is possible to use a gradient search method instead of the exhaustive search. This reduces the order of the optimisation process to:-

$$F(Q) = X^{Q-2} \quad (4.20)$$

Therefore we are able to evaluate the solution for six level quantisation, which is:-

$$\left(\frac{S}{N}\right) = 0.93K/\sigma^2 \quad (4.21)$$

This represents a loss of 0.32 dB over the analogue matched filter. This performance is achieved when:-

$$w_1 = 0.25\sigma$$

$$w_2 = 0.1625\sigma$$

$$w_3 = 0.8125\sigma \quad (4.22)$$

The worst case noise distribution is:-

*0 with probability 0.32*

*±1.02 each with probability 0.19*

## CHAPTER 4: EXTENSION OF PREVIOUS WORK

$\pm 0.78$  each with probability 0.11

$\pm 2.425$  each with probability 0.04 (4.23)

Quantisation is done using three uniformly distributed random variables,  $\beta_1$ ,  $\beta_2$  and  $\beta_3$  such that:-

$$-0.25\sigma < \beta_1 < 0.25\sigma$$

$$0.25\sigma < \beta_2 < 0.575\sigma$$

$$0.575\sigma < \beta_3 < 2.25\sigma \quad (4.24)$$

A received sample is quantised such that:-

$$\text{amplitude} = 1.0; |r| \leq \beta_2$$

$$\text{amplitude} = 1.410; \beta_2 < |r| \leq \beta_3$$

$$\text{amplitude} = 3.27; |r| > \beta_3$$

$$\text{polarity} = \text{sign}(r - \beta_1) \quad (4.25)$$

Fig. 4.4 shows simulation results for the six level case in its worst case noise. The simulation conditions are similar to those used for the four-level case in the previous chapter. The simulation results in fig. 4.4 show excellent correlation with the theory over the region of interest. As previously discussed, the output saturates at a level which can be predicted using equations 3.101, 3.104 and 3.56. In this case, for high input signal to noise ratios:-

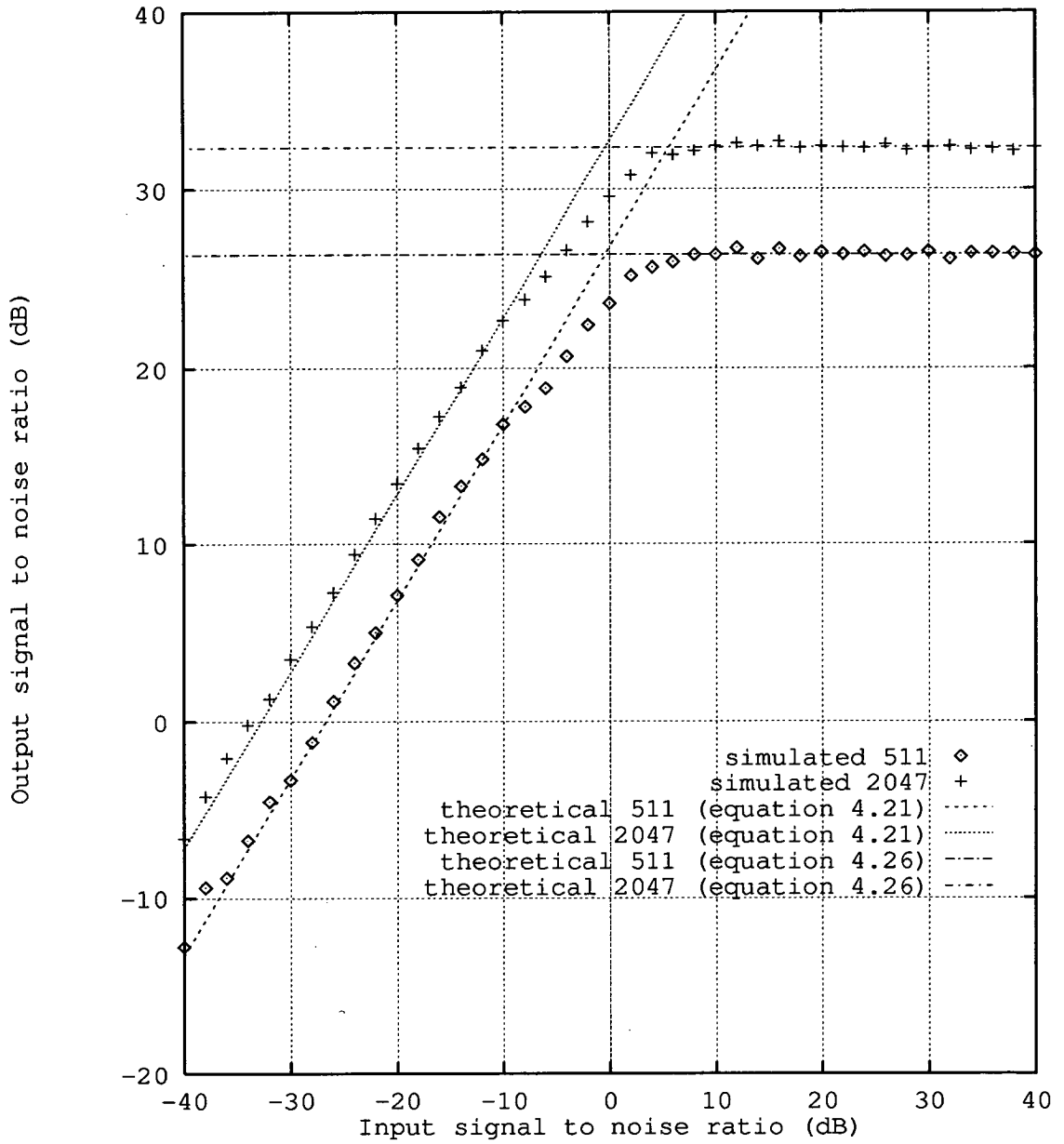


Fig. 4.4: Simulation results for a six-level digital matched filter optimised using the multi-level technique.

$$\frac{S}{N_{output}} = \frac{(2.23K)^2}{5.88K} \quad (4.26)$$

Graphs of this equation are shown in fig. 4.4.

Evaluating the solution for the eight level case is not so straight forward however. Even with the reduction in computational complexity facilitated by the use of the gradient search method, it is not possible to evaluate the solution for the eight level case with the same accuracy as before. The only way to find any sort of solution is to reduce the value of X in equation 4.17. The other optimisations were done with X set 100. In this case, the highest value that X can be set is around 30. Unfortunately, this makes the gradient search process dependent on the start point of the search. This can best be illustrated using the four level case as an example. Fig. 4.5 shows optimisation plots similar to the one in fig 3.4, but with the value of X decreasing. Fig. 4.5 shows that if you decrease the value of X, the smooth surface with its single global maximum is lost. When this happens, the gradient search is no longer guaranteed to find the optimal solution. The optimisation plots for X=12.5 and X=6.125 illustrate very well what happens in the eight level case with X=30. When the gradient search is applied, it tends to find incorrect solutions around  $w_1=0$ . The only way to find any kind of solution is to make the steps in the noise function search non-linear and unequal for different parameters. No further discussion of this rather unsatisfactory method will be included here. The solution it finds is also rather unsatisfactory, the worst case signal to noise ratio is given by:-

$$\left(\frac{S}{N}\right) = 1.14K/\sigma^2 \quad (4.27)$$

This suggests a minimum performance of 0.57 dB gain over the analogue matched filter! This solution is obviously incorrect. The true solution must lie between the loss of 0.32 dB for the six level case and the loss of approximately 0.15 dB quoted in [41] for an eight level DMF optimised for use in Gaussian noise. This solution is incorrect simply because

CHAPTER 4: EXTENSION OF PREVIOUS WORK

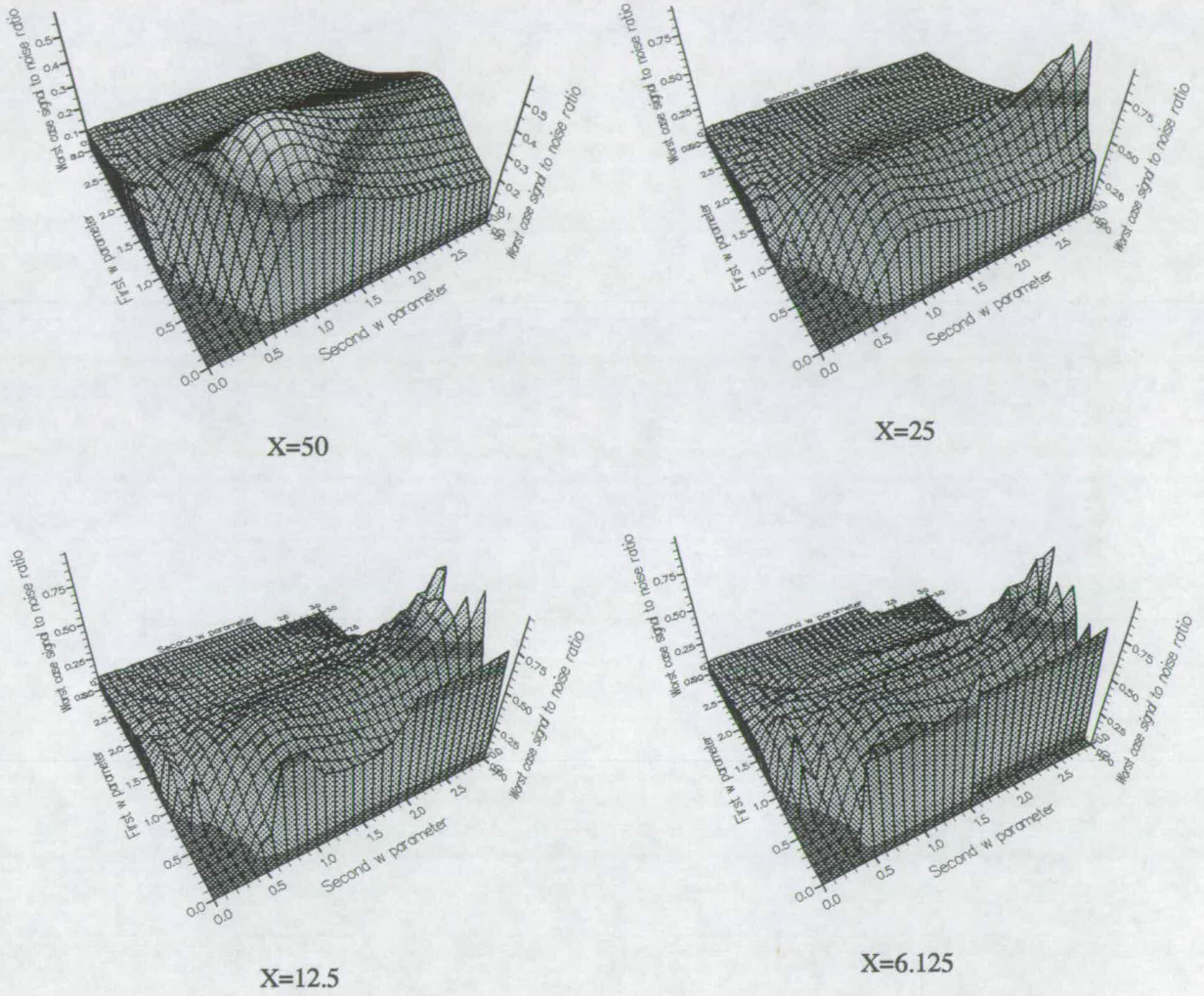


Fig. 4.5: Optimisation plots for the four level case with X varying.

## CHAPTER 4: EXTENSION OF PREVIOUS WORK

the number of noise cases tried is not enough. For the record, this performance is achieved when:-

$$w_1 = 0.103\sigma$$

$$w_2 = 0.244\sigma$$

$$w_3 = 0.150\sigma$$

$$w_4 = 0.739\sigma \quad (4.28)$$

The worst case noise distribution is supposedly:-

0 with probability 0.04

$\pm 0.360\sigma$  each with probability 0.151

$\pm 0.804\sigma$  each with probability 0.113

$\pm 1.10\sigma$  each with probability 0.183

$\pm 2.37\sigma$  each with probability 0.033 (4.29)

Quantisation is done using four uniformly distributed random variables,  $\beta_1$ ,  $\beta_2$ ,  $\beta_3$  and  $\beta_4$  such that:-

$$-0.103\sigma < \beta_1 < 0.103\sigma$$

$$0.103\sigma < \beta_2 < 0.591\sigma$$

## CHAPTER 4: EXTENSION OF PREVIOUS WORK

$$0.591\sigma < \beta_3 < 0.891\sigma$$

$$0.891\sigma < \beta_4 < 2.369\sigma \quad (4.30)$$

A received sample is quantised such that:-

$$\text{amplitude} = 1.0; |r| \leq \beta_2$$

$$\text{amplitude} = 5.175; \beta_2 < |r| \leq \beta_3$$

$$\text{amplitude} = 11.243; \beta_3 < |r| \leq \beta_4$$

$$\text{amplitude} = 22.079; |r| > \beta_4$$

$$\text{polarity} = \text{sign}(r - \beta_1) \quad (4.31)$$

Simulation results from this DMF are shown in fig. 4.6. The correlation between the simulation results and the theory of equation 4.27 is quite good, however there is a slight tendency for the simulation results to have lower output signal to noise ratios than the theory predicts. It is understandable for the results to be slightly better than predicted, (as may be the case in some of the earlier simulation results), because any slight statistical deviations from the worst case noise distribution will tend to improve the performance. The fact that in this case, the results of the simulation look slightly worse than the predicted theory only reflects the unsatisfactory nature of this optimisation. Final confirmation that this optimisation result is incorrect can be obtained by doing simulations in Gaussian noise. It is fundamentally true that a DMF cannot exceed the performance of an analogue matched filter in Gaussian noise. Fig. 4.7 shows simulation results for the eight level DMF in Gaussian noise. They show quite clearly that the guaranteed minimum performance predicted in equation 4.27 is incorrect. It is therefore



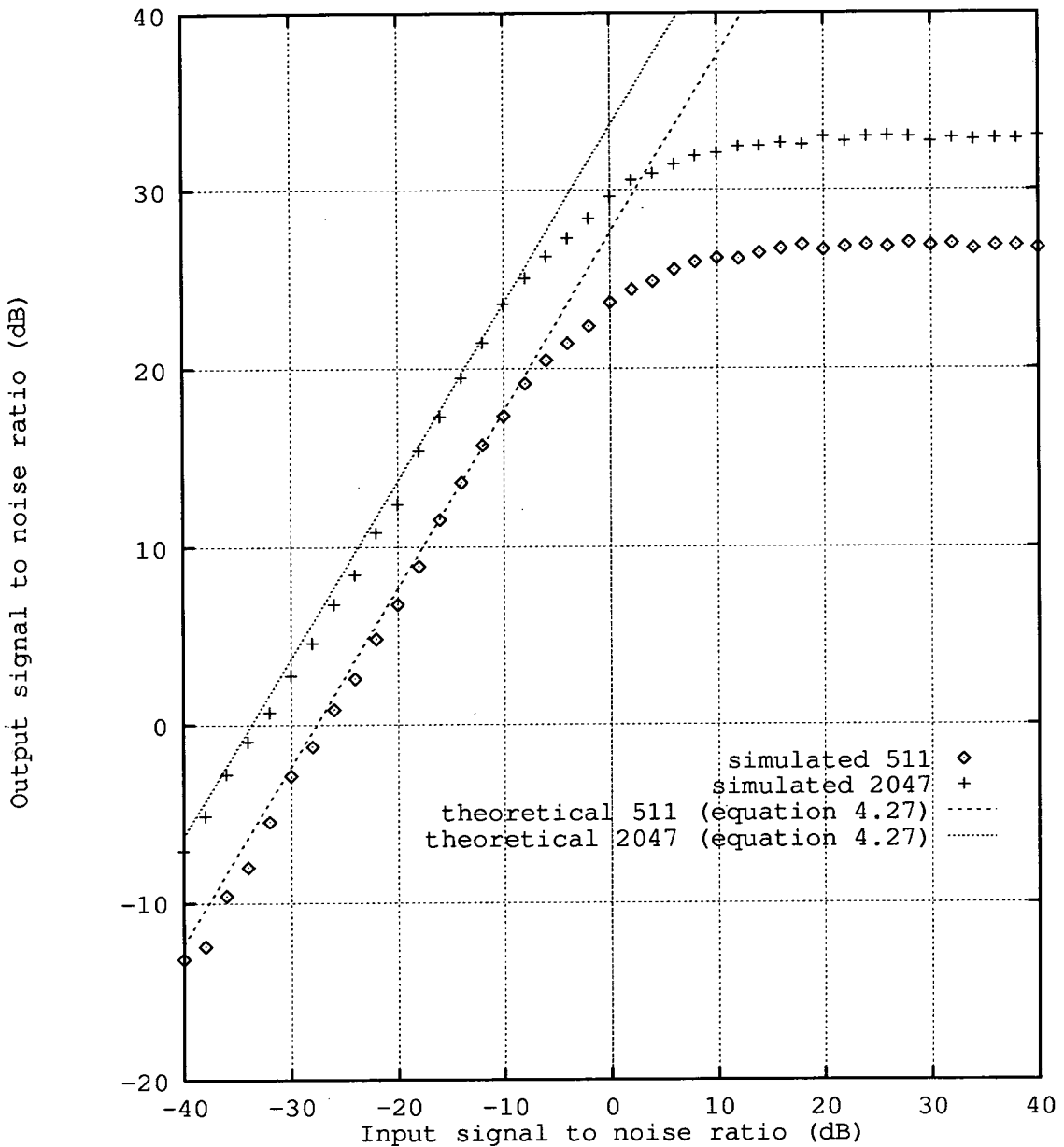


Fig. 4.6: Simulation results for the eight level DMF.

recommended that this DMF should not be used in any practical system and there will be no further discussion of it in this thesis.

## 4.2. Linear integer quantisation weights

Cahn's optimisation process produces a quantisation function which assigns floating point weights. In order to implement the matched filter in currently available hardware such as the devices manufactured by INMOS, MEDL and TRW or in custom designed hardware such as that found in [42], it is desirable that the weights in the quantisation function are linearly spaced integers. The exact value of the weights is unimportant, it is the ratio of the weights which defines the performance. Thus the binary DMFs (either the one detailed in Chapter 3 or in section 4.1.1) may be considered to have linear quantisation weights.

To find optimal solutions for larger numbers of quantisation levels, requires a search of all possible  $w$  values. Unfortunately, for reasons previously discussed, the amount of computer time required to do this becomes prohibitively large for any more than four quantisation levels. This is somewhat frustrating, as commercially available devices have up to three bit (eight level) quantisation and the linear integer solution for eight levels is expected to have a significant performance improvement over the four level solution.

To find the solution for four quantisation levels, we plot the worst case signal to noise ratio against the ratio of the two quantisation weights for many values of the  $w$  parameters. The results of doing this are shown in fig. 4.8. This graph reveals several interesting features. The two lines of points at the left of the graph and the line of points up from the origin are almost certainly incorrect. They appear due to the finite

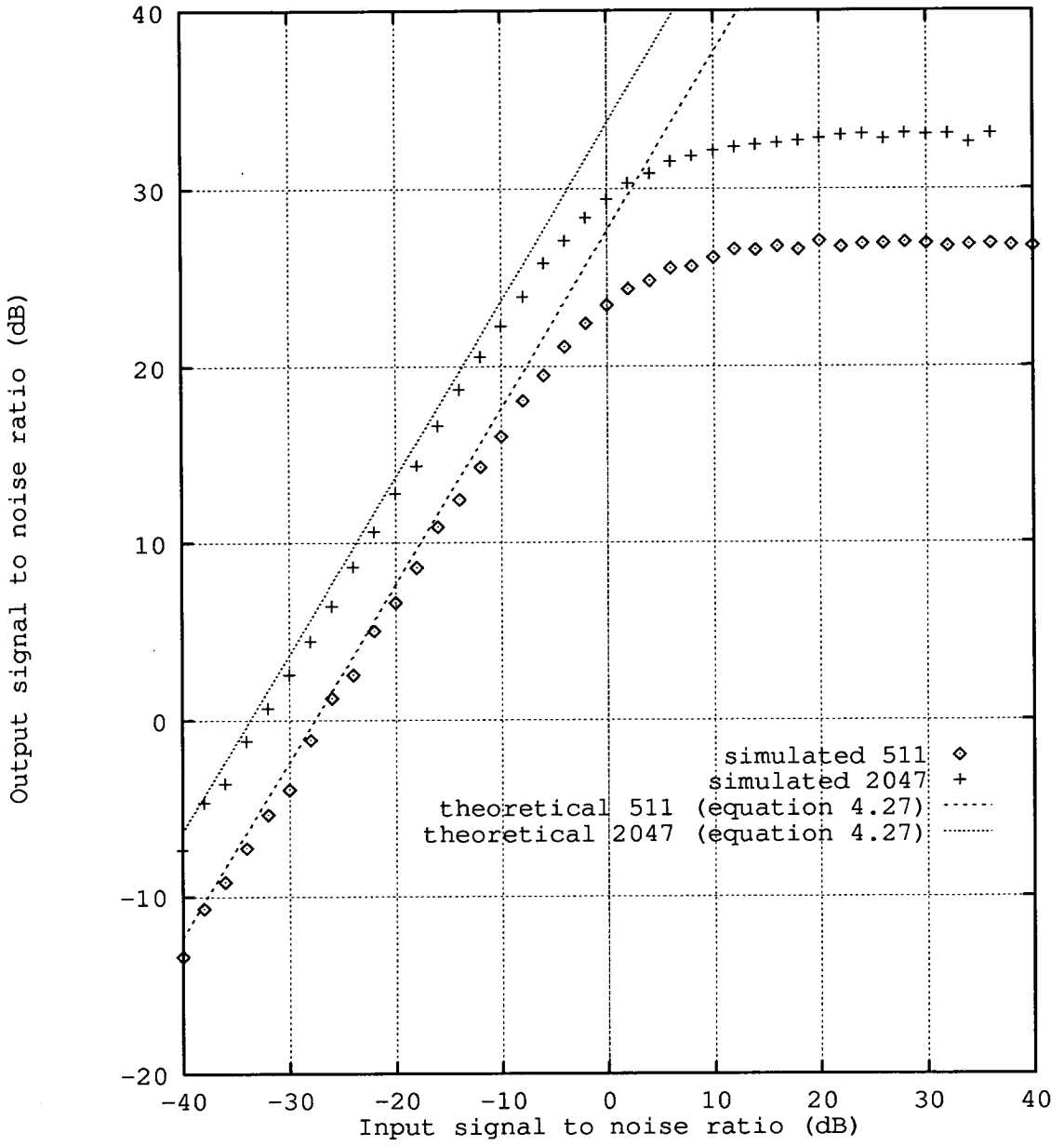


Fig. 4.7: Simulation results for the eight level DMF in Gaussian noise.

## CHAPTER 4: EXTENSION OF PREVIOUS WORK

number of noise distributions tried in the search for the worst case signal to noise ratio. The striped nature of the upper section of the graph is due to the finite number of  $w$  parameters tried. The point of interest however, is the largest worst case signal to noise ratio when the ratio of the two quantisation functions is 2. Looking at fig. 4.8, this would appear to give a worst case signal to noise ratio of around 0.5, or a loss of 3 dB over the equivalent analogue word matched filter. Searching back through the data used to generate fig. 4.8, we find a solution:-

$$\left(\frac{S}{N}\right) = 0.50K/\sigma^2 \quad (4.32)$$

This performance is achieved when:-

$$w_1 = 0.90\sigma$$

$$w_2 = 0.74\sigma \quad (4.33)$$

The worst case noise distribution is:-

$$0 \text{ with probability } 0.61$$

$$\pm 1.01 \text{ each with probability } 0.13$$

$$\pm 2.38 \text{ each with probability } 0.065 \quad (4.34)$$

Quantisation is done using two uniformly distributed random variables,  $\beta_1$  and  $\beta_2$  such that:-

$$-0.90\sigma < \beta_1 < 0.90\sigma$$

$$0.90\sigma < \beta_2 < 2.38\sigma \quad (4.35)$$

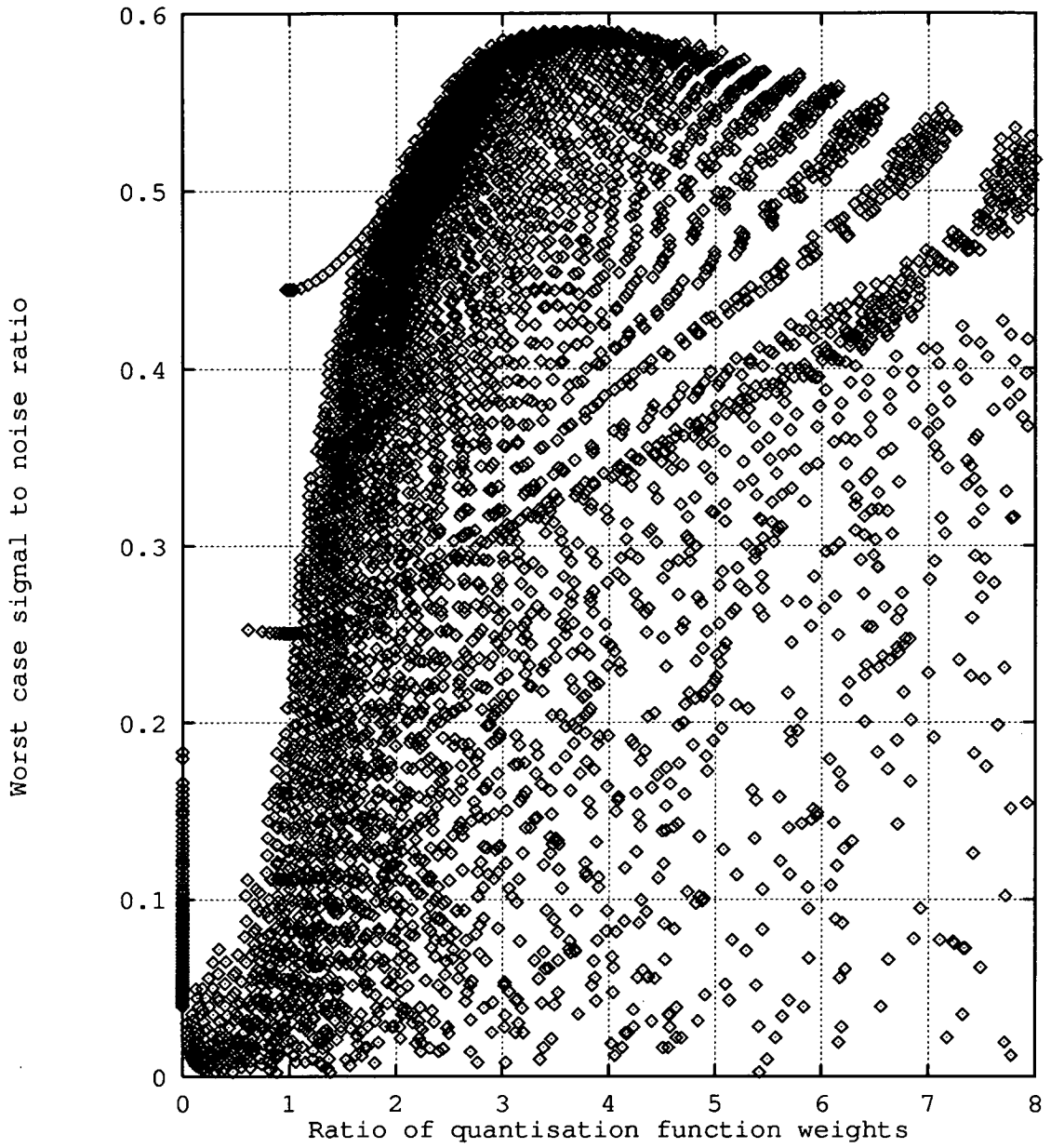


Fig. 4.8: Optimisation of a four level DMF with linear integer quantisation weights.

## CHAPTER 4: EXTENSION OF PREVIOUS WORK

A received sample is quantised such that:-

$$\text{amplitude} = 1.0; |r| \leq \beta/2$$

$$\text{amplitude} = 2.0; |r| > \beta/2$$

$$\text{polarity} = \text{sign}(r - \beta/2) \quad (4.36)$$

Simulation results for the four-level case with linear integer quantisation results are shown in fig. 4.9. Simulation conditions are again the same as those used for fig. 3.6. Good correlation with the theory in equation 4.27 is observed. Using the same method as for the non-integer quantisation case, the saturation level can be predicted. In this case it is:-

$$\left(\frac{S}{N}\right) = \frac{(1.37K)^2}{2.11K} \quad (4.37)$$

Graphs of this equation are shown in fig 4.9.

### 4.3. Improvements to Cahn's DMF

Two minor alterations can be made to Cahn's DMF, which appear to improve its performance.

The first is to replace the random sequence used as the reference for the matched filter with an m-sequence. M-sequences of length  $K$  have the property that their autocorrelation functions have a peak of height  $K$  and a non peak height (often referred to as peak side-lobe level) of  $-1$ . They are generated by using shift registers with some of

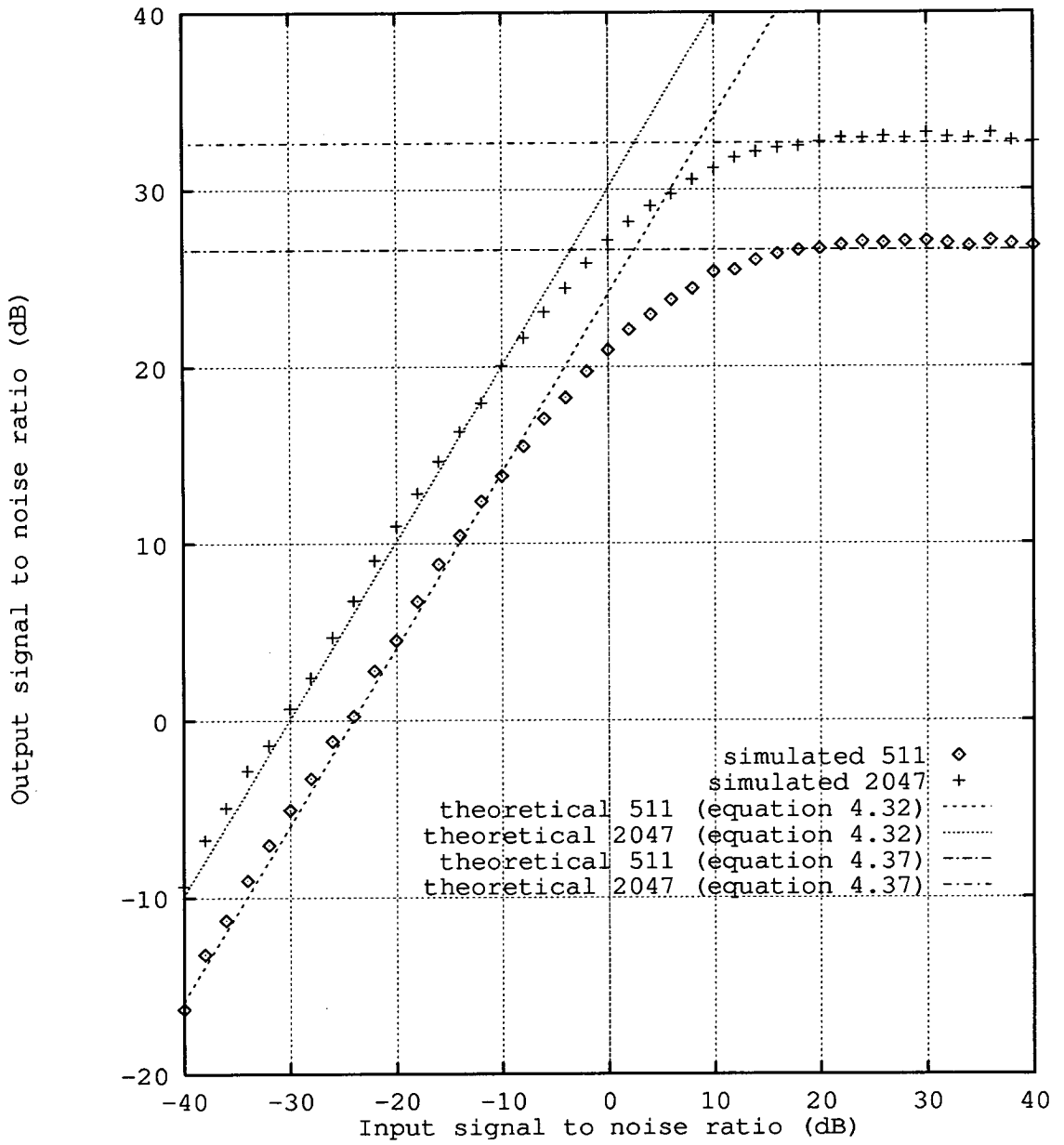


Fig. 4.9: Simulation results for the four level DMF with linear integer quantisation weights.

the taps EX-ORed together and fed back to the shift register input. Lists of the taps and/or methods of calculating the taps can be found in [14, 43]. However, these lists appear to contain a few errors. Lists of tap numbers which produce m-sequences of various lengths are contained in appendix A. The lists in appendix A are all the m-sequences for a particular number of taps and they have all been computer checked for the m-sequence autocorrelation properties. In a DMF at high values of input signal to noise level, it is the autocorrelation side lobes which define the noise level. Thus, if an m-sequence is used, the saturation level of the DMF is increased slightly. It is debatable whether or not this improvement is worthwhile on its own. At such high output signal to noise ratios, the data transfer may be considered perfect anyway.

The second improvement that may be made concerns the dither functions used in the quantisation process (the  $\beta$ 's). Instead of choosing them randomly using computer generated random numbers, we can use a function which is periodic with period K and whose amplitude is uniformly distributed. This improvement was first suggested by Turin [44], who suggested ramp functions. Another function with this property is the digital to analogue conversion of the taps in an m-sequence generator. This function is of course useful if the first improvement is already incorporated! It is important to note that when using these modified dither functions for multi-level systems, the different  $\beta$ 's must vary independently. If this condition is not observed, strange and inconsistent results are obtained. Examples of combinations which exhibit these undesirable properties are two ramp functions (amplitudes are linearly related) and two analogue to digital conversions of m-sequences (successive samples tend to both divide by two).

It is worth noting that neither of these two changes violates any of Cahn's assumptions, therefore the calculations of the guaranteed minimum performance are still valid. Simulation results of these improvements are shown in fig. 4.10. All the results shown in fig. 4.10 are for a 511 tap DMF. The points labelled "original" are for Cahn's original DMF, as shown in fig 3.6. The points labelled "modified dithers" are for Cahn's



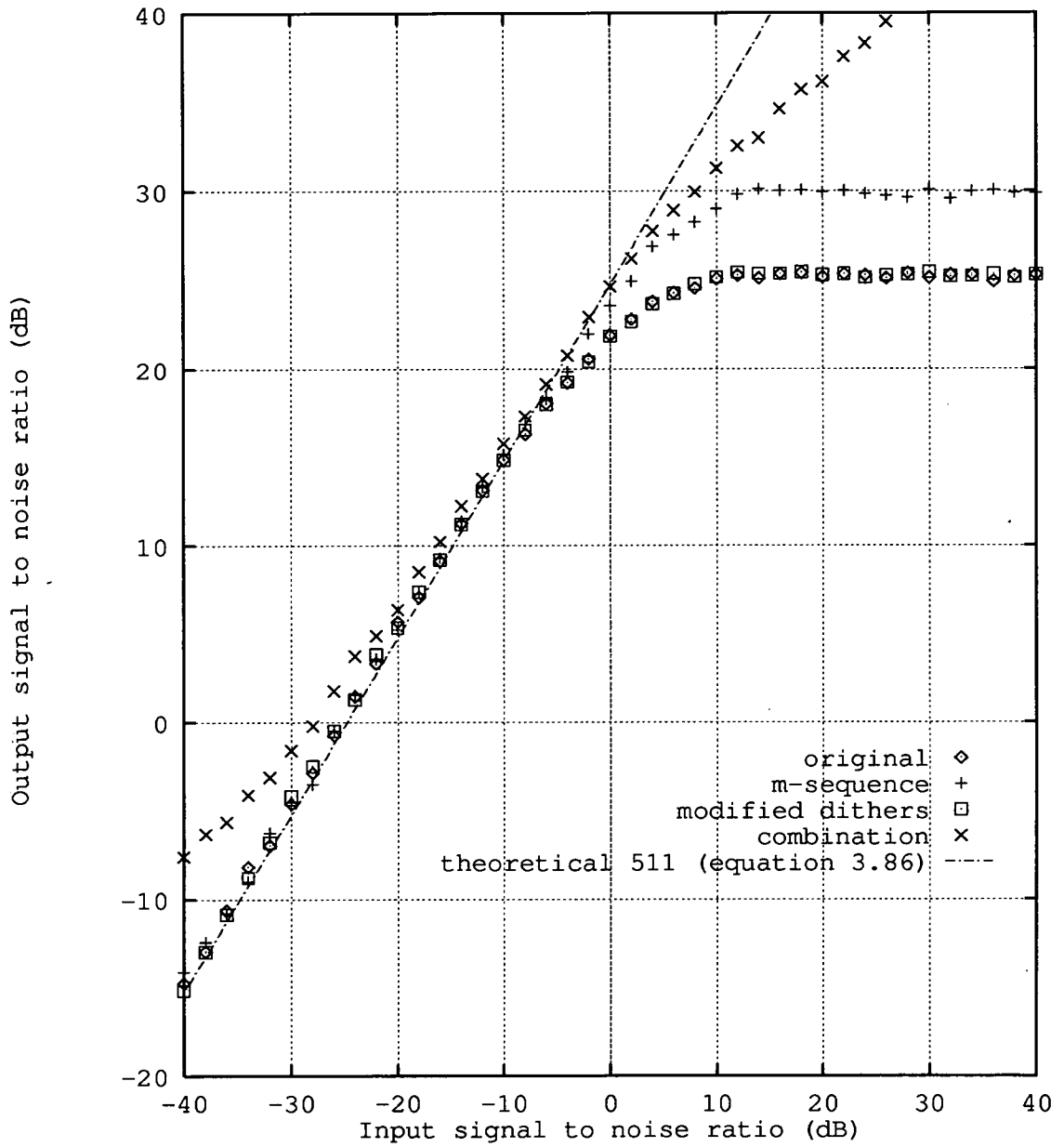


Fig. 4.10: Simulation results for the improvements to Cahn's DMF.

## CHAPTER 4: EXTENSION OF PREVIOUS WORK

DMF with the random dither functions replaced by a ramp function ( $\beta_1$ ) and an analogue to digital conversion of an m-sequence ( $\beta_2$ ). The points labelled "m-sequence" are for Cahn's DMF with the random matched filter code replaced by an m-sequence. Finally, the points labelled "combination" are for Cahn's DMF with modified dither functions and an m-sequence matched filter code. The calculated guaranteed minimum performance is also shown in fig. 4.10.

From fig. 4.10, we can see that just using the modified dither functions provides little if any improvement over the original DMF. Changing the matched filter code to an m-sequence provides a large increase in performance at high input signal to noise ratios. However, it makes little or no difference in the critical area for communications (0-10dB output signal to noise ratio). Combining the two improvements provides a general improvement in performance on all areas of the graph. This improvement is of the order of 1 dB over the critical area. It is worth noting that the improvements shown here are artificially enhanced by the fact that the simulations used here apply no modulation to the signal. When an m-sequence is modulated, ie inverted for transmission of a digital 0, its useful autocorrelation properties are lost on each transition. Since a transition occurs 50% of the time on average for a binary data sequence with equal probabilities of 1 and 0, it is reasonable to expect the performance improvement obtained from using the combination of modified dithers and the m-sequence spreading code to be 0.5 dB (half the improvement factor).

### 4.4. Chapter summary

In this chapter we have tried to extend Cahn's DMF to larger numbers of quantisation levels, but with limited success. However, we have found suggestions which

#### *CHAPTER 4: EXTENSION OF PREVIOUS WORK*

give a worthwhile improvement in performance with little penalty in terms of implementation complexity. We have also devised a method which allows us to implement Cahn's DMF on standard devices with linear binary quantisation levels. The most practical device we have developed is a four-level DMF with linear quantisation weights, modified dithers and an m-sequence matched filter code.

---

## 5. Impulsive noise and the clip to zero algorithm

---

In this chapter we look at the type of noise to which we expect the radio alarm channel to be subjected and derive a method of trying to combat the adverse effect it has on system performance.

### 5.1. Introduction to impulsive noise

Impulsive noise can be defined as interference which has significantly higher probability of large amplitudes than Gaussian noise with the same power. This noise appears in many communications environments and has many sources. The noise on telephone and computer networks is often impulsive because of switching spikes [45]. However, we are interested in the impulsive noise on radio channels. Impulsive noise is found in the LF, MF and HF radio bands. Sources are both man-made and natural. Man-made sources include discharges from car ignition systems, fluorescent lighting, motors and high power electrical equipment. Natural sources include lightning and other atmospheric conditions. Because of the nature of these sources and the changing properties of the HF radio channel, the impulsive noise found in the HF channels in which we are interested can be assumed to be time varying and site dependent. Thus the designer of a system operating in the HF band does not know a-priori the distribution of

the noise to which the system will be subjected.

## 5.2. Impulsive noise models

Many models have been proposed and used for impulsive noise ([46-51] for example). These vary from the extremely simple and easy to use, which have limited realism, to the physically based model proposed by Middleton [50, 51]. Middleton's model shows extremely good correlation with measured results including results taken at carrier frequencies close to the bands assigned to alarm schemes. This is despite some reservations about the measured results being dependent on the receiver used to make the measurements, expressed in [52]. We shall use the  $\varepsilon$ -mixture approximation to Middleton's model as proposed by Vastola [53]. This model is used because it is a close approximation to Middleton's model and is therefore thought to be a good model of atmospheric radio noise. The  $\varepsilon$ -mixture distribution is, however, easier to analyse theoretically and enables us to calculate theoretical results for some of the devices we shall look at later in this chapter. The probability density function (PDF) of the  $\varepsilon$ -mixture model,  $f_\varepsilon(x)$ , is a sum of two Gaussian PDFs  $f_0(x)$  and  $f_1(x)$  such that:-

$$f_\varepsilon(x) = (1 - \varepsilon)f_0(x) + \varepsilon f_1(x) \quad (5.1)$$

The ratio  $\gamma^2$  is given by  $\sigma_1^2(x)/\sigma_0^2(x)$ . The total power in the distribution is given by:-

$$\sigma^2 = (1 - \varepsilon)\sigma_0^2 + \varepsilon\sigma_1^2 \quad (5.2)$$

Thus an  $\varepsilon$ -mixture noise distribution is totally specified by  $\varepsilon$ ,  $\gamma^2$  and  $\sigma^2$ .

In the simulations we shall use two of the  $\varepsilon$ -mixture distributions shown in ([53], fig 4). The first case is  $\varepsilon = 0.259$  and  $\gamma^2 = 5715$ . This corresponds to  $A = 0.35$  and

$\Gamma' = 0.0005$  in Middleton's model. These parameters are shown to be an accurate model of the interference found in a 200 kHz channel with a bandwidth of 6 KHz. The dominant interferer is thought to be a nearby power line (see [54] ). The second case is  $\varepsilon = 0.0001$  and  $\gamma^2 = 201$ . These correspond to  $A = 0.0001$  and  $\Gamma' = 50$  in Middleton's model. These parameters are shown to be an accurate model of the interference found in a 1 MHz channel with a bandwidth of 1.2 kHz. The dominant interferer is thought to be ore-crushing machinery (see [55] ).

We shall also use a third  $\varepsilon$ -mixture distribution. The graph shown in ( [50], fig. 2.4) is for a channel close to the 27 MHz channel reserved for use in alarm schemes. Moreover, the dominant interferer is thought to be traffic 16 m from the measurement site. It is likely in a city environment that the receiver will be 16 m or closer to traffic. The data for this distribution is from [56] and it is interesting to note some of the characteristics observed. Most of the noise appears to radiate from a few vehicles, and therefore the distribution is highly time variant. The overall amount of noise is dependent on the level of traffic. Middleton used his full class B model for this interference, but we will simplify this by using his technique described in [51] to estimate the class A parameters as an approximation for this distribution. The result of doing this is that  $A = 0.01$  and  $\Gamma' = 0.25$ . These numbers can be converted to the  $\varepsilon$ -mixture model using the equations (see [53] ):-

$$\gamma^2 = 1 + \frac{1}{A\Gamma'} \quad (5.3)$$

and

$$\varepsilon = \frac{A}{1 + A} \quad (5.4)$$

Thus the  $\varepsilon$ -mixture parameters for the third case are  $\varepsilon = 0.0099$  and  $\gamma^2 = 401$ . Probability density functions for the three cases are shown in fig. 5.1. However, these

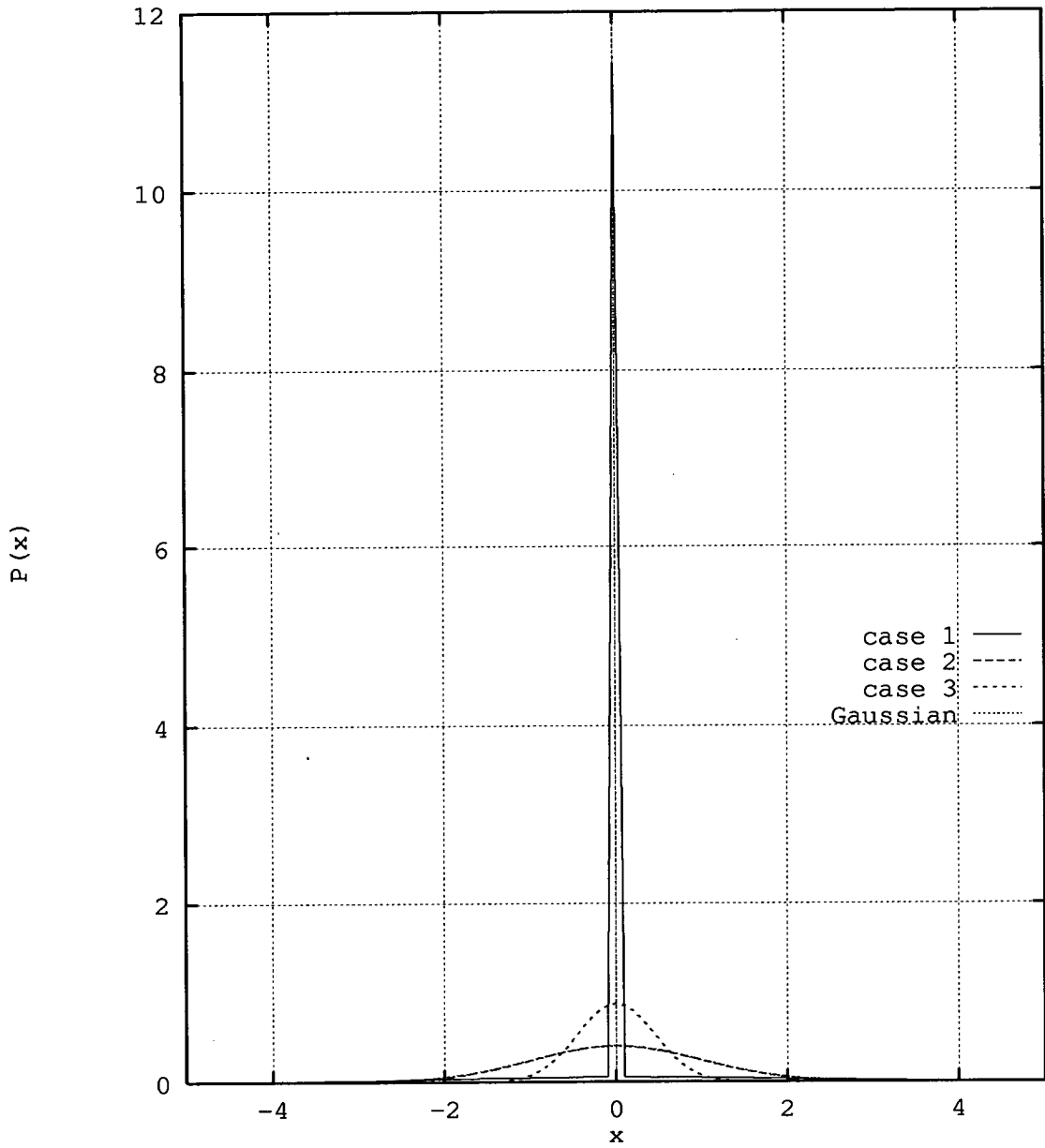


Fig. 5.1: Probability density functions for the three impulsive noise cases.

The Gaussian case and impulsive case 2 are indistinguishable.

diagrams are not particularly revealing, with much of the data in them at extremely low levels. When we come to look at clipping of signals later in this chapter, it is much more interesting to look at the envelope distribution for the impulsive noise cases, as in [53]. These graphs show amplitude against the probability of that amplitude being exceeded for a distribution. The envelope distributions for the three noise cases are shown in fig. 5.2. Envelope distributions are often shown with the x-axis plotted on Rayleigh graph paper. This is to emphasize the low y-axis values and show the Gaussian nature of some parts of the curve, which appear as a straight line when plotted in this manner. The only way to show that case 2 is non-Gaussian is by plotting in this manner (see [50] ).

In order to simulate systems operating in these impulsive interference environments, it is necessary to be able to generate samples from a random variable with the desired distribution. In a computer, the only random numbers available have a uniform distribution, thus we require a transform which takes uniformly distributed samples and turns them into samples with the required distribution. Unfortunately, there is no generalised method for doing this. In [39], a transformation is given for generating random samples with a Gaussian distribution. The method used for generating samples for the  $\varepsilon$ -mixture distribution is an approximation. We use the rejection method (see [39, 57] ), where the comparison function is a uniform distribution. We set  $p(x)$  in the uniform distribution to the maximum value of  $p(x)$  in the impulsive distributions. We set the range of the uniform distribution to  $[-W,+W]$ , where  $W$  is a large value beyond which the impulsive distribution has no significant probability. In the first two impulsive noise cases  $W$  was set to  $10\sigma$ . In the third case,  $W$  was set to  $100\sigma$  because fig. 5.2 shows that this distribution still has significant probability at  $10\sigma$  (20 dB above RMS value). It is worth noting that this method is both approximate and inefficient. The method is approximate because it ignores the content of the impulsive distribution below  $-W$  and above  $W$ . However,  $W$  has been set such that the impulsive distributions have no significant content outside the  $[-W,W]$  range and simulation results presented later in this



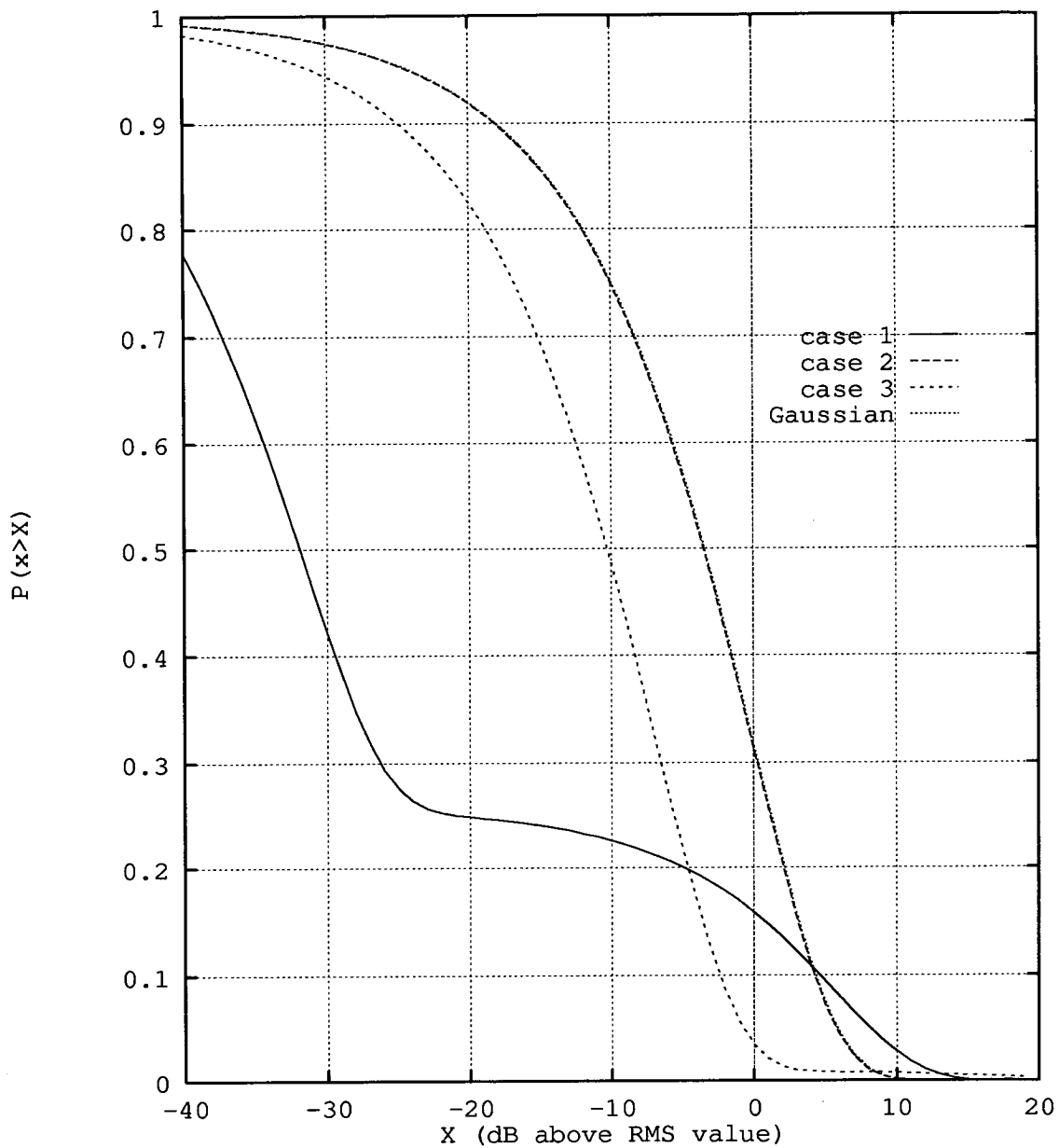


Fig. 5.2: Envelope distributions for the three impulsive noise cases. Again, the Gaussian case and impulsive case 2 are indistinguishable.

chapter show very good correlation with theoretical predictions. This method of generating impulsive noise samples is computationally very inefficient, because the rejection ratio is very high. Thus on average it takes many uniform samples to obtain one impulsive sample. Time series obtained using this method are shown in fig. 5.3. These time series are normalised, they have zero mean and variance one.

### 5.3. The effect of impulsive noise on conventional systems

The effect that impulsive noise has on conventional digital communications has been studied extensively, especially by Jain and Gupta (see [58-68] for example). It is shown that the performance of a conventional digital communication system can be severely degraded by impulsive noise. This can be illustrated by looking at the performance of a conventional system operating with assumed perfect linear demodulation and threshold detection as shown in fig. 5.4. Fig. 5.4 shows the BER for the  $\epsilon$ -mixture noise cases plotted against the receiver output signal to noise ratio. The BER for  $\epsilon$ -mixture noise is given by:-

$$BER = 1 - \int_{-\infty}^{\sqrt{\frac{s}{N}}} f_{\epsilon}(x) \quad (5.5)$$

From fig. 5.4, we can see that for better than extremely modest BERs, the signal to noise ratio required is vastly increased in impulsive noise when compared with Gaussian noise. What is potentially worse is that this degradation in performance is dependent on the exact distribution of the noise, as well as the signal to noise ratio at the receiver. The exact distribution of the impulsive noise in an HF radio channel is not known to the designer, therefore it is not possible to specify the system performance even if the

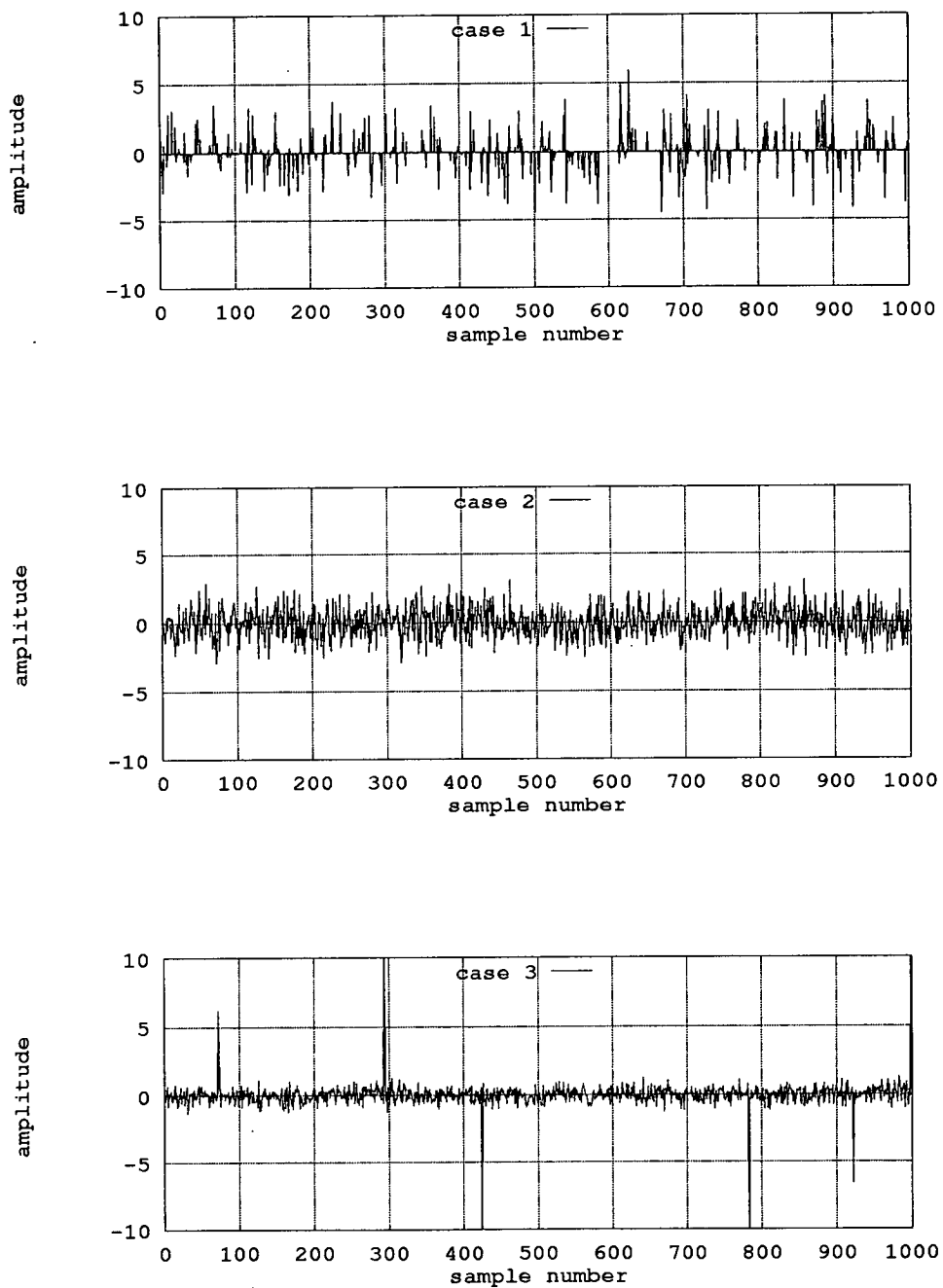


Fig. 5.3: Normalised time series for the impulsive noise distributions.

received signal to noise ratio can be estimated. The other point worthy of note from this work is that coherent systems are much more resistant to impulsive noise than non-coherent systems.

#### 5.4. The effect of impulsive noise on direct sequence spread spectrum systems

In this section we look at the performance of the digital matched filter in a DSSS system. We do not consider any non-linearities used to demodulate the signal, such as phase-locked loops. These will be discussed in the next chapter. The first matched filter we shall look at is the theoretical case with analogue word storage. We can use the central limit theorem [69, 70] to state that providing the matched filter has enough taps, the total noise output from the matched filter with N taps will be N times the average noise power in each input chip with a Gaussian distribution, regardless of the input noise distribution [71]. Thus, the performance of a DSSS system with matched filter demodulation should be unaffected by impulsive noise distributions, provided there are enough taps in the matched filter. It is difficult to define "enough taps", the number required depends on the ordinal impulsive distribution. However, the discussion in [69] indicates that it is relatively few. If we assume that the output of the matched filter has a Gaussian distribution, and that we can successfully find the correlation peaks, then the BER is given by:-

$$BER = 1 - erf\left(\frac{S}{N_{output}}\right) \quad (5.6)$$

Thus, if the above conditions are met, then we can predict the BER from the output signal to noise ratio of the matched filter using the curve in fig. 5.5. Also shown are BER simulations for the three impulsive noise cases and Gaussian noise. These results were obtained using a 511 tap matched filter with analogue word storage. Each BER is the

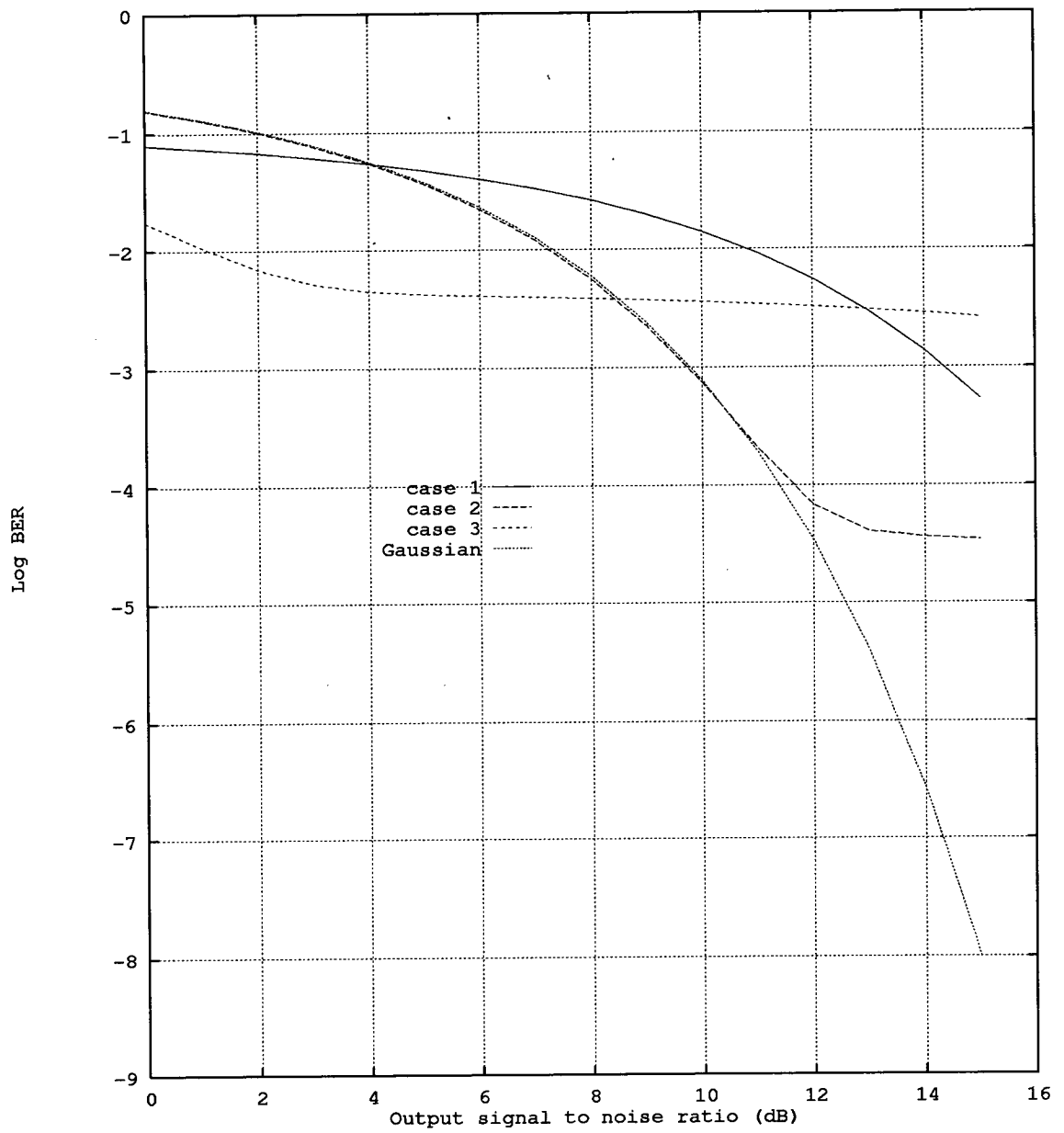


Fig. 5.4: Theoretical BER for the impulsive noise cases assuming perfect linear demodulation.

result of 25000 trials. This graph shows that the performance of the 511 tap matched filter is largely unaffected by the impulsive noise distributions. Thus, we shall assume that the output signal to noise ratio defines the BER performance of the matched filter according to equation 5.5.

It is also worth noting that the BER performance at high output signal to noise ratios of the impulsive case 1 and case 3 is already better than that obtained in a conventional system under similar circumstances (see fig 5.3).

### **5.5. Improving the performance of direct sequence spread spectrum systems in impulsive noise**

In the previous section, we saw that the matched filter in a DSSS receiver is largely unaffected by the input distribution. There are however indications that better performance can be achieved. In [72-74] there are results indicating that a hard limiting DMF receiver performs significantly better than a linear (analogue word) DMF. These results are repeated if we simulate one of the limited precision matched filters from the previous chapter in impulsive noise. Results obtained from doing this for Cahn's four level DMF with the two suggested improvements (see previous chapter) are shown in fig. 5.6. In this simulation, the DMF has 511 taps. Each simulation result is the average of 400 separate trials with the power measuring device assumed to be perfectly accurate. We can see that for the impulsive case 3, the performance exceeds the theoretical performance of an analogue word 511 tap DMF (processing gain 27.1 dB, shown on fig. 5.6 as "analogue theoretical"). This is due to the clipping of high amplitude samples during the quantisation process, which is equivalent to saturating an analogue to digital converter (ADC). Clipping a high amplitude sample destroys any signal information it

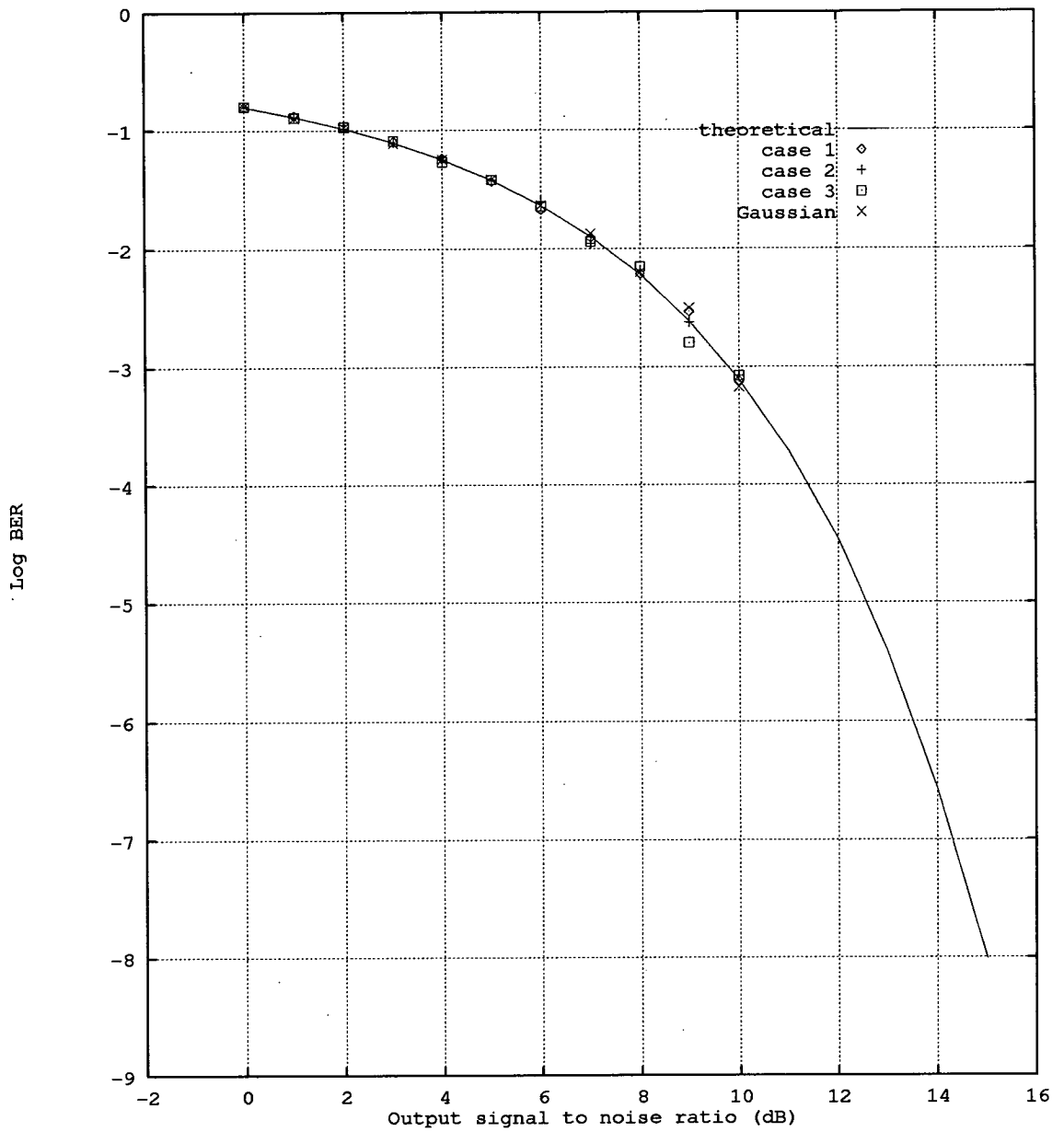


Fig. 5.5: Theoretical BER assuming Gaussian statistics at the DMF output and simulation results showing the BER for the three impulsive noise cases and Gaussian noise.

may have contained, but also reduces the contribution it makes to the noise at the output of the DMF. If, by clipping at a certain amplitude, the contribution to the noise is reduced by more than the loss in signal information on average, then the signal to noise ratio at the output will be enhanced. The logical extreme of this is to set to zero any signals whose amplitudes exceed a threshold  $a$ . We have called this process the clip to zero algorithm.

### 5.5.1. The clip to zero algorithm for analogue matched filters in Gaussian noise

We will consider the clipping of analogue matched filters in Gaussian noise for two reasons. Firstly, the  $\varepsilon$ -mixture model uses the sum of two Gaussian distributions to simulate impulsive noise. Thus if we can derive equations for the performance of a matched filter in Gaussian noise, we can calculate the performance in  $\varepsilon$ -mixture impulsive noise from them. Secondly, Gaussian noise is a special case of the  $\varepsilon$ -mixture distribution. It is the  $\varepsilon$ -mixture distribution that has the worst optimal performance.

The clip to zero algorithm sets to zero all signals whose amplitudes are greater than the threshold  $a = C\sigma$ , where  $C$  is the clipping factor as shown in fig. 5.7. If we normalise the signal amplitude to 1 and the noise power is  $\sigma^2$ , then the PDF at the input to the system is:-

$$f_g(x) = \frac{1}{2} \frac{1}{\sqrt{2\pi\sigma^2}} \exp\left\{-\frac{(x-1)^2}{2\sigma^2}\right\} + \frac{1}{2} \frac{1}{\sqrt{2\pi\sigma^2}} \exp\left\{-\frac{(x+1)^2}{2\sigma^2}\right\} \quad -a < x < a \quad (5.7)$$

$$= 0 \quad \text{elsewhere} \quad (5.8)$$

We shall use the output signal to noise ratio from the matched filter as the performance measure. This is defined as:-



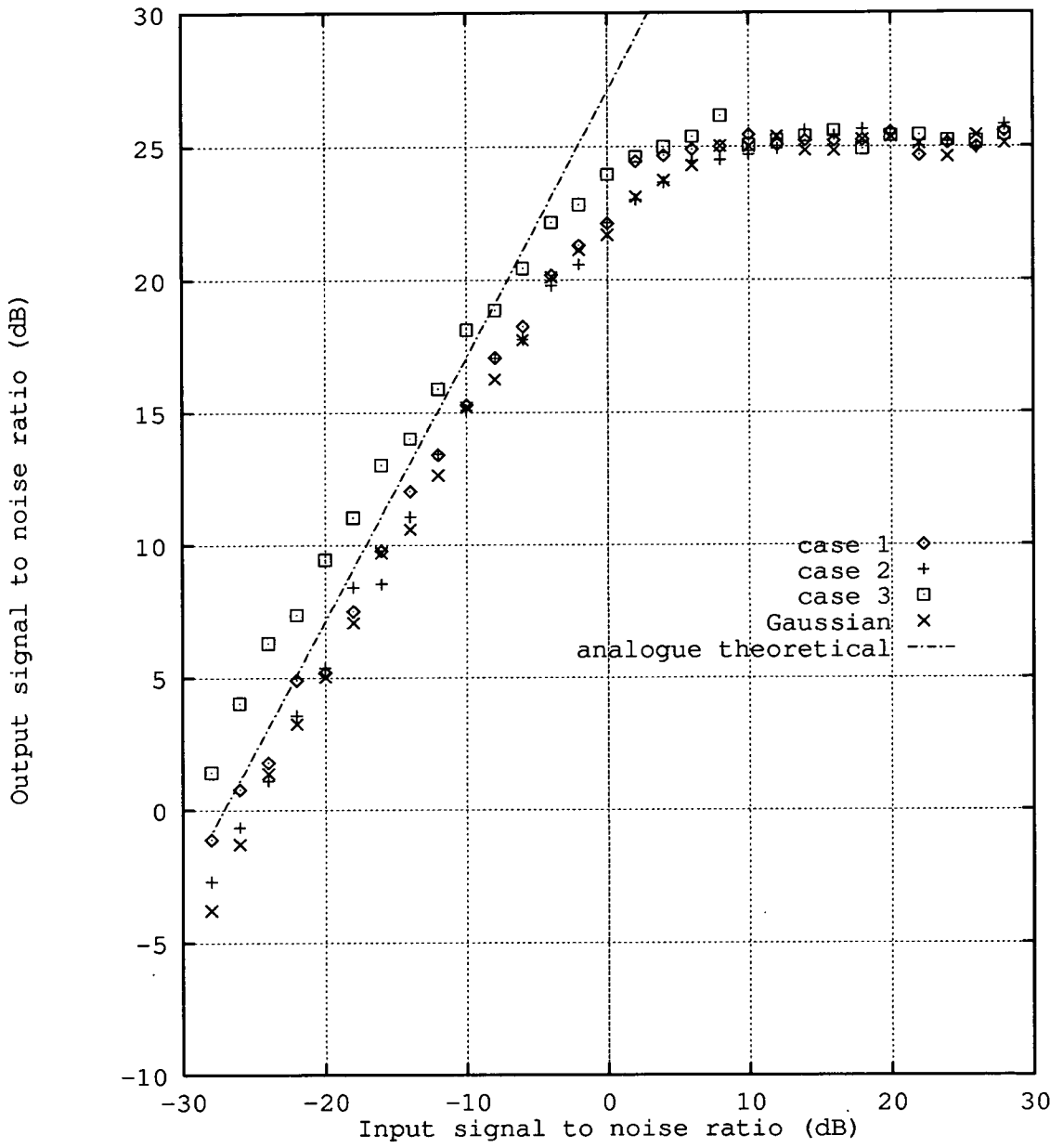


Fig. 5.6: Simulation of Cahn's four level DMF with the two improvements in impulsive noise.

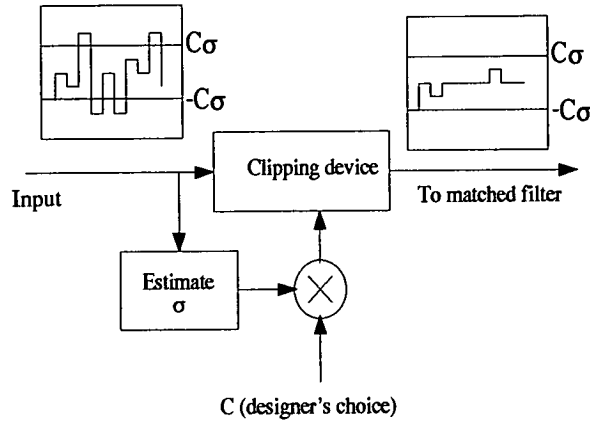


Fig. 5.7: Block diagram of the clip to zero algorithm.

$$\frac{S}{N_{out}} (dB) = 20 \log_{10} \left( \frac{\text{average correlation peak amplitude}}{\text{rms voltage with an uncorrelated input signal}} \right) \quad (5.9)$$

The average correlation peak amplitude is given by:-

$$E \left\{ \begin{array}{l} \frac{1}{\sqrt{2\pi\sigma^2}} \exp \left\{ -\frac{(x-1)^2}{2\sigma^2} \right\} \quad -a < x < a \\ 0 \quad \text{elsewhere} \end{array} \right\} \times \text{processing gain} \quad (5.10)$$

$E\{f(x)\}$  denotes the expected value of  $f(x)$ .

$$E \left\{ \begin{array}{l} \frac{1}{\sqrt{2\pi\sigma^2}} \exp \left\{ -\frac{(x-1)^2}{2\sigma^2} \right\} \quad -a < x < a \\ 0 \quad \text{elsewhere} \end{array} \right\} = \frac{1}{\sqrt{2\pi\sigma^2}} \int_{-a}^a x \exp \left\{ -\frac{(x-1)^2}{2\sigma^2} \right\} dx \quad (5.11)$$

$$\text{Substitute } t = \frac{x-1}{\sigma}, \quad x = (\sigma t + 1), \quad \frac{dx}{dt} = \sigma, \quad dx = \sigma dt$$

$$\begin{aligned}
 \frac{1}{\sqrt{2\pi\sigma^2}} \int_{-a}^a x \exp\left\{-\frac{(x-1)^2}{2\sigma^2}\right\} dx &= \frac{1}{\sqrt{2\pi}} \int_{\frac{-a-1}{\sigma}}^{\frac{a-1}{\sigma}} (\sigma t + 1) \exp\left\{\frac{-t^2}{2}\right\} dt \\
 &= \frac{\sigma}{\sqrt{2\pi}} \int_{\frac{-a-1}{\sigma}}^{\frac{a-1}{\sigma}} t \exp\left\{\frac{-t^2}{2}\right\} dt + \frac{1}{\sqrt{2\pi}} \int_{\frac{-a-1}{\sigma}}^{\frac{a-1}{\sigma}} \exp\left\{\frac{-t^2}{2}\right\} dt \\
 &= \frac{\sigma}{\sqrt{2\pi}} \left[ -\exp\left\{\frac{-t^2}{2}\right\} \right]_{\frac{-a-1}{\sigma}}^{\frac{a-1}{\sigma}} + \operatorname{erf}\left\{\frac{a-1}{\sigma}\right\} - \operatorname{erf}\left\{\frac{-a-1}{\sigma}\right\} \\
 &= \frac{\sigma}{\sqrt{2\pi}} \left( \exp\left\{\frac{-\left(\frac{-a-1}{\sigma}\right)^2}{2}\right\} - \exp\left\{\frac{-\left(\frac{a-1}{\sigma}\right)^2}{2}\right\} \right) + \operatorname{erf}\left\{\frac{a-1}{\sigma}\right\} - \operatorname{erf}\left\{\frac{-a-1}{\sigma}\right\} \quad (5.12)
 \end{aligned}$$

This result can also be inferred from formulae in [75]. The RMS voltage with an uncorrelated input signal is given by:-

$$\sqrt{\operatorname{Var}\{f_g(x)\} \times \text{processing gain}} \quad (5.13)$$

This means that the signal to noise ratio at the output This this is the standard deviation of the matched filter output, formed by multiplying the average variance of a single tap in the dmf by the number of taps in the dmf (the processing gain) and taking the square root.

Note that the expected value of the correlation peak (equation 5.10) is directly proportional to the processing gain and the RMS voltage with an uncorrelated signal (equation 5.13) is proportional to the square root of the processing gain. Thus the power signal to noise ratio is directly proportional to the processing gain (number of taps in the DMF) if the input noise power is fixed. However, attempting to increase the signal to noise ratio by having a larger processing gain will not result in any improvement in performance if this results in a corresponding increase in input noise power, for example if the transmission bandwidth is increased.

$$\text{Var}\left\{f_g(x)\right\} = \frac{1}{\sqrt{2\pi\sigma^2}} \int_{-a}^a x^2 \exp\left\{-\frac{(x-1)^2}{2\sigma^2}\right\} dx \quad (5.14)$$

Substitute  $t = \frac{x-1}{\sigma}$ ,  $x = (\sigma t + 1)$ ,  $\frac{dx}{dt} = \sigma$ ,  $dx = \sigma dt$

$$\frac{1}{\sqrt{2\pi\sigma^2}} \int_{-a}^a x^2 \exp\left\{-\frac{(x-1)^2}{2\sigma^2}\right\} dx = \frac{1}{\sqrt{2\pi}} \int_{\frac{-a-1}{\sigma}}^{\frac{a-1}{\sigma}} (\sigma t + 1)^2 \exp\left\{\frac{-t^2}{2}\right\} dt$$

$$= \frac{1}{\sqrt{2\pi}} \int_{\frac{-a-1}{\sigma}}^{\frac{a-1}{\sigma}} (\sigma t)^2 \exp\left\{\frac{-t^2}{2}\right\} + 2\sigma t \exp\left\{\frac{-t^2}{2}\right\} + \exp\left\{\frac{-t^2}{2}\right\} dt$$

$$= \frac{\sigma^2}{\sqrt{2\pi}} \left[ -t \exp\left\{\frac{-t^2}{2}\right\} \right]_{\frac{-a-1}{\sigma}}^{\frac{a-1}{\sigma}} + \frac{\sigma^2}{\sqrt{2\pi}} \int_{\frac{-a-1}{\sigma}}^{\frac{a-1}{\sigma}} \exp\left\{\frac{-t^2}{2}\right\} dt + \frac{\sqrt{2}\sigma}{\sqrt{\pi}} \int_{\frac{-a-1}{\sigma}}^{\frac{a-1}{\sigma}} t \exp\left\{\frac{-t^2}{2}\right\} dt + \frac{1}{\sqrt{2\pi}} \int_{\frac{-a-1}{\sigma}}^{\frac{a-1}{\sigma}} \exp\left\{\frac{-t^2}{2}\right\} dt$$

$$= \frac{\sigma^2}{\sqrt{2\pi}} \left( -\left(\frac{a-1}{\sigma}\right) \exp\left\{\frac{-\left(\frac{a-1}{\sigma}\right)^2}{2}\right\} + \left(\frac{-a-1}{\sigma}\right) \exp\left\{\frac{-\left(\frac{-a-1}{\sigma}\right)^2}{2}\right\} \right) + \sigma^2 \left( \text{erf}\left\{\frac{a-1}{\sigma}\right\} - \text{erf}\left\{\frac{-a-1}{\sigma}\right\} \right)$$

$$+ \frac{\sigma\sqrt{2}}{\sqrt{\pi}} \left( -\exp\left\{\frac{-\left(\frac{a-1}{\sigma}\right)^2}{2}\right\} + \exp\left\{\frac{-\left(\frac{-a-1}{\sigma}\right)^2}{2}\right\} \right) + \text{erf}\left\{\frac{a-1}{\sigma}\right\} - \text{erf}\left\{\frac{-a-1}{\sigma}\right\} \quad (5.15)$$

If we substitute equations 5.11 and 5.14 into equation 5.8, we can obtain the loss in Gaussian noise performance due to clipping, given by:-

$$Loss (dB) = 10\log_{10}(\text{processing gain}) - \left( \frac{S}{N_{out}} (dB) - 10\log_{10}\left(\frac{1}{\sigma^2}\right) \right) \quad (5.16)$$

Note that if we make  $a = C\sigma$ , as in fig. 5.7, and  $a \gg 1$ , the loss is approximately independent of the input signal to noise ratio. In spread spectrum systems,  $\sigma$  is usually  $\gg 1$ , thus the loss will be independent of the input signal to noise ratio provided  $A$  is not  $\ll 1$ . Also, if  $a \gg 1$  and  $C \gg 1$ , then the loss tends to 0 dB.

Fig. 5.8 shows plots obtained from the above equation, along with some simulation results. The simulations are of a 511 tap DMF with analogue word storage. Each point is the average of 400 independent trials. Perfect peak extraction and noise power measurement is assumed. Fig. 5.8 shows that the performance of the filter deteriorates as  $C$  decreases, demonstrating that clipping to zero at any level degrades the performance of the matched filter in Gaussian noise. The simulation results bear out the theoretical predictions.

### 5.5.2. The clip to zero algorithm in $\epsilon$ -mixture noise

It is possible to derive the performance of the clip to zero algorithm in  $\epsilon$ -mixture noise from the Gaussian case. The average correlation peak amplitude is given by:-

$$\left( (1 - \epsilon)E \left\{ \frac{1}{\sqrt{2\pi\sigma_0^2}} \exp \left\{ -\frac{(x-1)^2}{2\sigma_0^2} \right\} \right\} + \epsilon E \left\{ \frac{1}{\sqrt{2\pi\sigma_1^2}} \exp \left\{ -\frac{(x-1)^2}{2\sigma_1^2} \right\} \right\} \right) \times \text{processing gain} \quad (5.17)$$

The expected values can be calculated from equation 5.11, with the appropriate substitution for  $\sigma$ . The RMS voltage with an uncorrelated input signal is given by:-

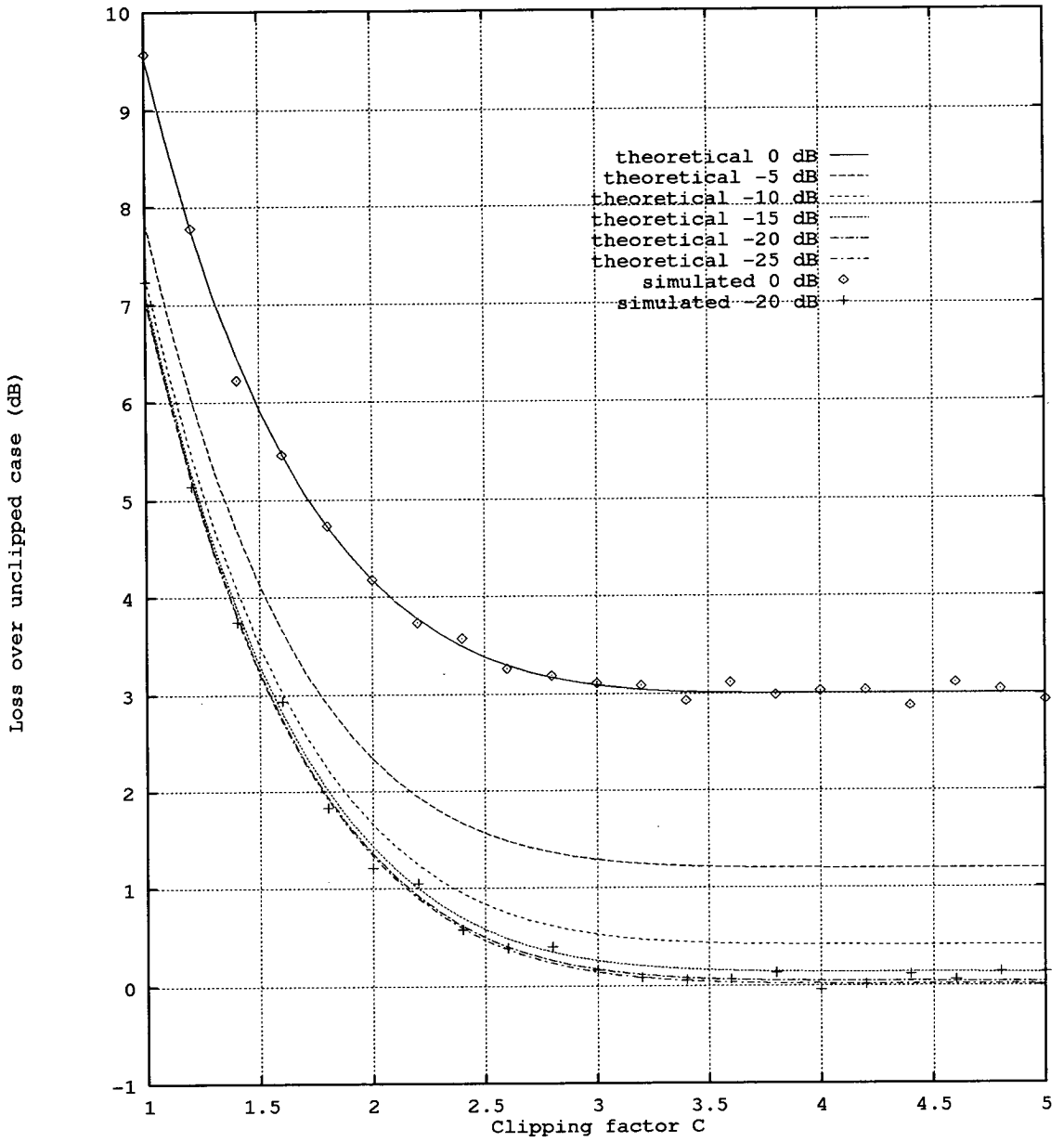


Fig. 5.8: Theoretical and simulation results for the clip to zero algorithm in Gaussian noise with input signal to noise ratio in the range 0 to -25 dB.

$$\sqrt{((1 - \epsilon)(\text{Var}\{f_0(x)\}) + \epsilon(\text{Var}\{f_1(x)\}))} \times \text{processing gain} \quad (5.18)$$

The variances can be calculated using equation 5.14, again with the appropriate substitutions for  $\sigma$ . Thus, substituting equations 5.16 and 5.17 into equation 5.8, we can obtain the output signal to noise from the matched filter in  $\epsilon$ -mixture noise.

Theoretical and simulation results are shown in fig. 5.9 and fig. 5.10. Simulation conditions are similar to those for the Gaussian case. Figs. 5.9 and 5.10 show performance results (expressed as a loss over the unclipped case) for the three  $\epsilon$ -mixture distributions. Fig. 5.9 shows the performance results for varying input signal to noise ratio clipping at  $C = 1.85$ , chosen to give a loss of approximately 2 dB at -10 dB input signal to noise ratio for the Gaussian noise case (see fig. 5.8). In fig. 5.10, the input signal to noise ratio was set to -15 dB, and the clipping factor  $C$  varied. This graph shows that large gains can be obtained if these impulsive distributions are clipped at the appropriate points.

### 5.5.3. Using the clip to zero algorithm

There are various methods of employing the clip to zero algorithm. The first is to set a fixed value for the clipping factor  $C$ . The worst performance this fixed value will produce is its performance in Gaussian noise. For example, if it is possible to sacrifice 2 dB of performance in Gaussian noise at low input signal to noise ratios, then  $C$  could be set to about 1.85 (see fig. 5.8). In return for this loss in Gaussian noise performance, a gain of approximately 5 dB in the case 1 impulsive noise and 6 dB in the case 3 impulsive noise (see fig. 5.10) would be obtained. In absolute level terms, one would expect the impulsive noise to contain more power than the Gaussian noise, because the

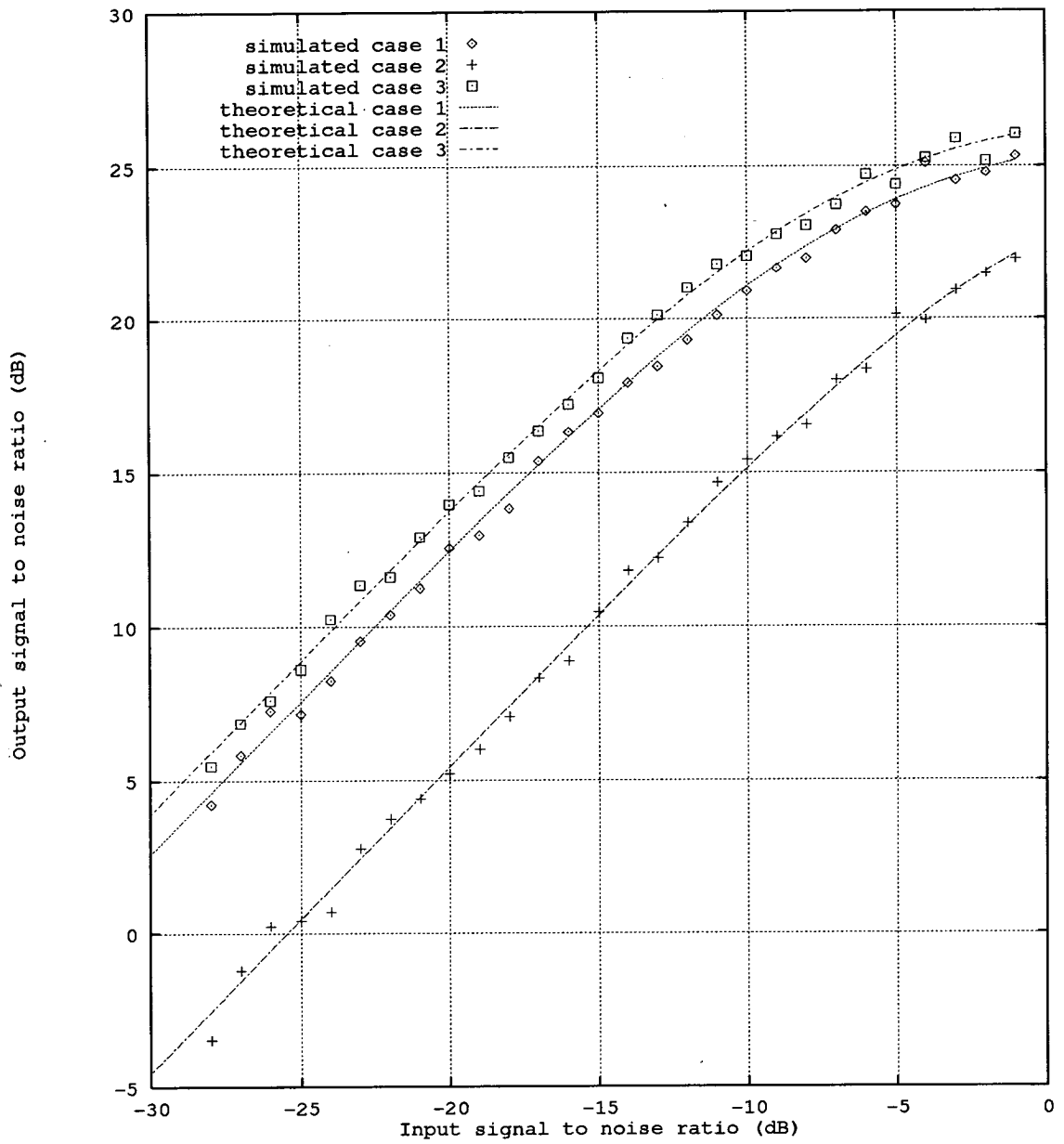


Fig. 5.9: Theoretical and simulation results for the clip to zero algorithm in the three impulsive noise cases (varying input signal to noise ratio).



impulsive noise can be thought of as the Gaussian noise floor plus a separate interference source. Therefore, this trade-off may help to average out performance, or help to build in a certain amount of immunity to impulsive noise.

The second method of employing the clip to zero algorithm is to apply adaptive clipping. By assuming local stationarity, an estimate of its  $\varepsilon$ -mixture statistics can be made using the methods described in [51]. The optimal clipping point can be calculated and applied. This method could produce significantly better results than the first method, for example the 13 dB gain in the case 3 at  $C = 0.4$  in fig. 5.10. However, this method has several drawbacks. It is much more computationally intense than the first method. In the alarm system case, it would take a considerable length of time to obtain enough samples to get a good estimate of the noise distribution. In this time, the distribution is certainly not stationary, see the example of traffic in [56]. Some impulsive noise distributions are not strictly  $\varepsilon$ -mixture distributions. These breaches in the assumptions will produce unpredictable results.

### **5.6. Combining guaranteed minimum performance digital matched filters with the clip to zero algorithm**

We can connect the clip to zero processor shown in fig. 5.7 in front of one of the limited precision DMFs discussed in chapters 3 and 4 as shown in fig. 5.11.

The overall performance of this new system has a guaranteed minimum performance of the original limited precision DMF plus the improvement from the clip to zero algorithm. The clip to zero algorithm has altered the noise distribution, but the guaranteed minimum performance of the DMF still applies.

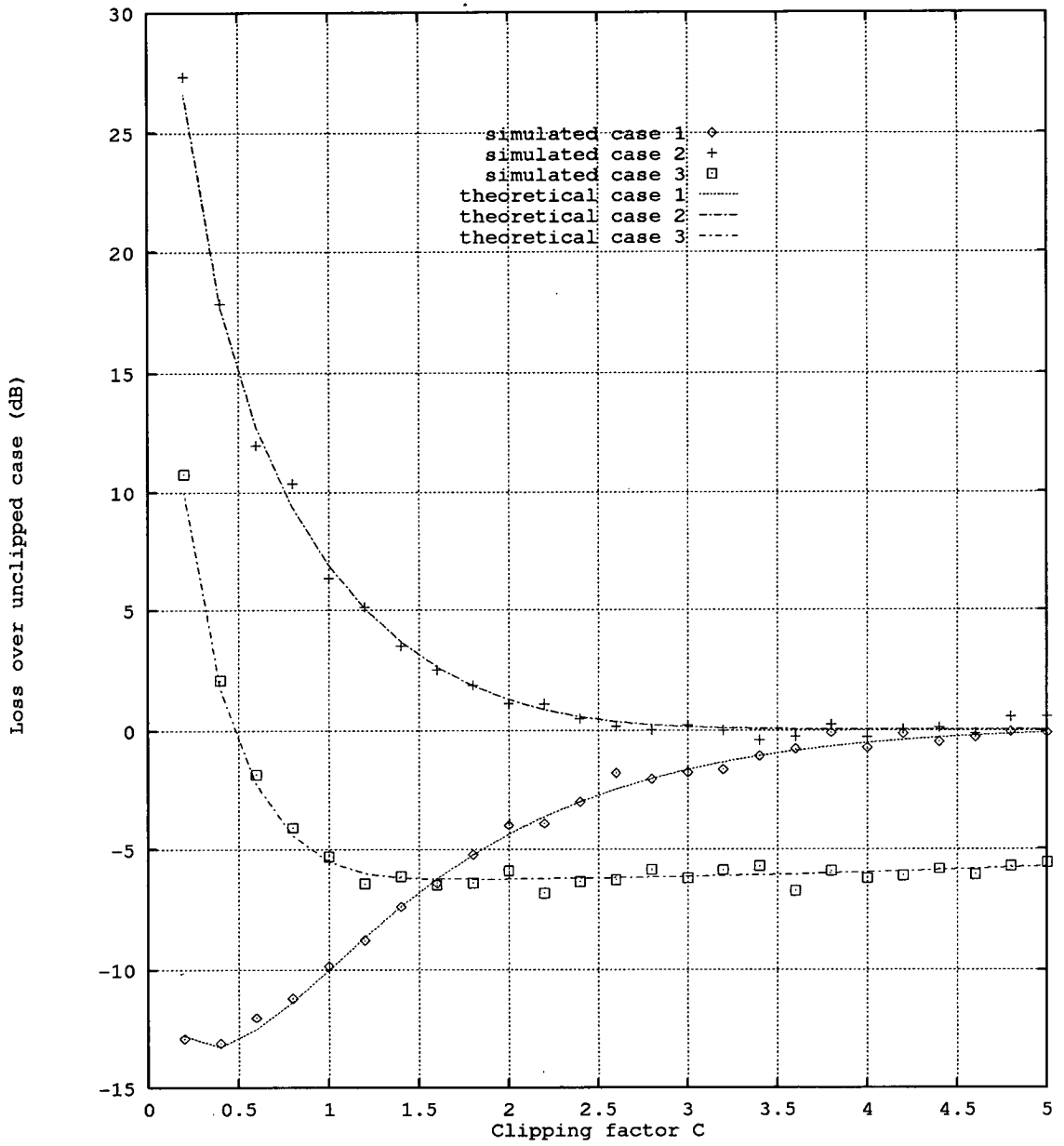


Fig. 5.10: Theoretical and simulation results for the clip to zero algorithm in the three impulsive noise cases (varying clipping factor).

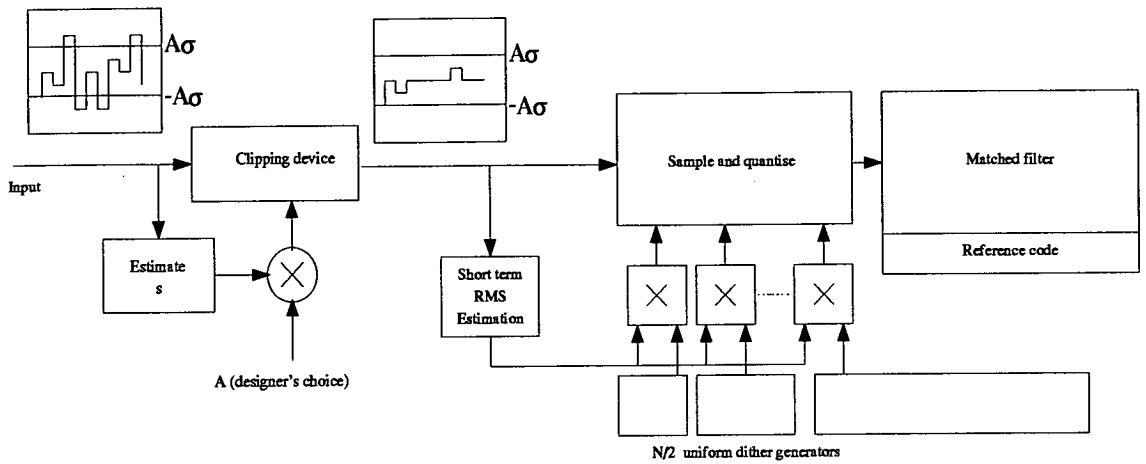


Fig. 5.11: Block diagram of the clip to zero algorithm combined with a limited precision DMF.

Simulation results for this type of combination are shown in fig 5.12 for Gaussian noise and the impulsive noise cases. The clip to zero algorithm has the clipping factor  $C$  set to 1.85. The limited precision DMF used in this example is Cahn's original DMF with the two improvements suggested in chapter 4. The DMF has 511 taps and each output signal to noise ratio is the average of 400 trials. The power measuring device for the clip to zero algorithm is assumed to be perfect. The second power measuring device is the average power of all previous samples in each of the 400 trials. This has the effect that it is highly erroneous at first, and may be significantly different from the original noise power.

In the Gaussian case (and the impulsive noise case 2, which is Gaussian for all useful purposes), the clip to zero algorithm should produce a loss of 2 dB. The guaranteed minimum performance of this particular DMF is -2.3 dB relative to an

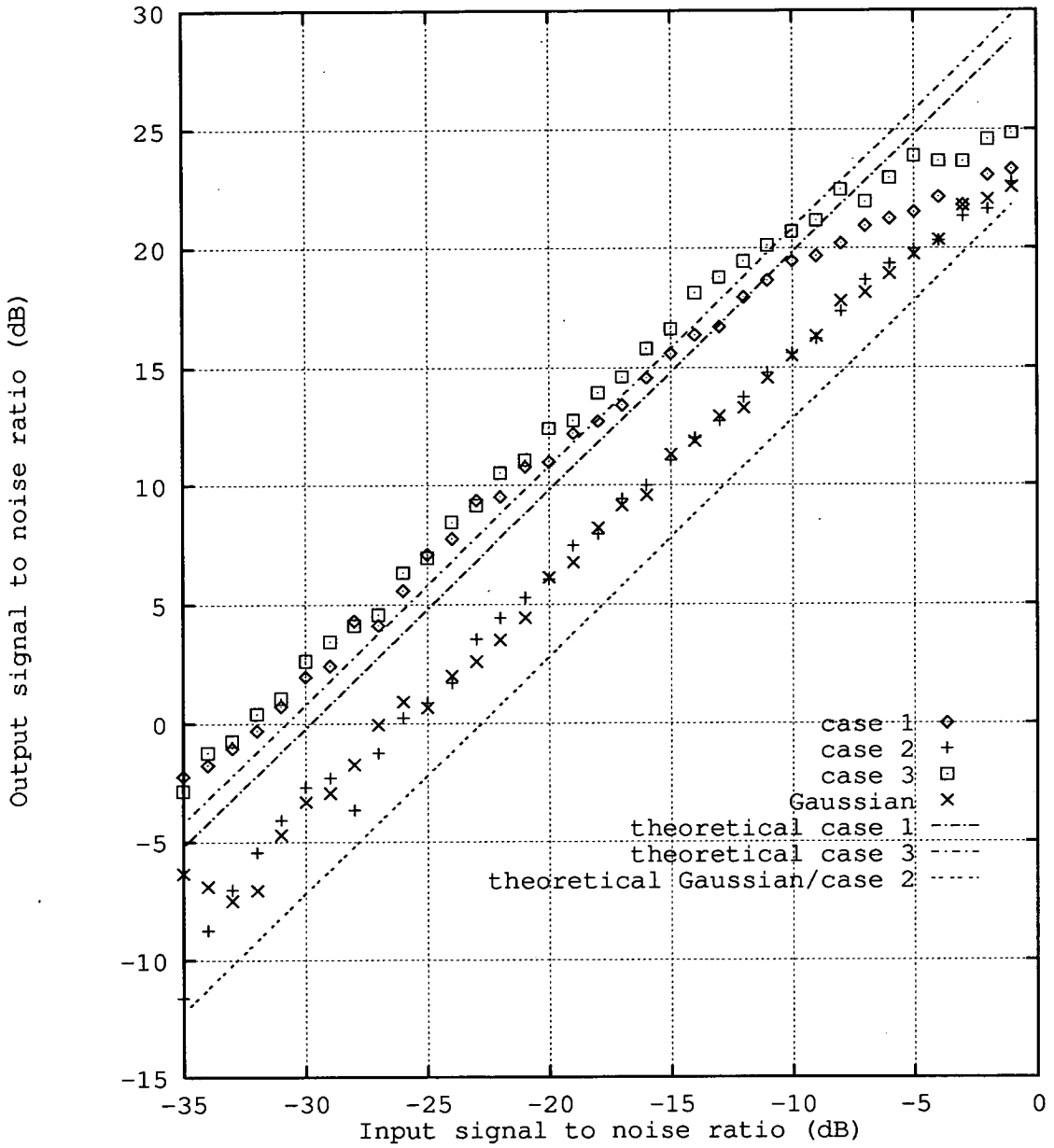


Fig. 5.12: Simulation results for the clip to zero algorithm combined with a limited precision matched filter.

analogue word DMF. Thus the overall guaranteed minimum performance of this DMF is a processing gain of:-

$$10\log(511) - 2 - 2.3 = 22.8\text{dB} \quad (5.19)$$

This minimum is shown on fig. 5.12 as "theoretical Gaussian/case 2". The actual simulation results for Gaussian noise and case 2 are considerably better than this worst case. There are two reasons for this. Gaussian noise is not the worst case noise for this DMF although it is close to the worst case (see fig. 5.6). More significant however, is the fact that the noise is not Gaussian when it reaches the DMF. The clip to zero algorithm has altered the noise distribution, and thus the DMF is performing considerably better than its original Gaussian performance.

In the impulsive case 1, the clip to zero algorithm gives a gain of 5 dB (see fig. 5.10). As before, the guaranteed minimum performance of this particular DMF is -2.3 dB relative to an analogue word DMF. Thus the overall guaranteed minimum performance of this DMF is a processing gain of:-

$$10\log(511) + 5 - 2.3 = 29.8\text{dB} \quad (5.20)$$

This minimum is shown on fig. 5.12 as "theoretical case 1". The simulation results consistently slightly exceed this guaranteed minimum because the matched filter is not operating in its worst case noise.

In the impulsive case 3, the clip to zero algorithm gives a gain of 6 dB (see fig 5.10). Again, the guaranteed minimum performance of this particular DMF is -2.3 dB relative to an analogue word DMF. Thus the overall guaranteed minimum performance of this DMF is a processing gain of:-

$$10\log(511) + 6 - 2.3 = 30.8\text{dB} \quad (5.21)$$

This minimum is shown on fig 5.12 as "theoretical case 3". Again, the simulation results

consistently slightly exceed this guaranteed minimum because the matched filter is not operating in its worst case noise.

It is also interesting to compare the results shown in fig. 5.12 with those in fig. 5.6. These graphs are for the same limited precision DMF, but fig. 5.12 is with the clip to zero algorithm before the DMF. The addition of the clip to zero algorithm has significantly improved the performance of the DMF in the impulsive cases 1 and 3, as would be expected. More surprisingly, the performance of the DMF has been marginally improved in the Gaussian and case 2 impulsive noise cases. This is despite the 2 dB sacrifice in worst case performance caused by clipping to zero at  $C = 1.85$ . The reduction in the noise power and change in the noise distribution is enough to improve the performance of the DMF by more than the 2 dB sacrificed in the clip to zero algorithm.

## 5.7. Chapter summary

In this chapter we have shown that spread spectrum systems have inherent advantages over conventional ones in impulsive interference. These natural advantages can be enhanced by the use of non-linear signal processing in the receiver, either by use of a non-linear clipping device in front of the matched filter or a limited precision matched filter, or both. If the non-linearity is not adaptive, these improvements in impulsive noise performance come at the expense of a small degradation in Gaussian noise performance.

---

## 6. System design

---

In this chapter, we develop an overall system design. The chapter starts with some preliminary decisions and assumptions. The design of a system is then discussed, from the macro level downwards, ie. from the consideration of multiple systems down to the transmitter/receiver components. The personnel required to service the alarm scheme will also be discussed. Finally, some discussion of the reliable range of the alarm scheme will be presented. The range is one of the most important parameters in trying to assess the feasibility of the scheme.

### 6.1. Preliminary assumptions and decisions

In order to constrain the number of unknowns in the design of the system, it is necessary to make a number of initial decisions and assumptions. They are set out below.

The system will be designed to operate within the specifications laid out in [11]. We shall assume that there is a maximum of 1024 clients for any one system. The time between a client pushing the alarm button and the alarm registering at the receiver should not normally be more than 60 seconds. This time is similar to the time required to make a phone call and small compared to the time the person responding to the alarm is likely to take to reach the client. We shall assume a processing gain of 511. Larger processing

gains may give very slightly better performance, but they increase the computational load at the receiver. We shall see later that the processing gain is not the factor which limits system performance anyway.

### 6.1.1. Transmission format

The choice of the transmission format in a digital communication system is normally a trade off between transmission power efficiency, resistance to the expected perturbations in the channel and receiver complexity. The possibilities include 100% amplitude modulation, sometimes referred to as on off keying (OOK), binary phase shift keying (BPSK), and binary frequency shift keying (BFSK) [76]. There is also a choice of detection methods for each transmission format.

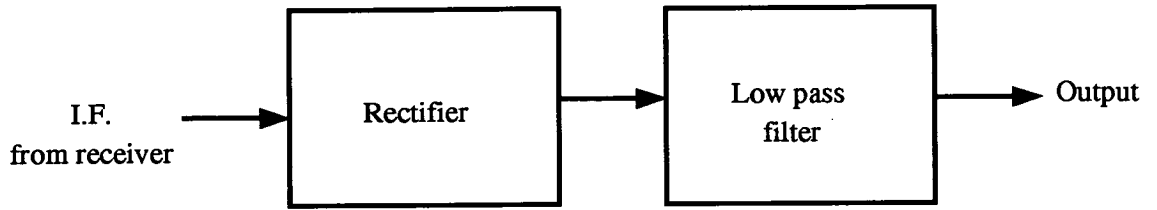
The choice of transmission format for the system is principally dictated by three important factors. Firstly, we expect the detection method to operate correctly when the signal to noise ratio in the transmission bandwidth is considerably less than 0 dB. Second, the overall error in the carrier frequency is likely to be comparable with the transmission bandwidth. The crystals used to generate the carrier frequency for the transmission may be assumed to have a minimum overall error of plus or minus 10 parts per million over their anticipated operating temperature range [77]. This means that the frequency error with a transmission frequency of 27 MHz will be plus or minus 270 Hz. Finally, it will be advantageous, though not strictly necessary, if the detection method is approximately linear. If the detection method is not linear, the noise PDF at the receiver will be altered. The performance of the DMFs and the clip to zero algorithm will be different from that predicted in the previous chapters if the noise PDF is altered.



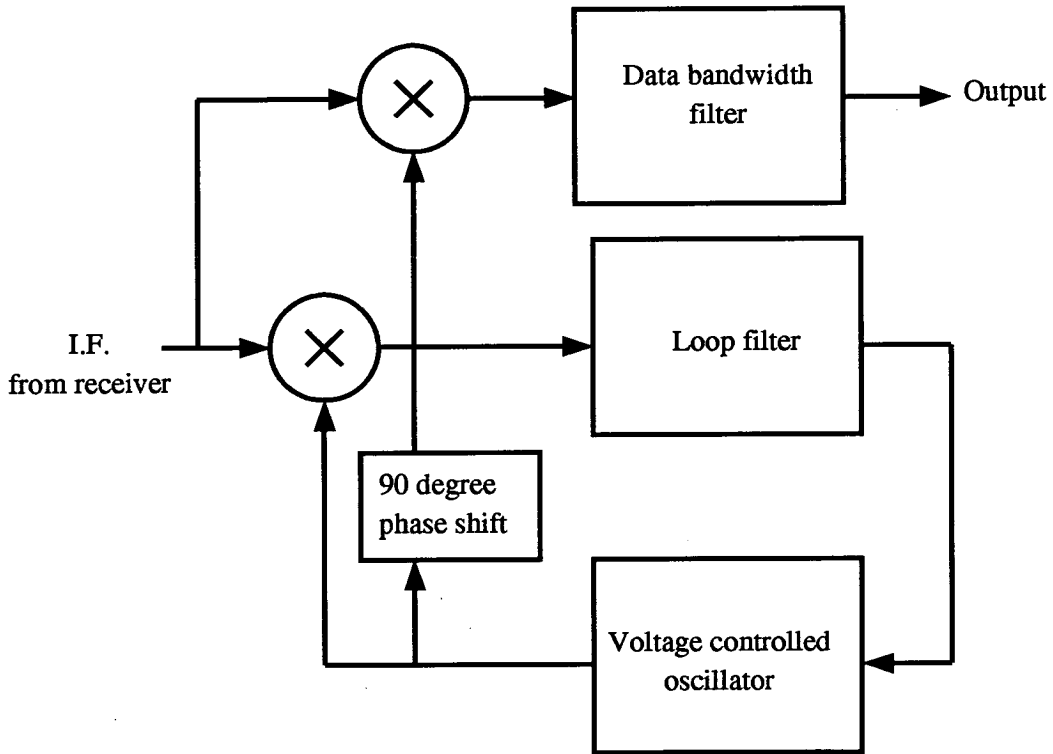
Often in direct sequence spread spectrum systems the signal is despread before it is demodulated, for example by using I and Q channels with a matched filter in each and combining. In this application, several problems exist with this method. The problems are associated with having to use digital matched filters because of the low data rate. Using I and Q channels means that there is already a doubling of the hardware required. However, to satisfy Nyquist criterion and avoid aliasing of the IF, the sampling rate would have to be increased and this will require a several fold increase in the number of taps required in the DMF. The combining process is also highly nonlinear. The effect of the interaction between this nonlinearity and the nonlinearity introduced by the use of limited precision digital matched filters is unclear. For these reasons we look at demodulating the signal before attempting to despread it.

There are two possibilities for the detection of OOK signals, non-coherent detection using an envelope detector and coherent detection using a phase-locked loop (see fig. 6.1 and [78, 79] ). The envelope detection method is completely unsuitable for two reasons. It has very poor performance at negative signal to noise ratios (see [80] ). This detection method is also inherently highly non-linear. Coherent detection of OOK is a strong possibility however. The phase-locked loop can have an effective noise bandwidth of far less than the transmission bandwidth, provided that the loop is given sufficient time to lock. This method will be discussed further in the last paragraph of this section.

For BPSK signals, there are also two possible demodulation schemes, the squaring loop and the Costas loop (see fig. 6.2 and [81, 82] ). These are normally highly efficient demodulation methods. However, they are of no use in this application. The reason for this is that when two signals with signal to noise ratios of less than 0 dB are multiplied together, the resulting signal has a much lower signal to noise ratio than either of the original signals. For example, if the two original signals have a signal to noise ratio of:-



a)



b)

Fig. 6.1: Detection methods for OOK, a) non-coherent envelope detection and b) coherent detection using a phase locked loop.

$$\frac{x^2}{y^2} \tag{6.1}$$

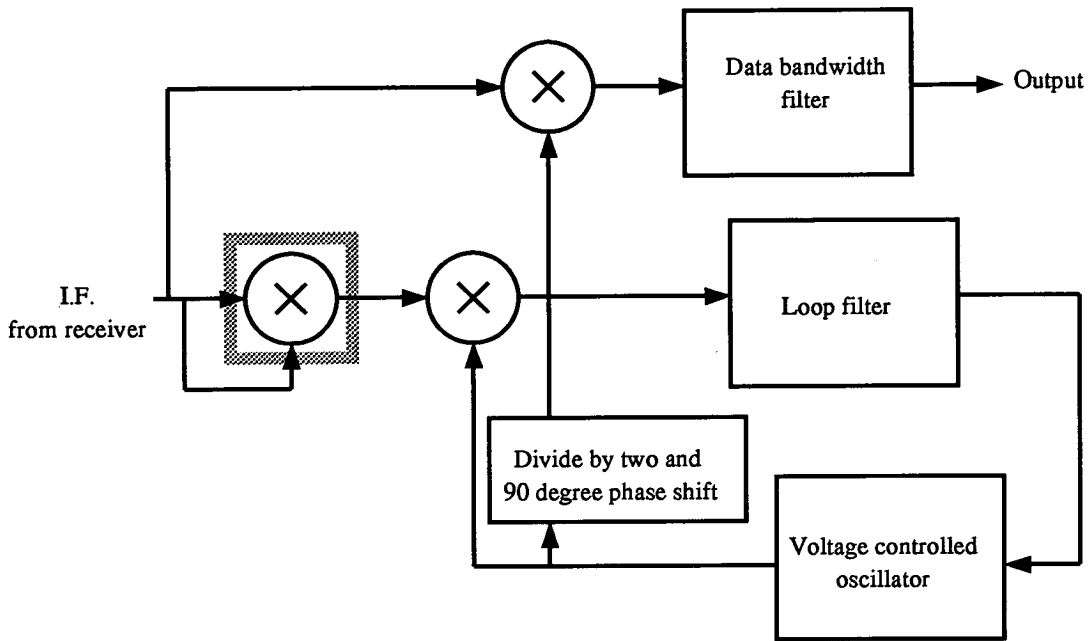
Then the output signal has signal to noise ratio is:-

$$\frac{x^4}{y^4} \tag{6.2}$$

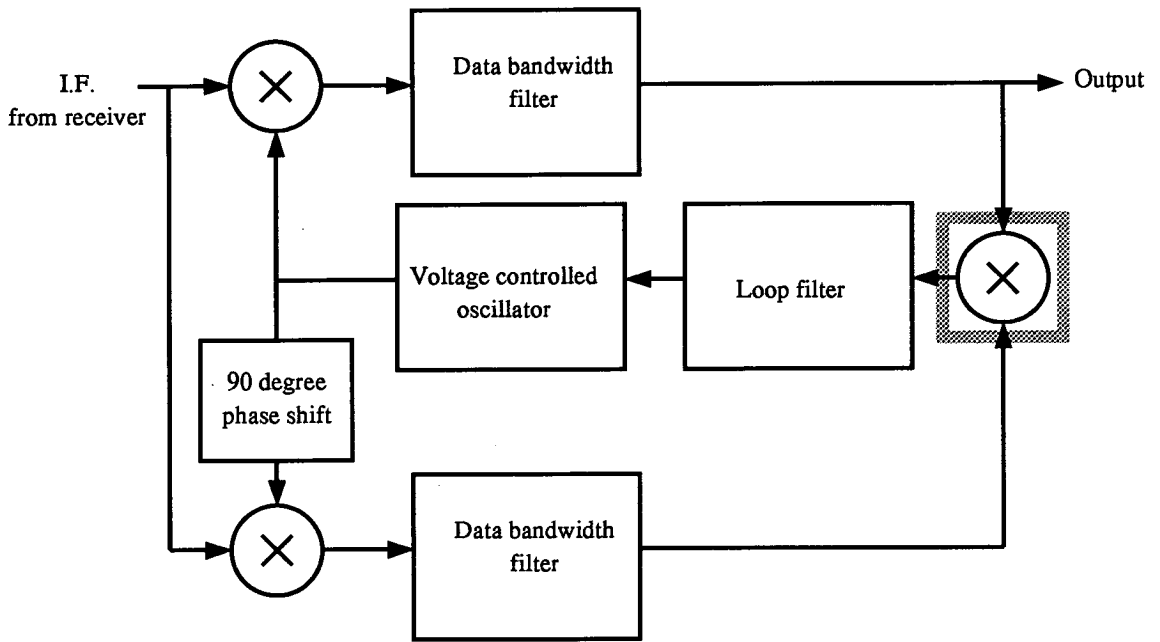
If  $x < y$ , ie. the original signal to noise ratio was less than 0 dB, then equation 6.2 is much less than equation 6.1. Thus the multiplier has severely degraded the signal to noise ratio. This applies to one of the multipliers in both the methods for demodulating BPSK signals. These multipliers are highlighted with a shaded square in fig. 6.2. Thus we dismiss the possibility of using BPSK.

The traditional methods for demodulating BFSK signals are shown in fig. 6.3 (see [79] ). In this form they are of little use in the system, as the decision box is highly non-linear and results in the premature loss of some of the information content of the signal. However, if the decision box is replaced by a subtraction, there are possibilities. The non-coherent method can be dismissed because of the poor performance of the envelope detectors at low signal to noise ratios. The coherent method is a possibility and will be compared with the coherent detection of an OOK signal in the next paragraph.

We have narrowed the possible transmission formats and detection methods down to two:- coherently detected OOK and coherently detected BFSK. If the phase detectors in the coherent BFSK system are phase locked loops, then the performances of these two systems are similar except for the following. The BFSK signal has twice as much average signal power as the OOK for the same peak power. However, this advantage is cancelled by the subtraction box used to replace the decision box in the traditional method for BFSK, as this doubles the noise power. In the BFSK system, the filters f1 and f2 can theoretically have narrower bandwidths than the filter in the OOK system. In practice however, the widths of the BFSK filters are likely to be dictated by the error in



a)



b)

Fig. 6.2: Detection methods for BPSK, a) squaring loop and b) Costas loop.

the carrier frequency and the practical tolerances of the filters, and are therefore likely to be a similar width to the filter in the OOK system. The phase-locked loop in the OOK system will lock twice as fast as the two phase-locked loops in the BFSK system if the locking pre-amble is a string of digital ones, ie. a tone at the carrier frequency. The OOK system is also simpler and closer to an ideal linear system than the BFSK system. Therefore we choose to use OOK as the transmission format, with coherent phase-locked loop detection. The details of the detection system will be discussed in the receiver section later in this chapter.

## 6.2. Multiple systems

To cover larger geographical areas and allow the possibility of more than one service provider in a given area, the method used for providing system diversity should be studied. The only way to provide true diversity between systems is to have adjacent or overlapping systems operate on different frequencies. In [11], there are four separate carrier frequencies. As the transmission requires far less bandwidth than is available in each of these channels, even with a spreading factor of 511, we can also subdivide each of these four channels. If we divide each channel into two, that gives us eight frequency independent channels. With co-operation from all service providers, this would enable us to set up a cellular structure similar to that used for mobile telephones (see fig. 6.4 and [83, 84] ). The structure in fig. 6.4 is based on 7 different frequencies (F1-F7). However, it is likely that occasionally a signal from a transmitter designed for one receiver system will arrive at another receiver. This may happen because a transmitter has been taken to the wrong geographical area or because of freak transmission characteristics. When this happens, it is important that the receiver does not generate a false alarm, but recognises

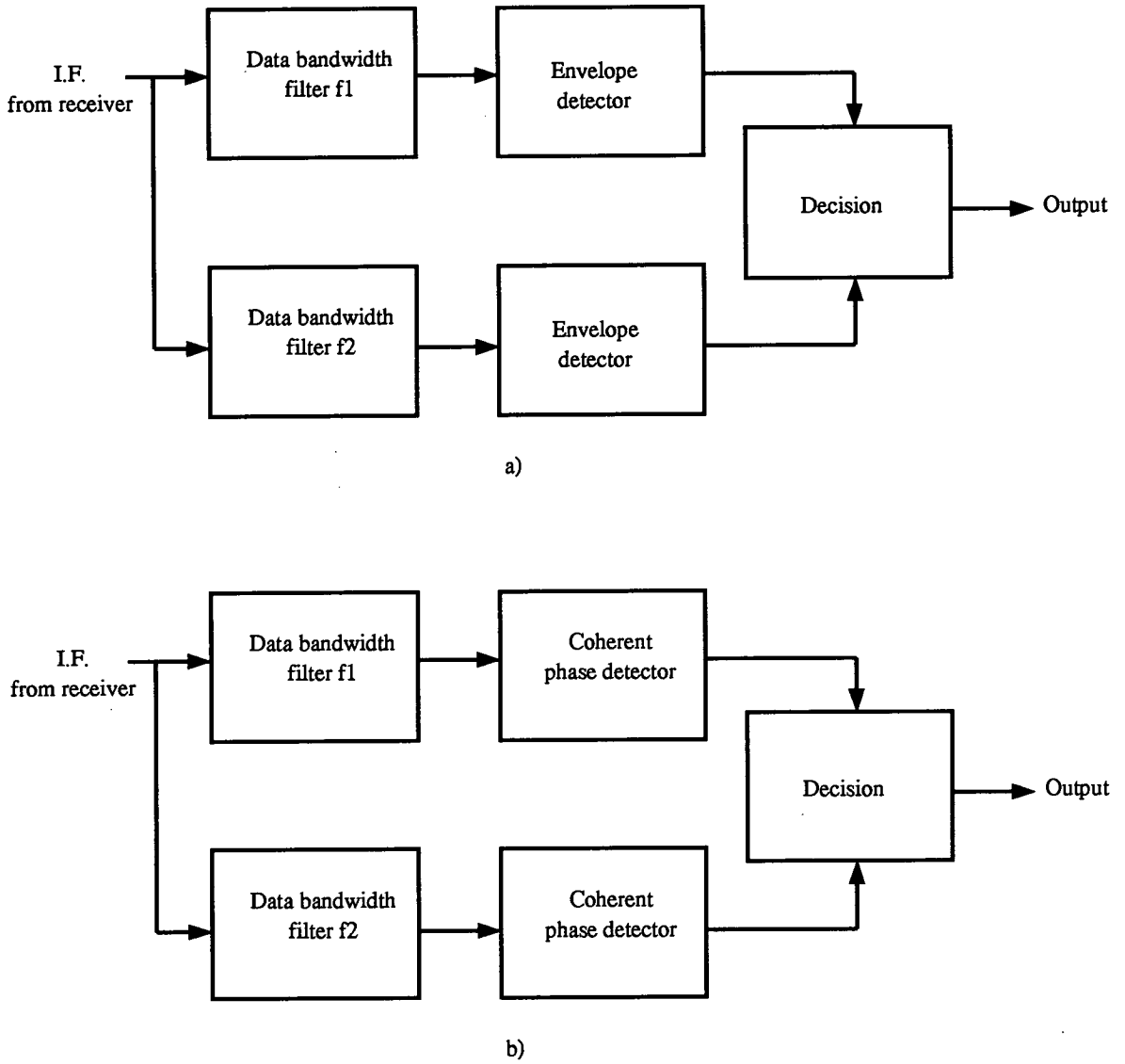


Fig. 6.3: Detection methods for BFSK, a) non-coherent detection and b) coherent detection.

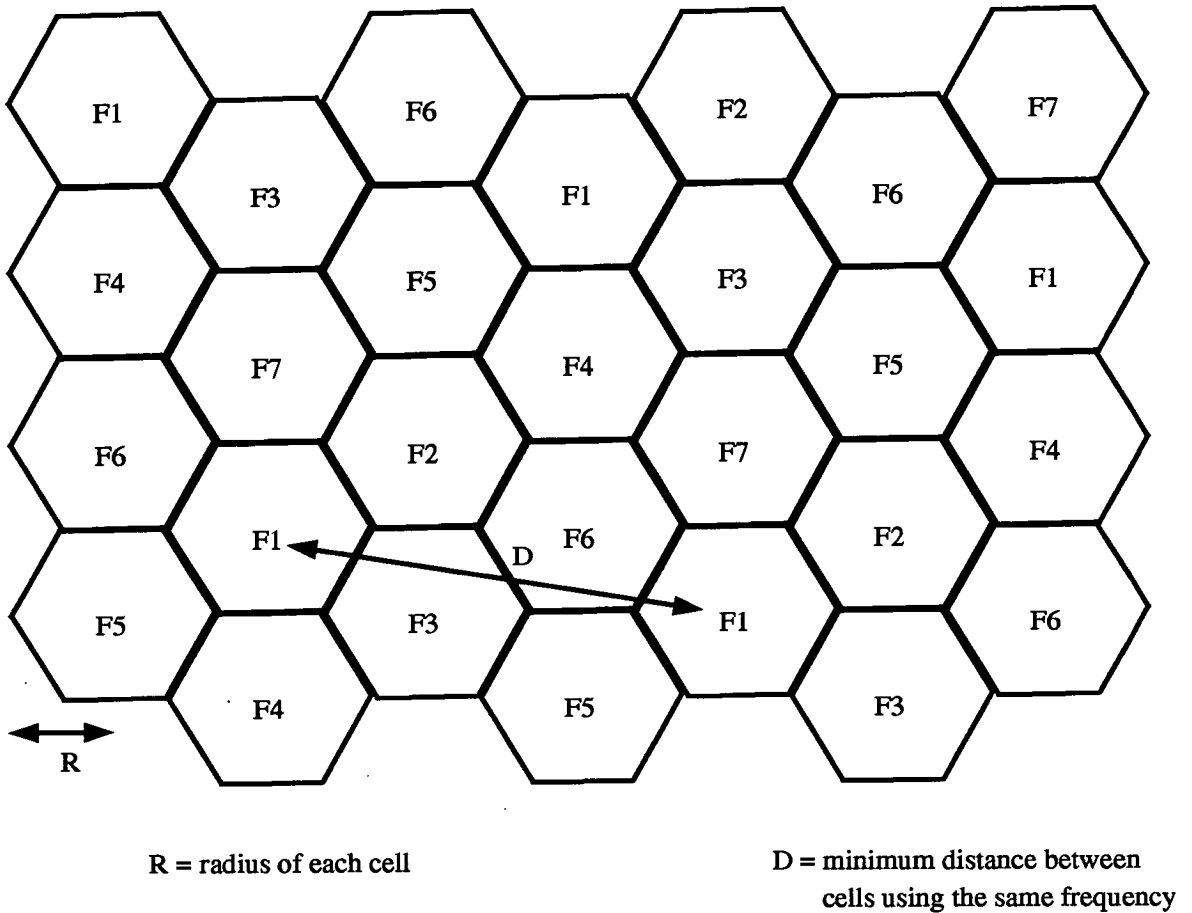


Fig. 6.4: Cellular structure for carrier frequency re-use.

that it is receiving a signal which should not occur. By assigning a different m-sequence spreading code to each system within a local area, this should be possible. There are 48 different m-sequence spreading codes available for a length 511 sequence (see appendix A). The mechanism for recognising incorrect signals will be discussed in more detail in the receiver section later in this chapter. We now go on to look at the structure of a single system.

### **6.3. A single system**

A single system would consist of one service centre, a small number of receivers and up to 1024 transmitters, as shown in fig. 6.5. The provision of more than one receiver is considered important for several reasons.

It is possible that a receiver may not receive the required signal to noise ratio. This may be because the receiver is in a shadow from a particular transmission, caused by an obstruction on the propagation path [85]. Careful siting of the receivers should reduce the possibility of this, but it is difficult to allow for obstructions close to the transmitter. Another reason for a receiver not receiving the required signal to noise ratio is that the antenna, which should be omni-directional to allow for all possible usage sites and angles, may become directional. This can happen because of reflectors local to the transmitter. Having more than one receiver reduces the possibility of all the receivers being in a directional null. Finally, an individual receiver may be unavailable some of the time because of strong local interference from a variety of other sources, for example a particularly noisy car (see 56), an illegal transmission or possibly interference from an adjacent cell (see previous section).

### **6.4. Transmitter design**

This section is split into three parts, the transmitted signal, transmitter operation and the design and physical construction of the transmitter.



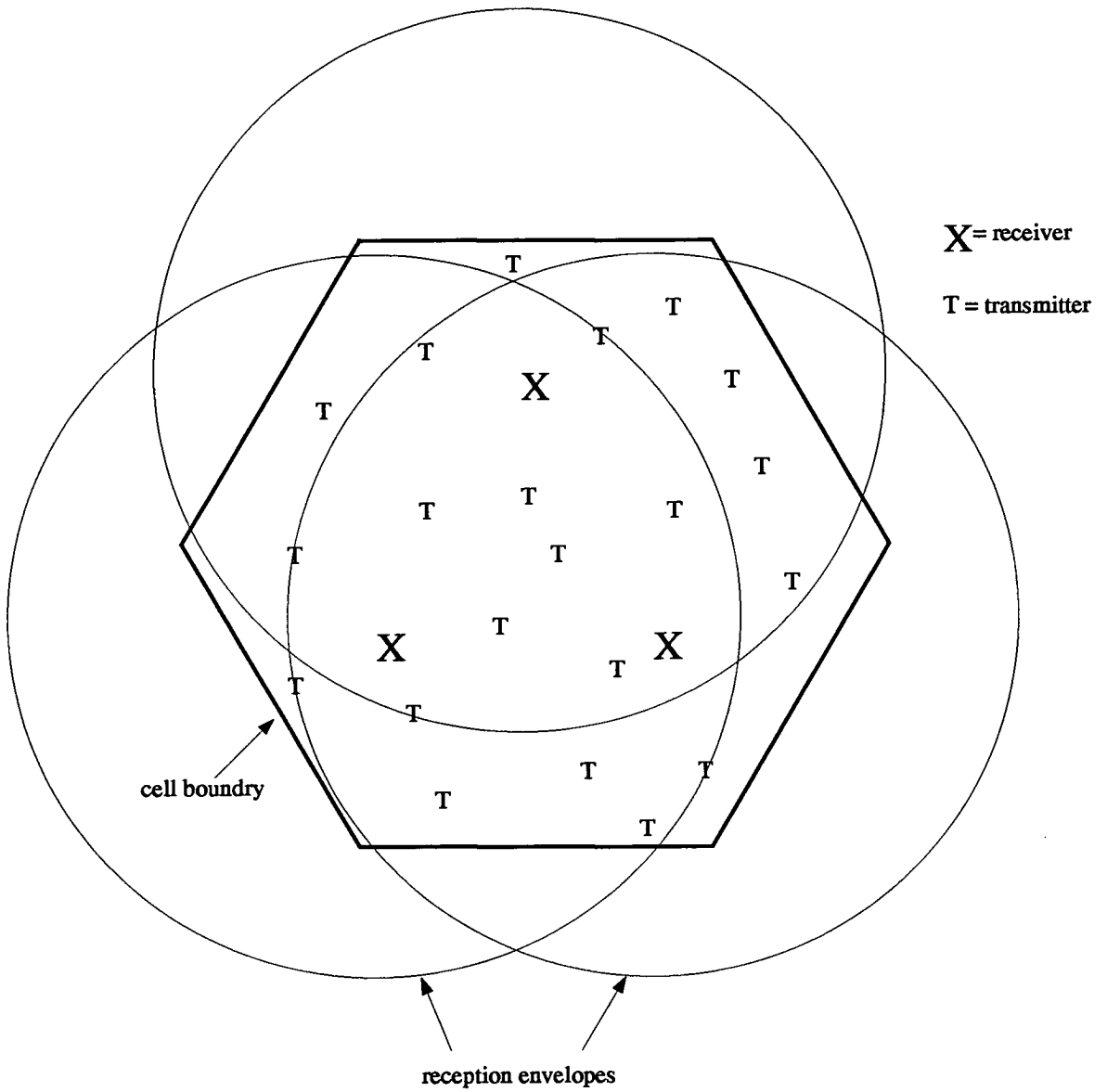


Fig. 6.5: Layout of a single system or cell.

### 6.4.1. The transmitted signal

The first important decision in the design of the transmitter is to decide what to transmit. We have already decided to allow 1024 users. This requires the transmission of

## CHAPTER 6: SYSTEM DESIGN

10 bits to identify uniquely each transmitter. As well as transmitting an alarm signal, a transmitter should also be able to transmit a cancellation signal, enabling a user who has accidentally triggered an alarm to cancel that alarm and save the respondent an unnecessary journey. A transmitter should also transmit a signal to indicate a low battery level substantially before the power of a transmission would be effected. This leaves us with three possible transmitted signals, alarm, cancel and low battery. This requires two information bits, with one state left free. This extra state could be used for an external trigger for example. This means that we have a total of 12 information bits to be transmitted. We require a very low bit error rate at the receiver for these 12 information bits. In order to reduce the bit error rate from the natural values given in fig. 5.5, we apply an error correcting block code to the transmission. The upper limit on the performance of error correcting block codes is described by the Hamming bound [86]. If we have  $K$  information bits and a total transmission of  $N$  bits then if:-

$$2^K \leq \frac{2^N}{1 + C_1 + C_2 + C_3 + \dots + C_t} \quad (6.3)$$

where

$$C_J = \frac{N!}{J!(N-J)!} \quad (6.4)$$

then it is possible to devise a code to correct  $t$  errors. In this case,  $K = 12$ . From these equations, it is reasonable to expect to correct two errors. From the Hamming bound, this requires  $N = 20$ , or 8 coding bits. In this type of transmission, the significant parameter is the probability of any error in the decoded 12 bit word. The probability of a word error plotted against the output signal to noise ratio from a receiver is shown in fig. 6.6 for the uncoded case and the block coded case as described above. It is assumed that the receiver output has Gaussian noise statistics. This is a good assumption in the case of this spread spectrum receiver, since as we have already seen, the noise distribution at the

output of a digital matched filter is always a good approximation to Gaussian. The probability of an error in the 12 bit word for the uncoded case is the probability of more than zero errors in 12 independent trials. If the BER is  $P_e$ , then the probability of a word error is:-

$$1 - (1 - P_e)^{12} \quad (6.5)$$

In the coded case, the probability of an error in the decoded 12 bit word is the probability of more than two errors in 20 bits. Again, if the BER is  $P_e$ , then the probability of a word error is:-

$$1 - \left( (1 - P_e)^{20} + 20P_e(1 - P_e)^{19} + 190P_e^2(1 - P_e)^{18} \right) \quad (6.6)$$

Fig. 6.6 shows that if we wish to achieve very low word error rates, then they can be achieved at lower output signal to noise ratio by using the block code. We also require a pre-amble to allow the phase-locked loop in the receiver to lock. To minimise the lock time with an OOK signal, the pre-amble should be all ones, ie. a carrier signal. This carrier signal should not be modulated by the spreading code. A reasonable time for this pre-amble is around 10 seconds. If we transmit the 20 bit data signal at one bit per second, this then gives us an overall transmission time of 30 seconds.

#### 6.4.2. Transmitter operation

In the event of the alarm button being pressed, the transmitter should immediately transmit an alarm signal, and then wait for a prescribed length of time plus a random period before re-transmitting. This waiting and transmitting cycle should repeat until the

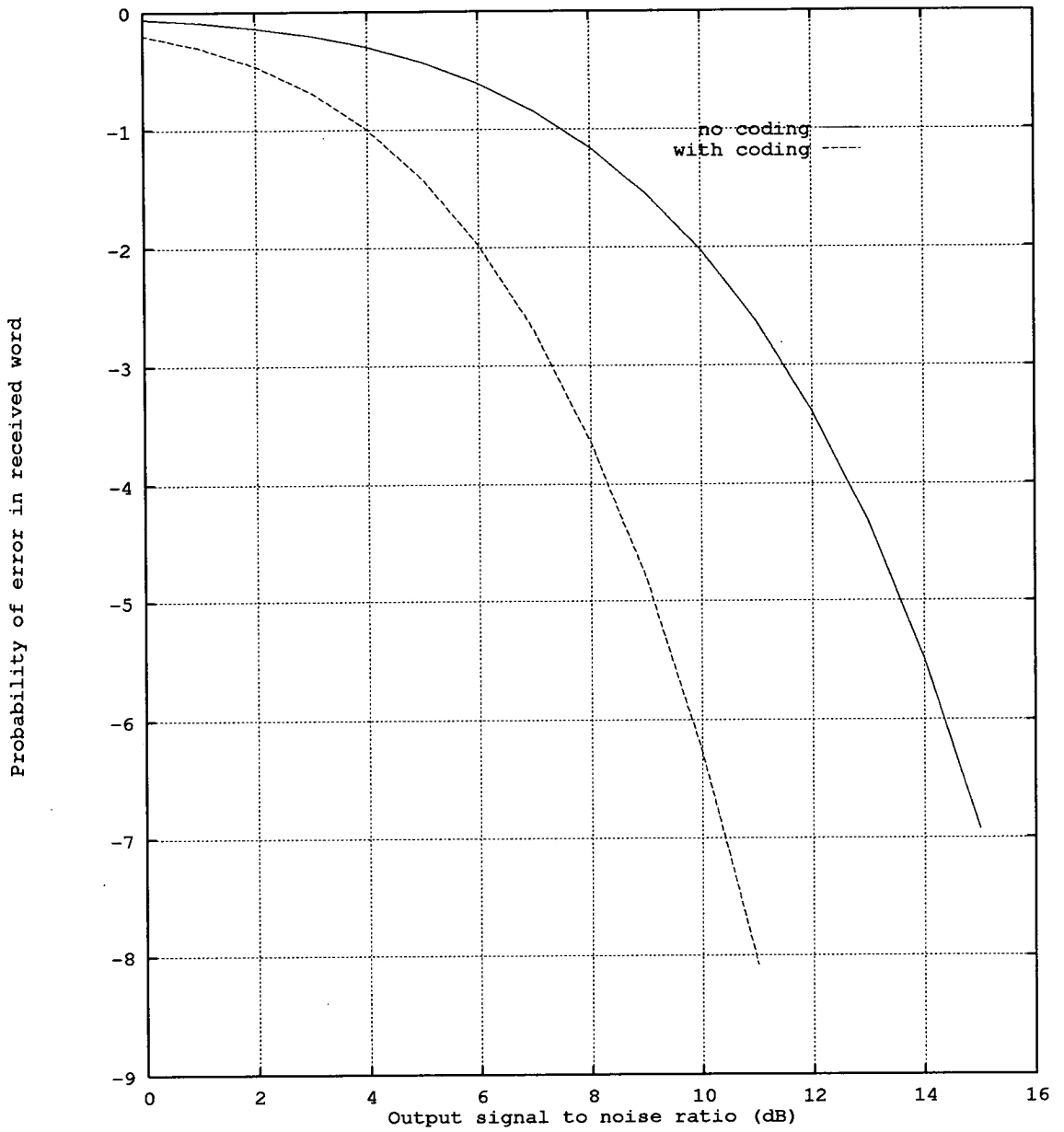


Fig. 6.6: The improvement in the probability of error in the received word achieved when using an error correcting block code.

alarm is cancelled. The prescribed waiting period is to allow the receiver to distinguish between successive transmissions. The random period is to allow for the clash of more than one transmission. This event is highly unlikely, previous trials have shown that alarms are rare occurrences. However, alarms cannot be assumed to be independent events, they are far more likely at certain times of day and local events like a power cut may result in several simultaneous alarms. The effect of simultaneous alarms will be discussed in more detail in the receiver section, but two signals cannot be simultaneously received. Therefore, it is necessary to have this random back-off period similar to that used in computer networks [87]. In the proposed system, it may be a good idea to link this random back-off period to the transmitter identity code, as this is unique to each client. Because of the retransmitting cycle, it is very important that the alarm signal is cancelled as soon as possible after the respondent reaches the client. Leaving transmitters on for long periods discharges the batteries and vastly increases the possibility of signal clashes.

In the event of the cancel button being pressed, the cancel signal should be transmitted once only, and then the transmitter reset. In the vast majority of cases, this will prevent unnecessary disturbance of the respondents. Occasionally, this cancel signal may be lost because of a clash between signals.

In the event of the battery strength being low, the transmitter should transmit the battery low signal once and then repeat this signal again after a prescribed period of time, say 24 hours.

### **6.4.3. Design and physical construction**

It is important that the transmitter be designed in such a way that the client cannot distort the signal, for example by frantically pressing the alarm button, or pressing the cancel button before the alarm signal has finished transmitting.

The transmitter should also provide some form of assurance that help is being called for when the alarm button is pressed. In terms of its physical construction, we have already said that the transmitter unit should be as small and unobtrusive as possible. In order to achieve this, it will be necessary to use programmable devices such as programmable read only memories (PROMs) to store the codes and programmable logic arrays (PLAs) for the logic. Fortunately, the circuitry required to generate OOK key signals is simple [88, 89]. The alarm buttons should be recessed to prevent accidental triggering because of knocks. In an ideal system, the transmitters should be regularly tested.

## **6.5. Receiver design**

The design of the receiver is far more complicated than the design of the transmitter. For this reason we break the design down in to more manageable blocks as shown in fig. 6.7. It is important that the whole receiver is extremely reliable. This may necessitate the use of redundancy in components and uninterruptable power supplies.

### **6.5.1. Demodulation**

We have already decided to demodulate the signal using a phase locked loop such as the one shown in fig. 6.8. The design of this loop shall now be discussed. There are

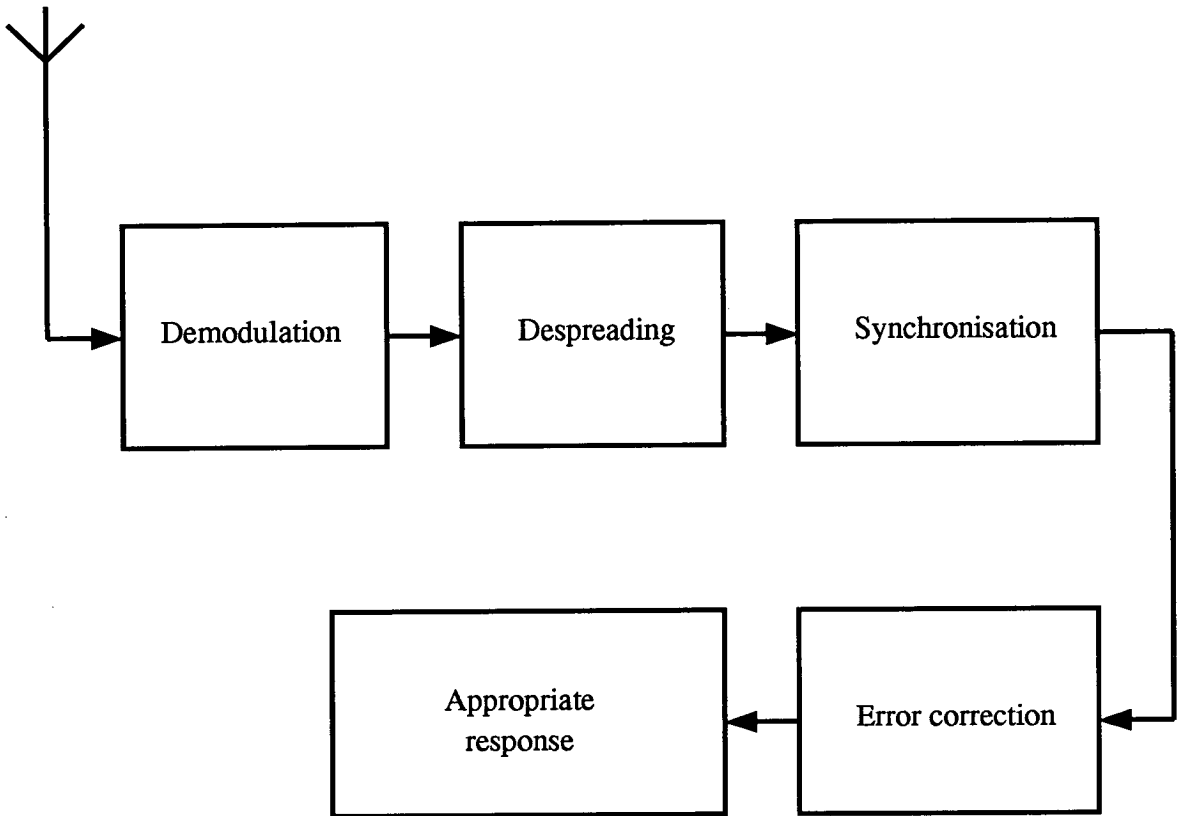


Fig. 6.7: Block diagram of the receiver.

several important parameters to be looked at in the design of a phase locked loop. These include the loop noise bandwidth, the time for the loop to lock, the steady state phase error, the probability of cycle slips and the stability of the loop. Whole books have been

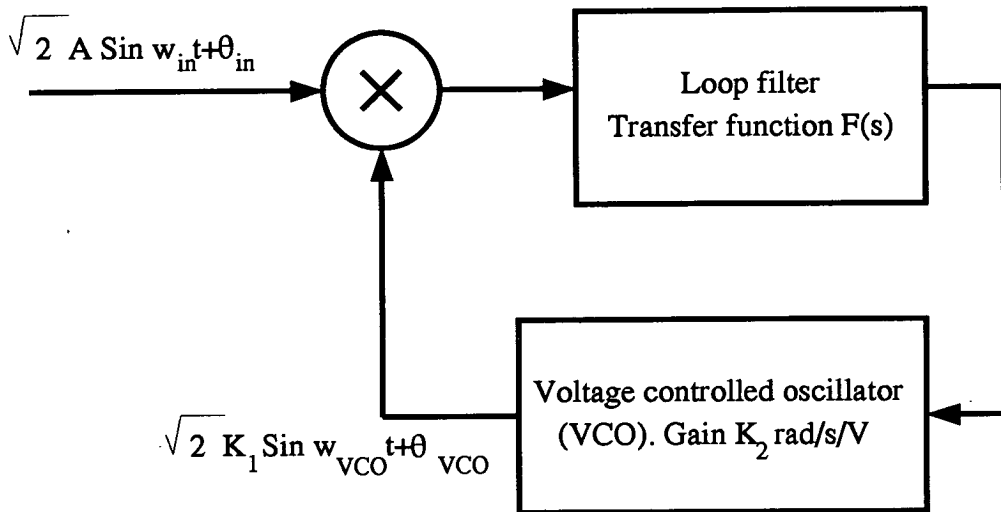


Fig. 6.8: Block diagram of the phase locked loop.

written on the design of phase locked loops and it would be unrealistic for us to attempt to explore exhaustively all possibilities in this thesis. As a result, the design detailed below may not be optimal. All the equations in this section are from work by A. J. Viterbi [90, 91].

The first important decision is to decide the order of the phase locked loop. The order of the loop is the order of the polynomial in  $s$  of the closed loop transfer function. A first order loop is guaranteed stable under all operating conditions, but has a long pull in time and a steady state phase error. A third order loop has good pull in characteristics, low loop noise bandwidth and no steady state error. It is not however, guaranteed stable under all circumstances. We shall use a second order phase locked loop, which has reasonable pull in characteristics and loop noise bandwidth. In its perfect form, it has no



steady state phase error and is guaranteed stable. A perfect second order phase locked loop has a loop filter transfer function:-

$$F(s) = 1 + \frac{a}{s} \quad (6.7)$$

If the loop has overall gain  $K = K_1 K_2$  rad/s/V and the input to the loop is  $\sqrt{2}A \sin w_{in}t$ , then loop noise bandwidth  $B_L$  is given by:-

$$B_L = \frac{AK + a}{4} \quad (6.8)$$

The pull-in time of the loop  $t$  is approximately:-

$$t = \frac{1}{a} \left( \frac{w_{VCO} - w_{in}}{AK} - \sin \theta \right)^2 \quad (6.9)$$

The natural frequency of the VCO is  $w_{VCO}$ ,  $\theta$  is the phase difference between the VCO and the input signal ( $\theta_{in} - \theta_{VCO}$ ). Thus the worst case pull-in time is given by:-

$$t = \frac{1}{a} \left( \frac{w_{VCO} - w_{in}}{AK} \right)^2 \quad (6.10)$$

We have already decided to allow 10 seconds for the pull-in time, so  $t = 10$ s. The best stability of the VCO and the carrier frequency can be assumed to be  $\pm 10$  parts per million. At 27 MHz, this means that  $w_{VCO} - w_{in}$  will be around 540 Hz, or 3393 rad/s. If we describe the loop gain  $G = AK$ , then from the worst case pull in time equation:-

$$10 = \frac{1}{a} \left( \frac{3393}{G} \right)^2 \quad (6.11)$$

or:-

$$a = \frac{1151245}{G^2} \quad (6.12)$$

Substituting this into the loop noise bandwidth equation, we obtain:-

$$B_L = \frac{G + \frac{1151245}{G^2}}{4} \quad (6.13)$$

We optimise this by differentiating with respect to  $G$  and setting to zero, ie.:-

$$1 - \frac{3453735}{G^3} = 0 \quad (6.14)$$

Thus  $G = 151.15$  and by substituting back into the pull in time equation,  $a = 50.4$ . The loop noise bandwidth is therefore 50.4 rad/s or 8.0 Hz. The validity of this calculation has been proved by extensive simulation using the signal processing worksystem (SPW) simulation package†. SPW is a time step based simulation package for communications. It is quicker to write simulations on the SPW rather than in a programming language such as 'C' because many of the blocks required in a communications system are included in the package. The disadvantage of using this package is that the simulation time is much longer than that required for a custom written program.

An example of the results from these simulations is shown in fig. 6.9. Fig. 6.9 shows the VCO input and the data output waveforms obtained from an SPW simulation of the above loop. These waveforms are sampled at 2000 samples/s. In this particular simulation,  $A = 1$  V,  $G = 151.15$  rad/s/V,  $w_{VCO} - w_{in} = 100\text{Hz} = 628$  rad/s. From the worst case pull in equation, the pull in time should be 0.34s. Fig. 6.9 shows the loop locking in exactly this time, with the VCO input settling to -4.15 V, ie. the VCO output exactly 100 Hz below its natural frequency.

In practice, this loop would be implemented as an imperfect second order loop, ie a third order loop. This is necessary to prevent the perfect integrator in the loop filter from drifting to infinity when there is no input signal because of offsets in the circuitry. With

†Signal Processing Worksystem and SPW are trademarks of Comdisco Systems Inc.

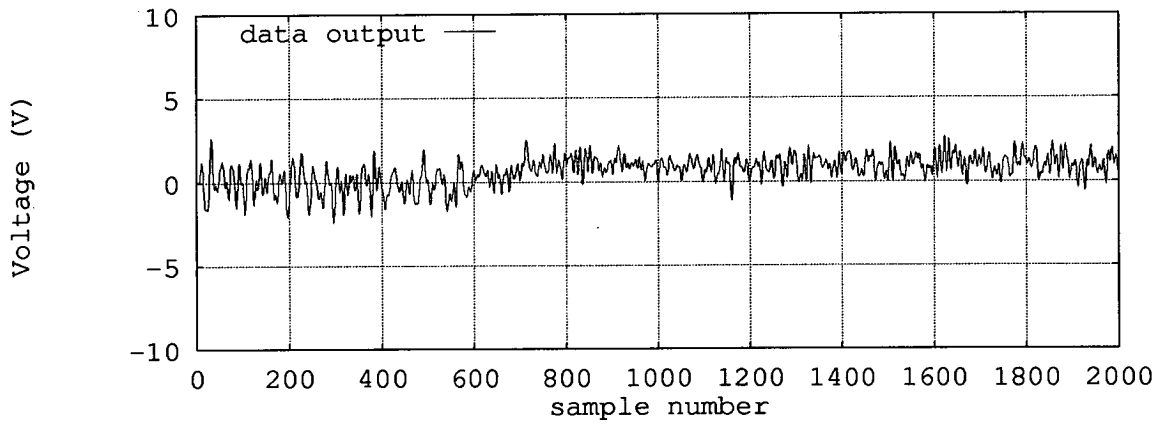
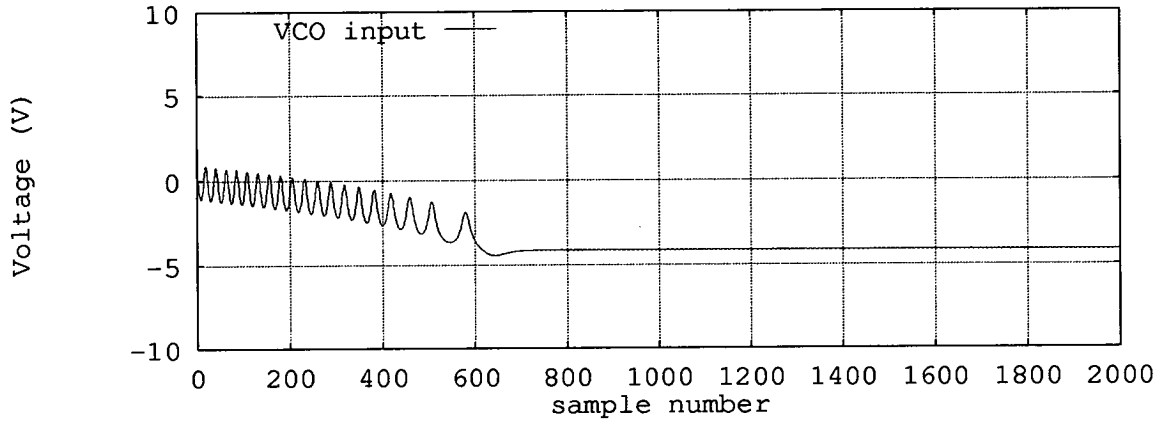


Fig. 6.9: SPW simulation results showing the accuracy of the pull-in time equation.

careful design, the imperfect second order loop should have the same dynamics as the perfect second order loop as discussed above. One factor we have not taken into account is the effect that impulsive noise will have on the loop. Because the loop is non-linear, it would require a great deal of work to calculate the effect of impulsive noise on a phase locked loop. It is hoped that the integrator in the loop filter transfer function will average the effect of impulsive spikes and therefore the performance of the loop will not be affected by impulsive noise.

The last important issue to address in the operation of this demodulation device is the action of the automatic gain controlled (AGC) amplifier which must precede the phase locked loop. In a more conventional system, this amplifier would operate on a waveform dominated by its signal component, therefore setting the correct signal amplitude into the phase locked loop would be easy. In the spread spectrum scenario however, the waveform on which the AGC amplifier will have to operate will be dominated by its noise component. Therefore, we must decide in advance the minimum signal to noise ratio in the loop bandwidth we expect the system to work in and set the AGC amplifier accordingly. This signal to noise ratio should be around 6 dB. This figure is chosen because it is only at this signal to noise ratio and above that the loop can be assumed to be operating in its linear region. It is important that the loop is operating in this region for three reasons. Firstly, the pull in time equation and the equivalent loop bandwidth equation are based on this assumption. Secondly, if the loop is operating outside this region, the noise PDF will be distorted and the performance of the non-linear devices discussed in chapters 3-5 will no longer be valid. Finally, at this loop signal to noise ratio, the probability of cycle slips will be acceptably low. Note that this 6 dB will have to take into account the fact that the modulation method is OOK.

A worthwhile calculation is the output signal to noise ratio of the matched filter when the signal to noise ratio within the 8 Hz loop bandwidth is 6 dB. The following calculation is an approximation. Assuming that the noise power is directly proportional

to bandwidth, and the data filter employed is 256 Hz wide in order to pass 511 chips/s, then the signal to noise ratio in this bandwidth will be -9 dB. With a processing gain of 511, the output signal to noise ratio from the matched filter will be 18 dB. From fig. 6.6, this will give an exceptionally low word error rate. This means that it is the demodulation method, and not the signal to noise ratio within the data bandwidth which is ultimately limiting performance.

### 6.5.2. Despreading

The signal is despread by parallel correlation with a reference m-sequence, ie. matched filtered. We have already decided to use a spreading gain of 511, therefore it might seem that we require a 511 tap filter. However, in order to reduce the maximum timing offset between the transmitted and the reference m-sequence to a fraction of one chip, it is necessary to oversample. Failure to reduce the maximum timing offset to a fraction of one chip will result in significant degradation in the signal to noise ratio at the output of the matched filter [14]. If we oversample by a factor of four, this means that we require a filter with 2044 taps. There are four possibilities for the implementation of this matched filter, discussed below.

The first method for implementing this filter is using commercially available matched filters from manufacturers such as INMOS, TRW and MEDL [92]. These devices can operate at extremely fast chip rates relative to the chip rate we wish to use. However, these devices have relatively few taps per package. These packages are cascadable to form filters with more taps. The drawback in using these devices for this application is the cost. The cheapest of these devices costs £54 for a 128 tap device. We would require 16 of these devices to implement the matched filter in the proposed system.

This would add substantially to the cost of each receiver.

The second method for implementing the matched filter despreading is to use a recirculating correlator based around a first in first out (FIFO) delay line as shown in fig. 6.10. The correlator in fig. 6.10 is a three bit (eight level) design. This architecture works by implementing a serial correlation on reception of each chip. The circuitry required to implement this architecture is relatively complex, but inexpensive. It does require relatively high clock rates, the fastest clock rate used to circulate the chips is approximately:-

$$C_r^2 O \quad (6.15)$$

$C_r$  is the chip rate and  $O$  is the oversampling. If  $C_r = 511/s$  and  $O = 4$  as previously assumed, then the maximum clock rate is 1 MHz. This is a very modest clock rate by current standards. A correlator based on this architecture was built during the course of this project and demonstrated to work. However, the complex timing logic and the large package count take their toll on design time, operational reliability and cost.

A third method for the implementation of this matched filter is to design an application specific integrated circuit (ASIC). A matched filter ASIC was designed by G. M. Blair [42] in connection with this project. This ASIC had several novel design features. However, this device has not been fabricated. Fabricating this device would only be economically viable if a large number of receivers was envisaged.

The final method for implementing the despreading matched filter is to sample the demodulated signal and do the matched filtering operation in software on a computer. By adding a small amount of hardware to the demodulating phase locked loop, we can generate a signal which indicates when the loop is locked. When this "in-lock" signal becomes true, the data output from the phase-locked loop can be sampled using a clock which can be exactly matched with the transmitter clock provided the probability of cycle slips in the phase locked loop is low. These samples should be stored until the maximum

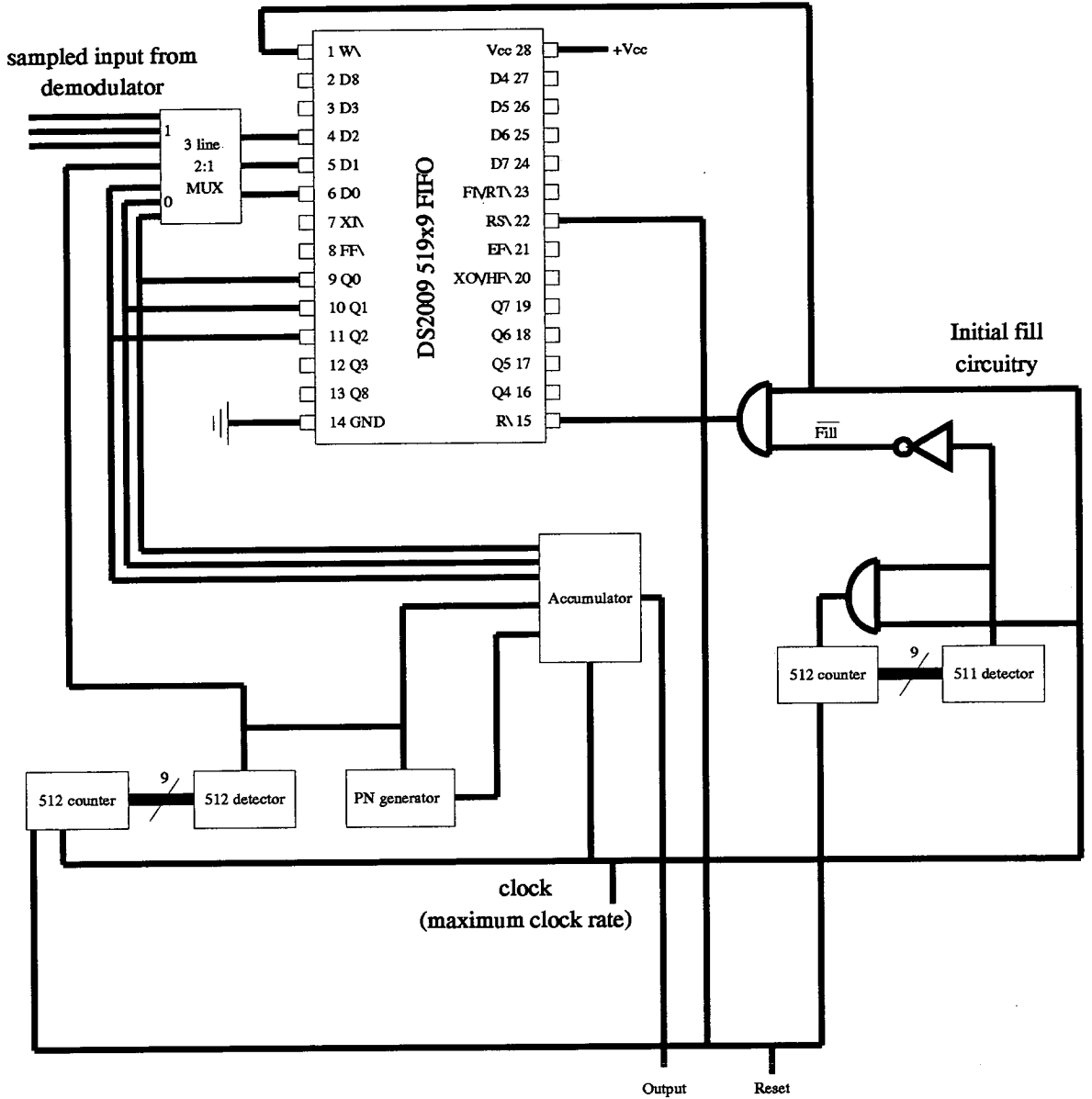


Fig. 6.10: A recirculating correlator.

length of a transmission is reached or the "in-lock" signal lost. The matched filtering operation can then be done on the computer. This method has many advantages. The non-linear devices discussed in chapters 3-5 can easily be implemented in software. The matched filtering operation does not have to be done in real time. Subsequent operations are also easy to implement in software. This method is effectively cost free, since the computer is required anyway to store and look up records for the clients and drive the auto-dial modem to call for help. In the following sections, we shall assume that the despreading operation is to be done in software.

### 6.5.3. Synchronisation

If we choose to use the software method of despreading the signal, then synchronisation will also be carried out in software. Having despread the signal using a matched filter, synchronisation is just a matter of extracting the positive or negative peaks from the correlation function. Providing the sampling process has not significantly distorted the signal in the time domain, this peak extraction is simple. There will be no significant time domain distortion of the signal if the sampling clock is an exact replica of the one used to generate the signal. This can be achieved by deriving the sampling clock from the VCO output in the phase locked loop. Providing the probability of cycle slips in the phase locked loop is low (as it will be if the 6 dB loop signal to noise ratio criterion is met), the VCO output can be used to reconstruct the transmission carrier, ie a signal directly related to one in the transmitter. The correlation peaks can be extracted by using a sliding comb structure which sums the modulus of samples which are 511 times  $O$  apart throughout the length of the stored signal. This operation should be repeated with an offset varying from 0 to 511 times  $O$  samples from the first stored sample, ie sliding the



comb along. The offset which gives the largest sum is the synchronisation point, and the transmitted bits can then be extracted.

A criterion can be set for no peaks found, for example if the sum of the largest offset from the sliding comb structure is not significantly bigger than the average sum. This enables us to detect when the phase locked loop is locking to a signal which is not generated by a transmitter from that particular system. This means we can detect when the receiver is being jammed.

#### **6.5.4. Error correction**

Error correction using the block code discussed in section 6.4.1 can most easily be achieved by generating a look up table to be stored on the receiver computer. The 20 bit received word can be used to look up the 12 transmitted information bits. In the particular case of the block code discussed in section 6.4.1, the Hamming bound (equation 6.2) is not an equality. Thus some received words cannot be uniquely decoded into 12 information bits. Because of the expected low error rates, the incidence of receiver words which cannot be decoded should be very low. If a receiver word which cannot be decoded is received, the receiver will have to wait for a repeat transmission to take any action.

### 6.5.5. Appropriate action

The appropriate action that the receiver computer should take for the variety of circumstances generated by the receiver circuitry is best illustrated by the flow chart in fig. 6.11.

A description of each of the action boxes is listed below.

#### Action A

If this action box is reached then the receiver is being jammed. The received signal should be recorded and stored for inspection and the system manager called by modem.

#### Action B

If this action box is reached, then the received word is not uniquely decodable. The receiver should wait for a re-transmission of the signal. This event is so unlikely that if it occurs twice in succession the system manager should be called by modem.

#### Action C

If this action box is reached then an alarm signal has been received. The receiver computer should start calling the list of respondents for the appropriate client by modem. These modem calls should only be considered answered if the respondent gives some indication of intelligent response, eg. putting down the receiver at a certain point in time or typing a code on their telephone. This avoids the possibility of children or a machine answering the telephone and not obtaining help for the client. If the respondent does not answer or fails to generate the required intelligent response, then the computer should call the next respondent on the list. The message passed to the respondent should include the name and address of the

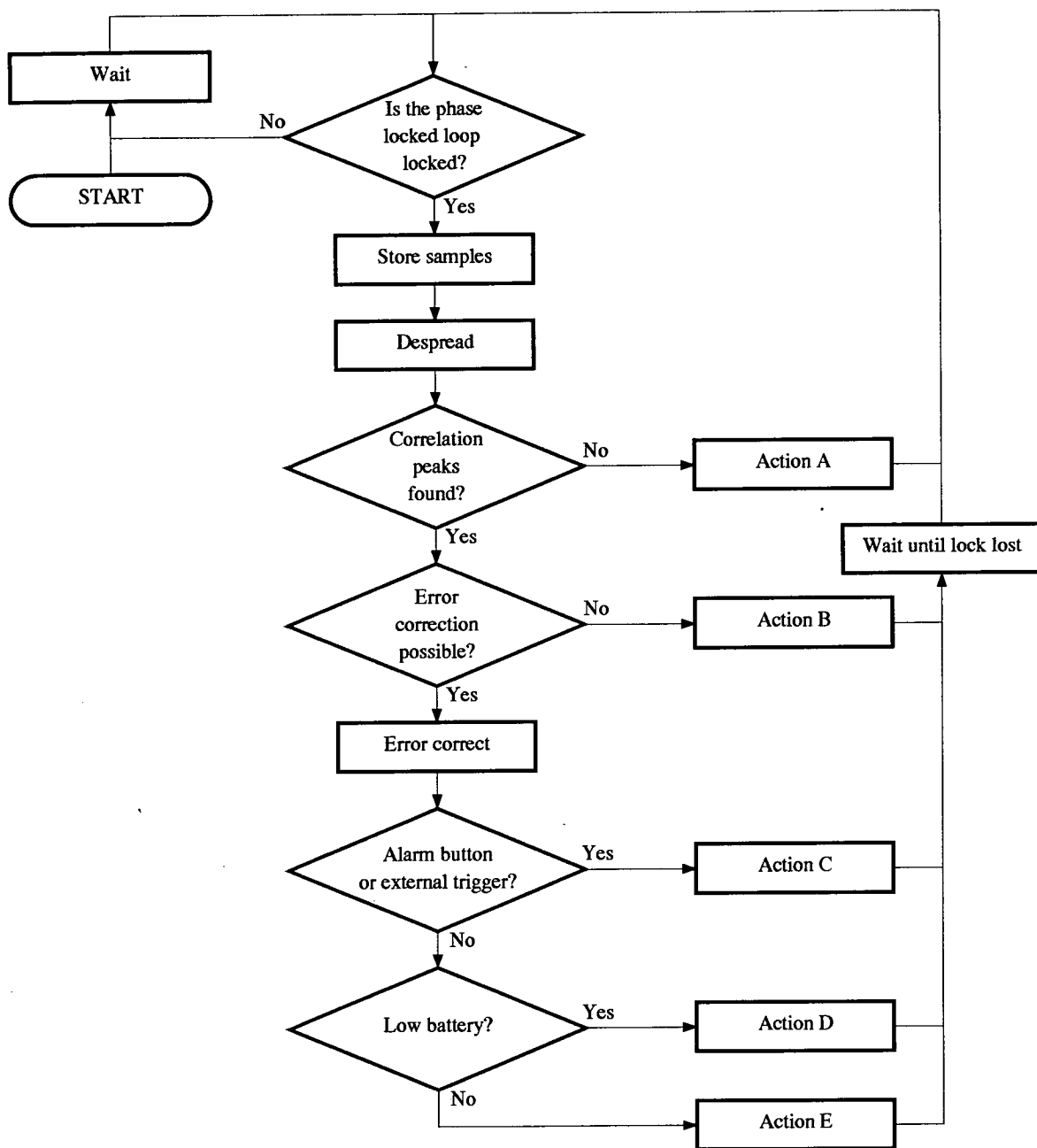


Fig. 6.11: Flow chart for the receiver response.

client and instructions to cancel the alarm when they reach the client. The respondent should be encouraged to listen to all the message to make sure that they receive all the necessary details. If the transmission is not cancelled within a reasonable length of time then the computer should seek another respondent.

#### Action D

If this action box is reached then a transmitter is indicating that its battery is low. This should be noted and brought to the attention of the system manager as soon as possible.

#### Action E

If this action box is reached than a transmitter is cancelling a previous alarm. The computer should call all the respondents that provided intelligent responses to the original alarm. It should interrupt the alarm call if necessary. If this box is reached, but no previous alarm exists, then this should be brought to the system managers attention.

As much information about received signals and action taken by the computer as possible should be stored on the computer and hard copied to a printer. This will facilitate better diagnosis of problems by the system manager. The stored information should contain things like date and time of received signal, an estimate of signal strength, respondents called, length of time until alarm cancelled etc. etc.

An example of a use of this information is if a receiver receives a cancel instruction but no alarm exists this will be brought to the attention of the system manager. By checking the information records, he may find that the alarm signal was received by other receivers and that the signal strength of the cancel signal at that particular receiver was weak. This is a perfectly normal state of affairs and nothing to worry about. Another example of the usefulness of these records is that the recording of a received jamming signal and an estimate of its strength may help in the identification of its source.

It is also very important that all the receivers within a single system can communicate to prevent duplication of alarm calls etc.

## **6.6. Personnel**

As indicated in the previous section, one full-time employee is recommended for each system. This employee shall be termed the system manager. The role of the system manager is very important and carries a large amount of responsibility. His or her duties would include the issuing of transmitters, the maintenance of client records and ensuring the maintenance and regular testing of transmitters including the replacement of transmitter batteries when necessary. The system manager will also have to be on call at all times to deal with receiver faults which could prevent the reception of alarm calls, such as jamming. For this reason, it is important that the system manager has a good understanding of the technical aspects of the system. The integrity of the system depends on the system manager and this should be reflected in the salary and stature offered with the job. The system manager will require a car and a mobile telephone. The cost of the system manager and his equipment is relatively large but, like the receiver costs, is divided amongst a large number of clients.

The most cost effective way of answering alarm calls is using friends, neighbours and volunteers, as used in other successful systems [8, 10]. It is important that the records of helpers for each client is kept up to date. If the receiver goes right through the list of helpers for one particular client without an acceptable response, then it may be possible to get the local police to answer these calls. If this is not possible, then the system manager will have to respond to these calls.

## 6.7. Range

One of the most important parameters when determining the economic success of the system is knowing the reliable range of a transmitter. If a single system can serve a large geographic area, eg. most of a city, then the number of clients will be high and the cost per client low. At first it may seem that we have all the information required to determine the range of the transmitter. We know that we require a 6 dB signal to noise ratio in an 8 Hz bandwidth. We also know that the transmission frequency will be approximately 27 or 35 MHz. Because of the relatively short range of the transmission, the signal will propagate by HF ground wave [85, 93, 94] There are ways of determining the range of HF transmissions, for example using the computer program GRWAVE [95], but these deterministic methods require the following information:-

- The transmission wavelength
- The surface impedance of the ground. This parameter is strongly dependent on the water content of the ground. This means that an HF transmission is dependent on the weather!
- The height above the ground and the type and directionality of the transmit and receive antennas
- The local topography, for example vegetation or urban, obstructions in the propagation path caused by hills etc.

Normally when designing a system of this type it would be prudent to make assumptions based on the expected worst case. In this system it is very difficult to determine a worst case for some of the parameters. Taking the transmission antenna as an example, a typical worst case assumption would normally be that the antenna is omni-

directional. In this particular case it is possible that the aerial becomes directional, but in the wrong direction because of local reflectors or the physical shape of a flexible antenna. Add to this the fact that the propagation of an HF wave is highly dependent on its polarisation and it is impossible to determine a worst case. The noise received at an HF receiver is also a highly variable and site dependent quantity. Therefore the only way to determine the reliable range of the transmitters in the proposed system is by a set of comprehensive measurements.

It is possible to draw comparisons between the proposed DSSS system and the systems currently available. In [1] many of the systems have speech links. To transmit speech, the noise bandwidth must be a minimum of 3 KHz. The noise power in a receiver is directly proportional to the noise bandwidth. Therefore, the system will receive a factor of 375 less noise power in its 8 Hz bandwidth. This does not take into account the fact that speech requires more than 6 dB signal to noise ratio to be intelligible. Adding to this the expected improvement in impulsive noise performance in the system proposed here, the signal to noise ratio in the receiver noise bandwidth in the new system should be around 1000 times greater than these speech systems. Assuming that the range is proportional to the square root of the power (not necessarily true in an HF system) then the range of the new system will be 33 times that of the old speech systems. This will give it a range of a few kilometres. It must be strongly emphasised that the above calculation is no more than an approximation and that several assumptions have been made. It is not known whether or not these speech systems operate under the restrictions imposed by [11]. It is expected that the new system will have much greater range than the old speech systems under the same restrictions. Whether or not this new system can have a range great enough to make a direct radio link economically viable can only be determined by measurement.

**6.8. Chapter summary**

In this chapter we have developed a system design for a DSSS alarm scheme and discussed some of the issues involved in the implementation of this scheme. It is shown that under similar restrictions, the proposed system should operate much better than some of the conventional systems currently in use. Some factors have not been taken into account fully in the new design, for example the effect of impulsive noise on the phase locked loop. It is also very difficult to establish with any certainty the reliable range of the new system.



---

## 7. Conclusions

---

The conclusions from this work can be spilt into three sections. The first section looks at the results obtained for limited precision matched filters. The second section looks at the results obtained for the clip to zero algorithm. The final section looks at the possibility of applying this work to a dispersed alarm scheme working by direct transmission of a spread spectrum system in the HF radio band.

### 7.1. Limited precision matched filters

It has been shown in chapters three and four that limited precision digital matched filters can be designed which have very good performance compared with analogue word matched filters. The number of quantisation levels required to achieve good performance is relatively small. If the quantisation levels are restricted to being linear, then this degrades performance. However, eight quantisation levels will produce a loss of a small fraction of one dB in either the linear or the non linear quantisation level case. This level of performance will almost always be acceptable in a communications system. Unfortunately, the computational time required to find the exact solution for eight level quantisation is too large to be practical. This type of limited precision digital matched filter will have many applications in other spread spectrum systems and in general signal processing.

## **7.2. The clip to zero algorithm**

It is shown in chapter 5 that employing this non linear algorithm before a matched filter produces good performance in impulsive noise. If this clipping is at a fixed level, then this improvement in impulsive noise performance is at the expense of a slight loss in Gaussian noise performance. Adaptive clipping offers the potential for very good performance. However, it is difficult to guarantee the performance of an adaptive system under all circumstances in a time varying environment.

Combining the clip to zero algorithm with limited precision digital matched filters is simple and the resulting performance is better than the worst case performance of the two devices separately. Again, this work should have applications outside the field of this study.

## **7.3. The feasibility of a spread spectrum alarm scheme**

A spread spectrum alarm scheme along the lines of the one described in chapter 6 will provide a large improvement over the radio link in conventional alarm schemes. Indeed, the performance of such a scheme is limited by practical considerations, such as carrier frequency stability and demodulation. The commercial feasibility of a direct transmission spread spectrum alarm scheme can only be decided if the reliable range of transmission is known. Therefore, this must remain an open question until some of the limitations of this work are addressed.

#### 7.4. Limitations of this work and suggestions for future work

It would be interesting to discover the exact performance of the limited digital matched filters with more than six quantisation levels. This could be achieved using the search method described in chapters 3 and 4 by using more processing power. A better way would be to develop an analytical optimisation technique. The basis of such a technique is conceptually simple. It is no more than a constrained optimisation. However, the complexity of the problem expands rapidly with the number of quantisation levels and only if the technique could be automated would there be any chance of obtaining the correct results.

The clip to zero algorithm is only one of several non-linear techniques that could be employed to provide enhanced performance in impulsive noise. Indeed, the limited precision digital matched filters are also non-linear and also provide enhanced performance over their linear (analogue word) equivalents in impulsive noise. To achieve the best performance in all types of noise, an adaptive version of the clip to zero algorithm should be developed. This will mean a study of all the parameters normally associated with adaptive filters, for example residual error and tracking ability. Then it will be possible to compare the performance of the clip to zero algorithm with other non-linear techniques.

To establish exactly the performance of a direct sequence spread spectrum alarm system operating in impulsive noise, more work is required. The effect that impulsive noise has on a phase locked loop is one aspect that could be studied theoretically. To establish the reliable range, it is important that a comprehensive set of measurements is done, under as wide a set of the circumstances as is likely to be encountered.

## References

1. "Alarms for elderly people," *Which?* (November 1989).
2. M. Abrahams, "Falls in the home," 28, *New age* (1985).
3. M. Abrahams, "Falls by the elderly: England and Wales," Age concern Scotland leaflet. (unpublished).
4. "Focus on falls," Age concern Scotland leaflet (1989).
5. A. J. Cambell, B. C. Allen, and G. S. Martinez, "Falls in old age: A study of frequency and related clinical factors," 10, *Age and ageing* (1981).
6. "Older People in the European Community:- some basic facts," Eurolink age leaflet (April 1989).
7. J. Bradshaw, M. Clifton, and J. Kennedy, "Found dead:- a study of old people found dead," Age concern England (1978).
8. "Alarm systems for the elderly: Report of a workshop held at the University of Leeds," Department of social policy and administration, University of Leeds (September 1980).
9. P. Thornton and G. Mountain, "A positive response: Developing community alarm services for older people," *Joseph Rowntree foundation* (1992).
10. S. N. Pockock and K. Grossfield, "A socially acceptable emergency alarm system," *Journal of medical engineering and technology*, 5, 2, pp. 68-72 (March 1981).
11. "Performance specification:- Transmitters and receivers for use in the short range emergency alarm systems for the aged and infirm operating at 27.450, 34.925, 34.950 and 34.975 MHz," Department of trade and industry, Radio-communications division (December 1986).

## REFERENCES

12. BS 5613, "Recommendations for: alarm systems for the elderly and others living at risk," *British standards institute* (1978).
13. C. E. Shannon, "A mathematical theory of communication," *Bell system technical journal*, 27, pp. 379-423 and 623-656 (1948).
14. R. C. Dixon, "Spread spectrum systems," John Wiley and sons, New York (1976).
15. L. A. Gerhart and R. C. Dixon, "Introduction-Special issue on spread spectrum communications," *IEEE transactions on communications*, 25, 8, pp. 745-747 (August 1977).
16. R. A. Scholtz, "The spread spectrum concept," *IEEE transactions on communications*, 25, 8, pp. 748-755 (August 1977).
17. L. Alcuri, G. Mamola, and E. Randazzo, "Asymptotic behaviour of bit error rate for bandpass direct-sequence spread-spectrum modulation systems," *Proceedings of the IEE, Part F*, 135, 5, pp. 487-495 (October 1988).
18. M. P. Ristenbatt, "Performance criteria for spread spectrum communications," *IEEE transactions on communications*, 25, 8, pp. 756-763 (August 1977).
19. D. L. Schilling, R. L. Pickholtz, and L. B. Milstein, "Spread spectrum goes commercial," *IEEE spectrum*, pp. 40-45 (August 1990).
20. L. C. Walters, "Shannon , coding and spread spectrum," *Electronics and wireless world* (March-April 1989).
21. D. J. Torrieri, "Principles of military communication systems," Artech house, Dedham, Massachusetts (1981).
22. G. R. Cooper and C. D. McGillen, "Modern communications and spread spectrum," *McGraw Hill book company*, New York (1986).

## REFERENCES

23. H. Matthews (ed.), "Surface wave filters: design construction and use," *John Wiley and sons*, New York (1977).
24. J. Gwvargiz, P. K. Das, and L. B. Milstein, "Adaptive narrow-band interference rejection in a DS spread-spectrum intercept receiver using transform domain signal processing techniques," *IEEE transactions on communications*, 37, 12, pp. 1359-1366 (December 1989).
25. M. Feldmann and J. Henaff, "Surface acoustic waves for signal processing," Artech house, Dedham, Massachusetts (1986, English translation 1989).
26. D. P. Morgan, "Surface-wave devices for signal processing," Elsevier science publishers, Amsterdam (1985).
27. R. H. Warring, "Radio control for modellers," *Lutterworth press*, London (1981).
28. K. S. Gilhousen, I. M. Jacobs, R. Padovani, A. J. Viterbi, L. A. Weaver, and C. E. Wheatley, "On the capacity of a cellular CDMA system," *IEEE transactions on vehicular technology*, Special issue on digital cellular (November 1990).
29. M. R. Heath and P. Newson, "On the capacity of spread spectrum CDMA for mobile radio," *Proc IEEE vehicular technology conference, Denver Colorado* (May 1992).
30. M. K. Varanasi and B. A. Aazhang, "Multistage detection in asynchronous code-division multiple access communications," *IEEE transactions on communications*, 38, 4, pp. 509-519 (April 1990).
31. A. J. Viterbi, "Very low rate convolutional codes for maximum theoretical performance of spread spectrum multiple-access channels," *IEEE journal on selected areas in communications*, 8, 4, pp. 641-649 (May 1990).
32. P. M. Grant, "Civillian spread spectrum - myth or ultimate reality?," *Electronics & Communication Engineering Journal* (January-February 1991).

## REFERENCES

33. P. K. Enge and D. V. Sarwate, "Spread-spectrum multiple-access performance of orthogonal codes: Impulsive noise," *IEEE transactions on communications*, 36, 1, pp. 98-106 (January 1988).
34. C. R. Cahn, "Performance of digital matched filter correlators with unknown interference," *IEEE transactions on communications*, 19, 6, pp. 1163-1172 (December 1971).
35. C. R. Cahn, "Worst interference for a coherent binary channel," *IEEE transactions on information theory*, 17, pp. 209-210 (March 1971).
36. J. V. Harrington, "An analysis of the detection of repeated signals in noise by binary integration," *IRE transactions on Information Theory*, 1, pp. 1-9 (March 1955).
37. G. Arfken, "Mathematical methods for physicists," Academic press inc., New York (1985).
38. I. G. Stiglitz, "Coding for a class of unknown channels," *IEEE transactions on information technology*, 12, 2, pp. 189-195 (April 1966).
39. W. H. Press, B. P. Flannery, S. A. Teukolsky, and W. T. Vetterling, "Numerical recipes in C - the art of scientific computing," *Cambridge University press*, Cambridge, UK (1988).
40. J. J. Freeman, "The action of dither in a polarity coincidence correlator," *IEEE transactions on communications*, 22, pp. 857-862 (June 1974).
41. M. Miyake, T. Kojima, N. Katoaka, and T. Fujino, "Design and performance of direct-sequence spread-spectrum Modem using soft decision digital matched filter," *Proceedings of the IEEE symposium on spread spectrum techniques and applications, King's College, London England*, pp. 135-139 (September 1990).

## REFERENCES

42. G. M. Blair, "Bit serial correlator with a novel clocking scheme," *Proceedings of the seventeenth European solid state circuits conference*, pp. 157-160 (September 1991).
43. W. W Peterson and E. J. Weldon, "Error correcting codes," *MIT press*, Cambridge, USA (1972).
44. G. L. Turin, "An introduction to digital matched filters," *Proceedings of the IEEE*, 64, 7, pp. 1092-1112 (July 1976).
45. J. Cook, "Peak amplitude of impulsive noise as a function of signalling rate for baseband PAM systems," *American national standards institute telecommunications committee*, Doc. T1E1.4/90-207 (December 1990).
46. M. P. Shinde and S. N. Gupta, "A model of HF atmospheric noise," *IEEE transactions on electromagnetic compatibility*, 16, 2, pp. 71-75 (May 1974).
47. CCIR, "World distribution and characteristics of atmospheric radio noise," *International telecommunication union, Geneva, Switzerland, Rep. 322* (1964).
48. Feldman, D. A., "An atmospheric noise model with application to low frequency navigation systems.," *Ph.D. dissertation, Massachusetts Institute of Technology* (Cambridge 1972).
49. A. D. Spaulding and J. S. Washburn, "Atmospheric radio noise: worldwide levels and other characteristics," *U.S. Department of Commerce, NTIA Report*, pp. 85-173 (1985).
50. D. Middleton, "Statistical-physical models of electromagnetic interference," *IEEE transactions on electromagnetic compatibility*, 19, 3, pp. 106-126 (August 1977).
51. D. Middleton, "Procedures for determining the parameters of the first-order canonical models of class A and class B electromagnetic interference," *IEEE transactions on electromagnetic compatibility*, 21, 3, pp. 190-208 (August 1979).



## REFERENCES

52. A. M. D. Turkmani, "Prediction of error rate in FSK data communications systems subjected to impulsive noise," *Proceedings of the IEE, part F*, 134, pp. 633-642 (December 1987).
53. K. S. Vastola, "Threshold detection in narrow-band non-Gaussian noise," *IEEE transactions on communications*, 32, 2, pp. 134-139 (February 1984).
54. E. C. Bolton, "Simulating LF atmospheric noise at 660, 76, 200KHz," *Office of telecommunications, Technical memorandum OT-TM-97* (1972).
55. J. W. Adams, W. D. Bensema, and M. Kanda, "Electromagnetic noise, Grace mine," *National bureau of standards technical note 654 (U. S.)* (1974).
56. R. A. Shepard, "Measurements of amplitude probability distributions and power of Automobile ignition noise at HF," *IEEE transactions on vehicular technology*, 23, 3, pp. 72-83 (August 1974).
57. W. J. Kennedy and J. E. Gentle, "Statistical computing," *Marcel Dekker inc.*, New York (1980).
58. L. R. Halstead, "On binary data transmission error rates due to combinations of Gaussian and impulsive noise," *IEEE transactions on communications*, 11, 4, pp. 428-435 (December 1963).
59. J. S. Engel, "Digital transmission in the presence of impulsive noise," *Bell systems technical journal*, 44, pp. 1699-1743 (October 1965).
60. V. K. Jain and S. N. Gupta, "Binary baseband signals in combination with continuous and impulsive noise and ISI," *Electronic letters*, 48, pp. 82-83 (February 1978).
61. V. K. Jain and S. N. Gupta, "Error probability of binary signal perturbed by intersymbol interference and impulsive atmospheric noise," *IEEE transactions on electromagnetic compatibility*, 20, 4, pp. 352-353 (May 1978).

## REFERENCES

62. S. N. Gupta and V. K. Jain, "Binary and m-ary communication systems in impulsive atmospheric radio noise in tropics," *Pacific telecommunication conference*, PTG-79, pp. 8-9 (January 1979).
63. S. N. Gupta and V. K. Jain, "Binary communication system performance in atmospheric noise," *Proceedings of the IEE*, 126, 1, pp. 43-44 (January 1979).
64. V. K. Jain and S. N. Gupta, "Digital communication systems in impulsive atmospheric radio noise," *IEEE transaction on aerospace electronic systems*, 15, 2, pp. 228-236 (March 1979).
65. S. N. Gupta and V. K. Jain, "Performance of DPSK systems in impulsive radio noise with intersymbol interference," *Proceedings of the IEEE*, 40, 4, pp. 169-171 (December 1979).
66. V. K. Jain and S. N. Gupta, "Optimum receiver for impulsive atmospheric radio noise," *Proceedings of the IEE*, 128, Pt F, pp. 189-192 (August 1981).
67. V. K. Jain and S. N. Gupta, "Performance of DPSK system in impulsive atmospheric radio noise with varying impulse rates and intersymbol interference," *Electronic letters*, 19, pp. 999-1000 (November 1983).
68. V. K. Jain and S. N. Gupta, "Performance of binary baseband polar signals in white Gaussian and impulsive atmospheric radio noise with varying impulse rates and ISI," *Journal of electrical and electronic engineering*, pp. 65-68 (March 1985).
69. M. Kendall and J. K. Ord, "Time series," *Edward Arnold*, London (1990).
70. A. Gelb, "Applied optimal estimation," *The MIT press*, Cambridge, USA (1989).
71. P. A. Kullstam, "Spread spectrum performance analysis in arbitrary interference," *IEEE transactions on communications*, 25, 8, pp. 848-853 (August 1977).

## REFERENCES

72. B. Aazhang and H. V. Poor, "Performance of DS/SSMA Communications in impulsive channels - Part I: Linear correlation receivers," *IEEE transactions on communications*, 35, 11, pp. 1179-1188 (November 1987).
73. B. Aazhang and H. V. Poor, "Performance of DS/SSMA Communications in impulsive channels - Part II: Hard-Limiting Correlation Receivers," *IEEE transactions on communications*, 36, 1, pp. 88-97 (January 1988).
74. B. Aazhang and H. V. Poor, "An Analysis of Nonlinear Direct-Sequence Correlators," *IEEE transactions on communications*, 37, 7, pp. 723-731 (July 1989).
75. J. K. Patel and C. B. Read, "Handbook of the normal distribution," Marcel Dekker inc., New York (1982).
76. W. R. Bennett, "Introduction to Signal Transmission," *McGraw-Hill Book Company*, New York (1970).
77. International Quartz Devices, "Shortform crystal catalogue 1991/92," *IQD Limited* (1991).
78. D. Sakrison, "Communication theory: transmission of waveforms and digital information," *John Wiley and sons*, New York (1968).
79. P. F. Panter, "Modulation noise, and spectral analysis," *McGraw-Hill book company*, New York (1965).
80. A. Grumet, "Demodulation effect of an envelope detector at low signal to noise ratios," *Proceedings of the institute of radio engineers*, 50, 10, pp. 2133-2134 (October 1962).
81. J. G. Proakis, "Digital communications," *McGraw-Hill book company*, New York (1983).

## REFERENCES

82. J. P. Costas, "Synchronous communications," *Proceedings of the institute of radio engineers*, 44, 12, pp. 1713-1718 (December 1956).
83. W. C. Y. Lee, "Mobile communications engineering," *McGraw-Hill*, New York (1982).
84. V. H. MacDonald, "The cellular concept," *Bellsystems technical journal*, 58, 1, pp. 15-42 (January 1979).
85. N. Maslin, "HF communications: a systems approach," *Pitman publishing*, London (1987).
86. P. M. Grant, C. F. N. Cowan, B. Mulgrew, and J. H. Dripps, "Signal processing and coding," *Chartwell-Bratt*, Bromley, UK (1989).
87. T. G. Robertazzi, "Computer networks and systems: queueing theory and performance evaluation," *Springer-Verlag*, New York (1990).
88. G. J. King, "Radio circuits explained," *Newnes technical books*, London (1971).
89. H. I. F. Peel, "Radio for Examination," *Cleaver-Hume press limited*, London (1961).
90. A. J. Viterbi, "Principles of coherent communications," *McGraw-Hill book company*, New York (1975).
91. A. J. Viterbi, "Phase-locked loop dynamics in the presence of noise by Fokker-Planck techniques," *Proceedings of the IEEE*, 51, 12, pp. 1737-1753 (December 1963).
92. J. Eldon, "Correlation... A powerful technique for digital signal processing," *TRW LSI products Inc.* (1981).
93. S. Rotheram, "Ground-wave propagation part 1: Theory for short distances," *Proceedings of the IEE part F*, 128, 5, pp. 275-284 (October 1981).

## REFERENCES

94. S. Rotheram, "Ground-wave propagation part 2: Theory for medium and long distances and reference propagation curves," *Proceedings of the IEE part F*, 128, 5, pp. 285-295 (October 1981).
95. CCIR, "Ground wave propagation curves for frequencies between 10 kHz and 30 MHz," *Recommendation 368-3, study group 5, ITU, Kyoto* (1978).

---

## **Appendix A: Verified m-sequences**

---

This appendix contains lists of m-sequences that have been verified by checking the autocorrelation function of each potential code up to a code length of 8192. This list is exhaustive. Each code is given as a list of the taps which should be EX-ORed together as the feedback term for a shift register m-sequence generator. The taps are numbered from the input (tap 1) to the output (tap N).

## APPENDIX A: VERIFIED M-SEQUENCES

taps = 2 code length = 3 total no. codes = 1

[1 2]

taps = 3 code length = 7 total no. codes = 2

[1 3] and [2 3]

taps = 4 code length = 15 total no. codes = 2

[1 4] and [3 4]

taps = 5 code length = 31 total no. codes = 6

[2 5], [3 5], [1 2 3 5], [1 2 4 5], [1 3 4 5] and [2 3 4 5]

taps = 6 code length = 63 total no. codes = 6

[1 6], [1 3 4 6], [5 6], [1 2 5 6], [2 3 5 6] and [1 4 5 6]

taps = 7 code length = 127 total no. codes = 18

[1 7], [3 7], [1 2 3 7], [4 7], [2 3 4 7], [1 2 5 7], [1 3 5 7], [3 4 5 7], [1 2 3 4 5 7], [6 7], [1 3 6 7], [1 4 6 7], [2 4 6 7], [2 5 6 7], [1 2 3 5 6 7], [4 5 6 7], [1 2 4 5 6 7] and [2 3 4 5 6 7]

taps = 8 code length = 255 total no. codes = 16

[2 3 4 8], [1 3 5 8], [2 3 5 8], [2 3 6 8], [1 2 3 4 6 8], [1 5 6 8], [2 5 6 8], [3 5 6 8], [4 5 6 8], [1 2 7 8], [2 3 7 8], [3 5 7 8], [1 6 7 8], [1 2 3 6 7 8], [1 2 5 6 7 8] and [2 4 5 6 7 8]

taps = 9 code length = 511 total no. codes = 48

[4 9], [1 3 4 9], [5 9], [2 3 5 9], [1 4 5 9], [3 4 6 9], [1 2 3 4 6 9], [3 5 6 9], [1 2 3 5 6 9], [1 2 4 5 6 9], [2 3 4 5 6 9], [1 2 7 9], [2 4 7 9], [1 5 7 9], [2 5 7 9], [1 2 3 5 7 9], [1 2 4 5 7 9], [2 3 4 5 7 9], [1 2 3 6 7 9], [4 6 7 9], [1 3 4 6 7 9], [2 4 5 6 7 9], [3 4 5 6 7 9], [1 4 8 9], [2 4 8 9], [1 2 3 4 8 9], [1 5 8 9], [4 5 8 9], [1 3 4 5 8 9], [1 2 3 6 8 9], [1 3 4 6 8 9], [5 6 8 9], [1 3 5 6 8 9], [2 3 5 6 8 9], [1 4 5 6 8 9], [1 2 3 4 5 6 8 9], [2 7 8 9], [1 2 3 7 8 9], [2 4 5 7 8 9], [3 4 5 7 8 9], [1 2 6 7 8 9], [1 3 6 7 8 9], [2 3 6 7 8 9], [2 4 6 7 8 9], [3 4 6 7 8 9], [1 5 6 7 8 9], [3 5 6 7 8 9] and [1 3 4 5 6 7 8 9]

taps = 10 code length = 1023 total no. codes = 60

[3 10], [1 3 4 10], [1 2 5 10], [2 3 5 10], [2 5 6 10], [1 2 3 5 6 10], [7 10], [1 3 7 10], [2 6 7 10], [1 2 4 6 7 10], [1 2 5 6 7 10], [1 4 5 6 7 10], [1 2 3 4 5 6 7 10], [2 3 8 10], [3 4 8 10], [1 5 8 10], [4 5 8 10], [2 3 4 5 8 10], [1 6 8 10], [1 2 4 6 8 10], [1 3 5 6 8 10], [2 7 8 10], [1 2 3 7 8 10], [1 2 4 7 8 10], [5 7 8 10], [1 2 6 7 8 10], [2 5 6 7 8 10], [1 2 4 5 6 7 8 10], [1 3 4 5 6 7 8 10], [1 4 9 10], [2 4 9 10], [2 5 9 10], [1 2 4 5 9 10], [1 6 9 10], [1 2 3 6 9 10], [1 3 4 6 9 10], [3 4 5 6 9 10], [1 2 3 4 5 6 9 10], [3 7 9 10], [2 4 5 7 9 10], [6 7 9 10], [1 4 6 7 9 10], [1 2 3 4 6 7 9 10], [2 3 4 5 6 7 9 10], [1 2 4 8 9 10], [2 3 4 8 9 10], [5 8 9 10], [3 4 5 8 9 10], [1 2 6 8 9 10], [2 3 6 8 9 10], [2 4 6 8 9 10], [3 4 6 8 9 10], [1 5 6 8 9 10], [2 3 4 5 6 8 9 10], [2 3 7

## APPENDIX A: VERIFIED M-SEQUENCES

89 10],[14789 10],[45789 10],[1346789 10],[1456789 10] and [3456789 10]

taps = 11 code length = 2047 total no. codes = 176

[2 11],[124 11],[135 11],[235 11],[126 11],[156 11],[256 11],[456 11],[13456 11],[237 11],[247 11],[12347 11],[357 11],[457 11],[12367 11],[467 11],[567 11],[12567 11],[13567 11],[24567 11],[238 11],[148 11],[258 11],[358 11],[13458 11],[23458 11],[268 11],[368 11],[468 11],[13468 11],[14568 11],[24568 11],[1234568 11],[178 11],[12378 11],[13578 11],[23578 11],[34578 11],[12678 11],[34678 11],[25678 11],[1245678 11],[9 11],[129 11],[149 11],[249 11],[359 11],[369 11],[569 11],[23569 11],[34569 11],[1234569 11],[279 11],[479 11],[23479 11],[12579 11],[13579 11],[14579 11],[24579 11],[24679 11],[1234679 11],[35679 11],[1235679 11],[45679 11],[1345679 11],[189 11],[389 11],[489 11],[14589 11],[1234589 11],[689 11],[13689 11],[34689 11],[1234689 11],[25689 11],[1235689 11],[2345689 11],[12789 11],[13789 11],[14789 11],[24789 11],[1235789 11],[1245789 11],[2345789 11],[36789 11],[1346789 11],[2346789 11],[1256789 11],[2356789 11],[13 10 11],[23 10 11],[34 10 11],[1234 10 11],[1246 10 11],[56 10 11],[1356 10 11],[1456 10 11],[27 10 11],[37 10 11],[1247 10 11],[1347 10 11],[2347 10 11],[1457 10 11],[123457 10 11],[1267 10 11],[2367 10 11],[1467 10 11],[2467 10 11],[1567 10 11],[3567 10 11],[124567 10 11],[18 10 11],[1238 10 11],[2348 10 11],[1258 10 11],[2358 10 11],[68 10 11],[1268 10 11],[2468 10 11],[3468 10 11],[1568 10 11],[123568 10 11],[4568 10 11],[1478 10 11],[123478 10 11],[3578 10 11],[134578 10 11],[234578 10 11],[3678 10 11],[124678 10 11],[134678 10 11],[5678 10 11],[125678 10 11],[245678 10 11],[29 10 11],[2349 10 11],[59 10 11],[1259 10 11],[1359 10 11],[1459 10 11],[3459 10 11],[1269 10 11],[1369 10 11],[2469 10 11],[123469 10 11],[4569 10 11],[134569 10 11],[234569 10 11],[79 10 11],[1479 10 11],[123479 10 11],[1579 10 11],[134579 10 11],[123679 10 11],[234679 10 11],[145679 10 11],[345679 10 11],[1389 10 11],[3489 10 11],[4589 10 11],[124589 10 11],[234689 10 11],[135689 10 11],[235689 10 11],[245689 10 11],[1789 10 11],[4789 10 11],[124789 10 11],[134789 10 11],[125789 10 11],[235789 10 11],[245789 10 11],[236789 10 11],[146789 10 11],[256789 10 11] and [356789 10 11]

taps = 12 code length = 4095 total no. codes = 144

[146 12],[356 12],[13456 12],[23456 12],[347 12],[467 12],[13567 12],[128 12],[12348 12],[158 12],[13458 12],[12368 12],[12468 12],[568 12],[13568 12],[278 12],[14578 12],[34678 12],[1234678 12],[239 12],[12459 12],[23459 12],[12569 12],[14569 12],[1234569 12],[34579 12],[679 12],[13679 12],[12389 12],[23489 12],[589 12],[34589 12],[1234589 12],[23689 12],[45689 12],[34789 12],[15789 12],[35789 12],[12 10 12],[45 10 12],[1245 10 12],[1236 10 12],[2346 10 12],[1256 10 12],[2456 10 12],[1257 10 12],[2357 10 12],[1467 10 12],[1238 10 12],[2348 10 12],[2368 10 12],[1478 10 12],[2678 10 12],[124678 10 12],[234678 10 12],[135678 10 12],[39 10 12],[1269 10 12],[2469 10 12],[3469 10 12],[2579 10 12],[234579 10 12],[2489 10 12],[3489 10 12],[1689 10 12],[2689 10 12],[245689 10 12],[3789 10 12],[235789 10 12],[145789 10 12],[12345789 10 12],[6789 10 12],[1246 11 12],[2346 11 12],[47 11 12],[1247 11 12],[3457 11 12],[123567 11 12],[1348 11 12],[2458 11 12],[68 11 12],[2568 11 12],[134568 11 12],[1378 11 12],[4578 11 12],[234578 11 12],[3678 11 12],[123678 11 12],[125678 11 12],[1349 11 12],[1359 11 12],[1459 11 12],[3569 11 12],[1379 11 12],[4679 11 12],[5679 11 12],[245679 11 12],[1389 11 12],[1489 11 12],[123489 11 12],[124689 11 12],[4789 11 12],[125789 11 12],[12345789 11 12],[6789 11 12],[146789 11 12],[2 10 11 12],[4 10 11 12],[124 10 11 12],[125 10 11 12],[236 10 11 12],[127 10 11 12],[12347 10 11 12],[257 10 11 12],[13457 10 11 12],[267 10 11 12],[367 10 11 12],[12367 10 11 12],[14567 10 11 12],[128 10 11 12],[158 10 11 12],[168 10 11 12],[468 10 11 12],[13468 10 11 12],[24568 10 11 12],[278 10 11 12],[378 10 11 12],[249 10 11 12],[349 10 11 12],[12359 10 11 12],[269 10 11 12],[469 10 11 12],[12569 10 11 12],[14569 10 11 12],[12379 10 11 12],[15679 10 11 12],[489 10 11 12],[13489 10 11 12],[12589 10 11 12],[45689 10 11 12],[34789 10 11 12],[1345789 10 11 12],[2345789 10 11 12],[36789 10 11 12],

taps = 13 code length = 8191 total no. codes = 630



## APPENDIX A: VERIFIED M-SEQUENCES

[13413],[12513],[24513],[14613],[25613],[1235613],[13713],[23713],[1234713],[25713],[1235713],[1345713],[2345713],[16713],[36713],[56713],[1456713],[23813],[24813],[35813],[1235813],[1345813],[16813],[1256813],[1356813],[3456813],[37813],[1247813],[2347813],[123457813],[67813],[1267813],[2367813],[123467813],[1567813],[4567813],[134567813],[34913],[25913],[1245913],[2345913],[16913],[1346913],[2346913],[3456913],[123456913],[37913],[1247913],[1347913],[1457913],[123457913],[2367913],[123567913],[124567913],[134567913],[28913],[1258913],[1358913],[1268913],[2468913],[3468913],[123568913],[4568913],[234568913],[1278913],[2378913],[2478913],[1578913],[3578913],[4578913],[124578913],[134578913],[5678913],[235678913],[345678913],[131013],[141013],[12341013],[251013],[351013],[23451013],[461013],[12461013],[561013],[23561013],[1234561013],[171013],[13471013],[23471013],[24571013],[1234571013],[671013],[12671013],[13671013],[15671013],[381013],[12481013],[23481013],[581013],[23581013],[34581013],[14681013],[24681013],[15681013],[45681013],[1245681013],[12781013],[13781013],[24781013],[34781013],[1234781013],[1235781013],[2345781013],[26781013],[1236781013],[1246781013],[1356781013],[191013],[291013],[491013],[23591013],[1234591013],[13691013],[14691013],[34691013],[35691013],[1245691013],[1345691013],[12791013],[14791013],[34791013],[45791013],[1245791013],[2345791013],[16791013],[1356791013],[2456791013],[14891013],[35891013],[1345891013],[1236891013],[1246891013],[2346891013],[1356891013],[1456891013],[3456891013],[17891013],[47891013],[57891013],[3457891013],[1267891013],[1367891013],[123467891013],[123567891013],[4567891013],[121113],[341113],[12341113],[151113],[451113],[13451113],[23451113],[261113],[12561113],[24561113],[271113],[13571113],[23571113],[1234571113],[23671113],[24671113],[1234671113],[15671113],[35671113],[1345671113],[381113],[12381113],[481113],[13481113],[13581113],[24581113],[1234581113],[681113],[13681113],[24681113],[1245681113],[2345681113],[781113],[14781113],[1234781113],[1235781113],[1245781113],[2345781113],[16781113],[1246781113],[1456781113],[2456781113],[191113],[12391113],[23491113],[591113],[14591113],[24591113],[23691113],[35691113],[1235691113],[45691113],[1345691113],[2345691113],[25791113],[35791113],[45791113],[26791113],[1246791113],[1346791113],[1356791113],[1456791113],[891113],[24891113],[15891113],[25891113],[1235891113],[1245891113],[16891113],[36891113],[2356891113],[123456891113],[27891113],[1247891113],[1347891113],[2357891113],[1457891113],[3467891113],[2567891113],[234567891113],[123101113],[5101113],[135101113],[235101113],[12345101113],[6101113],[236101113],[456101113],[137101113],[237101113],[247101113],[157101113],[12357101113],[23457101113],[267101113],[467101113],[12467101113],[567101113],[12567101113],[13567101113],[238101113],[348101113],[358101113],[12358101113],[12458101113],[13458101113],[268101113],[13468101113],[12568101113],[24568101113],[378101113],[12378101113],[12578101113],[13578101113],[24578101113],[15678101113],[45678101113],[2345678101113],[129101113],[149101113],[249101113],[359101113],[369101113],[12369101113],[13469101113],[23469101113],[569101113],[13569101113],[12379101113],[479101113],[12479101113],[23479101113],[13579101113],[14579101113],[34579101113],[1234679101113],[1345679101113],[2345679101113],[289101113],[389101113],[489101113],[12489101113],[1234589101113],[689101113],[13689101113],[23689101113],[34689101113],[1234689101113],[25689101113],[35689101113],[24789101113],[25789101113],[1235789101113],[45789101113],[1236789101113],[2346789101113],[1256789101113],[2356789101113],[2456789101113],[123456789101113],[121213],[241213],[341213],[12351213],[361213],[12361213],[12561213],[34561213],[1234561213],[471213],[571213],[24571213],[1234571213],[671213],[14671213],[34671213],[25671213],[1235671213],[281213],[12381213],[24581213],[12681213],[23681213],[1234681213],[15681213],[45681213],[1345681213],[15781213],[35781213],[1245781213],[26781213],[36781213],[1346781213],[56781213],[1356781213],[2356781213],[1456781213],[123456781213],[391213],[12391213],[23491213],[12591213],[34591213],[13691213],[14691213],[34691213],[25691213],[791213],[14791213],[34791213],[1234791213],[35791213],[1245791213],[1345791213],[16791213],[1246791213],[1346791213],[1256791213],[12891213],[24891213],[1235891213],[46891213],[2346891213],[2456891213],[1247891213],[1347891213],[1357891213],[3457891213],[67891213],[1267891213],[2467891213],[1567891213],[2567891213],[124567891213],[134567891213],[3101213],[134101213],[125101213],[6101213],[236101213],[123

## APPENDIX A: VERIFIED M-SEQUENCES

4 6 10 12 13], [3 5 6 10 12 13], [1 2 4 5 6 10 12 13], [1 3 4 5 6 10 12 13], [1 2 7 10 12 13], [1 4 7 10 12 13], [3 4 7 10 12 13], [2 5 7 10 12 13], [2 3 4 5 7 10 12 13], [3 6 7 10 12 13], [1 3 4 6 7 10 12 13], [1 2 5 6 7 10 12 13], [3 4 5 6 7 10 12 13], [2 3 8 10 12 13], [1 2 3 4 8 10 12 13], [2 5 8 10 12 13], [4 5 8 10 12 13], [1 2 4 5 8 10 12 13], [2 6 8 10 12 13], [1 2 3 6 8 10 12 13], [2 3 4 6 8 10 12 13], [2 3 5 6 8 10 12 13], [1 4 5 6 8 10 12 13], [1 2 3 4 5 6 8 10 12 13], [2 3 4 7 8 10 12 13], [5 7 8 10 12 13], [3 4 5 7 8 10 12 13], [2 3 6 7 8 10 12 13], [2 4 6 7 8 10 12 13], [3 4 6 7 8 10 12 13], [1 5 6 7 8 10 12 13], [3 5 6 7 8 10 12 13], [1 2 3 5 6 7 8 10 12 13], [9 10 12 13], [1 3 9 10 12 13], [1 2 3 4 9 10 12 13], [2 5 9 10 12 13], [1 2 3 5 9 10 12 13], [1 3 4 5 9 10 12 13], [3 6 9 10 12 13], [4 6 9 10 12 13], [1 3 4 6 9 10 12 13], [1 4 5 6 9 10 12 13], [2 4 5 6 9 10 12 13], [4 7 9 10 12 13], [1 3 4 7 9 10 12 13], [2 3 4 7 9 10 12 13], [2 3 5 7 9 10 12 13], [1 3 6 7 9 10 12 13], [1 4 6 7 9 10 12 13], [2 4 6 7 9 10 12 13], [1 5 6 7 9 10 12 13], [1 2 3 5 6 7 9 10 12 13], [2 8 9 10 12 13], [1 2 3 8 9 10 12 13], [1 3 4 8 9 10 12 13], [5 8 9 10 12 13], [2 3 5 8 9 10 12 13], [3 4 5 8 9 10 12 13], [6 8 9 10 12 13], [1 2 6 8 9 10 12 13], [1 4 6 8 9 10 12 13], [4 5 6 8 9 10 12 13], [1 2 4 5 6 8 9 10 12 13], [1 3 7 8 9 10 12 13], [2 4 7 8 9 10 12 13], [3 4 7 8 9 10 12 13], [1 5 7 8 9 10 12 13], [2 6 7 8 9 10 12 13], [1 2 3 6 7 8 9 10 12 13], [4 6 7 8 9 10 12 13], [1 2 4 6 7 8 9 10 12 13], [2 3 4 6 7 8 9 10 12 13], [5 6 7 8 9 10 12 13], [1 4 5 6 7 8 9 10 12 13], [1 1 11 12 13], [2 11 12 13], [1 2 4 11 12 13], [2 3 4 11 12 13], [1 2 5 11 12 13], [1 4 5 11 12 13], [1 3 6 11 12 13], [3 4 6 11 12 13], [3 5 6 11 12 13], [4 5 6 11 12 13], [1 5 7 11 12 13], [4 5 7 11 12 13], [1 3 4 5 7 11 12 13], [3 6 7 11 12 13], [1 2 3 6 7 11 12 13], [5 6 7 11 12 13], [1 4 5 6 7 11 12 13], [3 4 5 6 7 11 12 13], [8 11 12 13], [1 2 8 11 12 13], [1 3 8 11 12 13], [1 4 8 11 12 13], [4 5 8 11 12 13], [1 2 3 6 8 11 12 13], [1 2 5 6 8 11 12 13], [2 3 5 6 8 11 12 13], [1 7 8 11 12 13], [2 7 8 11 12 13], [1 2 4 7 8 11 12 13], [5 7 8 11 12 13], [1 2 5 7 8 11 12 13], [2 3 5 7 8 11 12 13], [1 3 6 7 8 11 12 13], [2 3 6 7 8 11 12 13], [1 4 6 7 8 11 12 13], [1 2 3 5 6 7 8 11 12 13], [1 2 4 5 6 7 8 11 12 13], [2 3 4 5 6 7 8 11 12 13], [1 2 9 11 12 13], [3 5 9 11 12 13], [1 2 3 5 9 11 12 13], [2 3 4 5 9 11 12 13], [4 6 9 11 12 13], [2 3 4 6 9 11 12 13], [5 6 9 11 12 13], [1 2 5 6 9 11 12 13], [1 4 5 6 9 11 12 13], [2 4 5 6 9 11 12 13], [3 7 9 11 12 13], [3 4 5 7 9 11 12 13], [1 2 3 4 5 7 9 11 12 13], [2 3 6 7 9 11 12 13], [1 4 6 7 9 11 12 13], [2 4 6 7 9 11 12 13], [1 2 3 4 6 7 9 11 12 13], [2 5 6 7 9 11 12 13], [3 5 6 7 9 11 12 13], [1 3 4 5 6 7 9 11 12 13], [4 8 9 11 12 13], [1 3 5 8 9 11 12 13], [2 3 5 8 9 11 12 13], [2 4 5 8 9 11 12 13], [1 2 3 4 5 8 9 11 12 13], [1 4 6 8 9 11 12 13], [3 4 6 8 9 11 12 13], [1 5 6 8 9 11 12 13], [2 5 6 8 9 11 12 13], [1 2 3 5 6 8 9 11 12 13], [4 5 6 8 9 11 12 13], [1 2 4 5 6 8 9 11 12 13], [1 3 7 8 9 11 12 13], [3 4 7 8 9 11 12 13], [2 5 7 8 9 11 12 13], [3 5 7 8 9 11 12 13], [1 2 4 5 7 8 9 11 12 13], [1 3 4 5 7 8 9 11 12 13], [4 6 7 8 9 11 12 13], [1 2 5 6 7 8 9 11 12 13], [1 4 5 6 7 8 9 11 12 13], [1 2 3 4 5 6 7 8 9 11 12 13], [2 3 10 11 12 13], [1 4 10 11 12 13], [2 4 10 11 12 13], [1 2 3 4 10 11 12 13], [1 5 10 11 12 13], [2 5 10 11 12 13], [1 3 4 5 10 11 12 13], [1 2 3 6 10 11 12 13], [2 3 4 6 10 11 12 13], [2 3 5 6 10 11 12 13], [1 7 10 11 12 13], [1 2 3 7 10 11 12 13], [2 3 4 7 10 11 12 13], [1 2 5 7 10 11 12 13], [1 3 5 7 10 11 12 13], [3 4 5 7 10 11 12 13], [1 2 6 7 10 11 12 13], [3 5 6 7 10 11 12 13], [1 3 4 5 6 7 10 11 12 13], [2 3 4 5 6 7 10 11 12 13], [1 8 10 11 12 13], [1 2 4 8 10 11 12 13], [1 3 4 8 10 11 12 13], [5 8 10 11 12 13], [2 3 5 8 10 11 12 13], [1 4 5 8 10 11 12 13], [2 4 5 8 10 11 12 13], [6 8 10 11 12 13], [2 3 6 8 10 11 12 13], [2 5 6 8 10 11 12 13], [3 5 6 8 10 11 12 13], [2 3 4 5 6 8 10 11 12 13], [7 8 10 11 12 13], [2 4 7 8 10 11 12 13], [4 5 7 8 10 11 12 13], [1 2 4 5 7 8 10 11 12 13], [1 6 7 8 10 11 12 13], [4 6 7 8 10 11 12 13], [1 3 4 6 7 8 10 11 12 13], [1 2 5 6 7 8 10 11 12 13], [1 3 5 6 7 8 10 11 12 13], [3 4 5 6 7 8 10 11 12 13], [2 9 10 11 12 13], [3 9 10 11 12 13], [1 2 3 9 10 11 12 13], [1 3 4 9 10 11 12 13], [1 3 5 9 10 11 12 13], [1 2 3 4 5 9 10 11 12 13], [6 9 10 11 12 13], [1 4 6 9 10 11 12 13], [2 5 6 9 10 11 12 13], [3 5 6 9 10 11 12 13], [1 3 7 9 10 11 12 13], [1 5 7 9 10 11 12 13], [2 3 4 5 7 9 10 11 12 13], [2 6 7 9 10 11 12 13], [1 2 4 6 7 9 10 11 12 13], [2 3 4 6 7 9 10 11 12 13], [5 6 7 9 10 11 12 13], [3 4 5 6 7 9 10 11 12 13], [2 3 8 9 10 11 12 13], [3 4 8 9 10 11 12 13], [1 2 3 4 8 9 10 11 12 13], [2 5 8 9 10 11 12 13], [1 2 4 5 8 9 10 11 12 13], [2 3 4 5 8 9 10 11 12 13], [1 6 8 9 10 11 12 13], [2 6 8 9 10 11 12 13], [3 6 8 9 10 11 12 13], [4 6 8 9 10 11 12 13], [1 2 4 6 8 9 10 11 12 13], [5 6 8 9 10 11 12 13], [1 7 8 9 10 11 12 13], [3 7 8 9 10 11 12 13], [4 7 8 9 10 11 12 13], [1 3 5 7 8 9 10 11 12 13], [2 4 5 7 8 9 10 11 12 13], [1 5 6 7 8 9 10 11 12 13], [1 2 4 5 6 7 8 9 10 11 12 13] and [2 3 4 5 6 7 8 9 10 11 12 13]

---

## Appendix B: ORIGINAL PUBLICATIONS

---

The following publications have arisen from work contained in this thesis:

D. G. M. Cruickshank and J. H. Dripps, "Digital matched filters in unknown interference", Proceedings of the sixth international conference on digital processing of signals in communications, IEE conference publication 340, pp. 16-21, September 1991

D. G. M. Cruickshank and J. H. Dripps, "Improved matched filter performance in impulsive noise", Proceedings of the 4th Bangor communications symposium, pp. 149-152, May 1992

D. G. M. Cruickshank and J. H. Dripps, "Design of a spread spectrum system for use in impulsive noise", Proceedings of the IEE colloquium on spread spectrum techniques for radio communications systems, Digest no. 1992/161, paper no. 7, June 1992

DIGITAL MATCHED FILTERS IN UNKNOWN INTERFERENCE

David G. M. Cruickshank and James H. Dripps

University of Edinburgh

ABSTRACT

This paper examines the performance of Digital Matched Filters with multi-level quantisation and dither in various types of impulsive interference. The work of Cahn [1] is extended to eight quantisation level devices. It is then limited to binary quantisation steps to enable simple implementation using digital circuitry. Improvements to Cahn's device suggested by Turin [2] are incorporated and the performance of the device evaluated in a variety of interference cases. The device is then further modified by a new suggestion, setting to zero inputs that are outside the region in which any information can be extracted. The performance of this new device is then discussed.

1. INTRODUCTION

The performance of a multi-quantisation level Digital Matched Filter (DMF) in Gaussian noise is well documented [3], but the performance of DMF's in impulsive interference is not well known. It has been shown that binary correlator matched filters have excellent properties in impulsive interference of the type found in the radio frequency (RF) bands [4], but that they have poor performance in Gaussian interference [5]. In this paper we shall develop a multi-level DMF which has similar performance to an analogue matched filter in Gaussian noise while retaining most of the desirable performance of a binary correlator matched filter in impulsive interference.

2. BACKGROUND

In Cahn's original paper, he used the work of Stiglitz [6] to show that it was possible to design a DMF with a guaranteed minimum performance. The calculations were then performed for a four level system, showing that the worst case performance of the four level system was 2.3 dB below the performance of an analogue system. It was stated in Cahn's paper that this method could be extended to DMF's with a higher number of quantisation levels. One of the problems with this solution is that the quantisation levels used are not linearly spaced and therefore cannot be represented by simple digital circuitry.

3. EXTENSION OF CAHN'S WORK

3.1 Increased quantisation levels

Extending Cahn's work to higher quantisation levels

using a simple serial search algorithm would rapidly become impossible as the number of search points is proportional to  $N^{((3q/2)-2)}$ .  $N$  is a fixed parameter relating to the desired accuracy and  $q$  is the number of quantisation levels ( $q=2$  for a binary correlator etc.). In the rest of this section we shall use the same notation as Cahn. If we observe a surface plot of the  $w$  parameters against their worst case signal to noise ratio as used in Cahn's optimisation for a binary (Fig. 1) and a four level system (Fig. 2), we see that it is a smooth function with a global maximum. The  $w$  parameters are the maximum amplitudes of the dither function for each quantisation amplitude. Thus for the binary case there is only one  $w$  parameter, marked  $w$  in Fig. 1. and there are two  $w$  parameters for the four-level case, marked  $w_1$  and  $w_2$  in Fig. 2. Assuming that this smoothness extends to systems with a larger number of quantisation levels, we can use a gradient search algorithm to find their global maximum. This reduces the number of search points to being proportional to  $0.5qN^{(q-2)}$ , and enables calculation of the maximum guaranteed signal to noise ratio for up to 8 levels, shown in table 1. †

q	loss in processing gain
2	8.3dB
4	2.3dB
6	0.3dB
8	0.0dB

Table 1: Number of quantisation levels vs the worst case loss in processing gain when compared with an analogue matched filter (non-linear quantisation steps).

In reality, the worst case loss for the eight level case is not 0.0dB, as this would constitute the perfect analogue case, towards which a digital approximation can only tend. The experiment has achieved this result due to the finite number of noise pdf's used to discover the worst case noise. The true loss is likely to be less than 0.1dB. It was hoped to extend this optimisation process to sixteen levels, but the result would appear to be 0.0dB for the same reason as above.

† Note that the loss given for a binary correlator ( $q=2$ ) is not the same as that quoted by Cahn (4.8dB). The reason for this is that Cahn did not apply the same restrictions to his binary analysis as he did to his four level analysis, in particular the dither function used by Cahn in his binary analysis did not have a uniform distribution.

### 3.2 Linear quantisation steps

Cahn's search method does not provide linear quantisation steps, for example his four level optimal solution has the quantisation steps 1.00 and 3.85. This would be extremely difficult to implement in digital hardware. It is possible to find a worst case solution with linear quantisation steps at the expense of a small loss in guaranteed minimum signal to noise ratio. These solutions can be found by plotting the worst case quantisation step against the worst case signal to noise ratio for a large number of  $w$  values. The envelopes of these plots yield the best solution for each quantisation step. We can then pick the solutions that have linear quantisation steps. This is shown for the four level case in Fig. 3 and for the six level case in Fig. 4. Note that the six level case has already been simplified by taking the largest value of signal to noise ratio in a localised area, thus reducing the number of points. The numerical results of this are shown in table 2.

q	loss in processing gain
2	8.3dB
4	3.0dB
6	0.5dB
8	-

Table 2: Number of quantisation levels vs the worst case loss in processing gain when compared with an analogue matched filter (linear quantisation steps).

Note that the result for binary quantisation is the same as that shown in table 1, as a single amplitude may be considered linear. Unfortunately, it has not yet been possible to obtain a result for eight levels. The reason for this is that there is no obvious way of ensuring that the optimal solution has linear quantisation steps when testing  $w$  values. Thus solutions can only be found by trial and error. In the eight-level case, this process would take a prohibitive amount of computer time.

### 4. IMPROVEMENTS TO CAHN'S DMF

Turin [2] has suggested some improvements that can be made to Cahn's circuitry. He suggested that if the uniformly distributed function used to generate the dithers is a resetting triangular ramp, the performance of Cahn's DMF will be improved.

Turin demonstrated this using the binary quantisation case. Simulation has shown that this is also true for multi-level quantisation, with the improvement even more marked than that observed by Turin (see section 5.2). However, this does not apply if you use triangular waves for each dither in a multi-level system, as triangular waves have a fixed phase relationship and this means that the dithers are proportional to each other when they should be at least pseudo-independent. This problem may be avoided by using another

function that is equivalent to sampling a uniform distribution without replacement. An example is a maximal length pseudo-noise sequence (m-sequence) generator with each tap as a parallel input bit to a digital to analogue (D/A) converter. Care should be taken when using this method too, as a D/A conversion of an m-sequence generator with a small number of taps tends to divide by two on each clock pulse, bringing interdependence of the dither functions again. This can be avoided by taking two precautions, mixing randomly the connections between the m-sequence generator and the D/A and using an m-sequence generator with many feedback taps. An alternative practical solution may be to use a PROM containing the tap settings of an m-sequence addressed with different m-sequences for each required dither.

A small improvement in performance at high input signal to noise ratios is obtained using a m-sequence in place of the random code that Cahn used, but this improvement is largely academic as the output signal to noise ratio is already large.

### 5. CLIP TO ZERO ALGORITHM

It has been shown that binary correlator DMF's have good properties in impulsive interference [4]

and we shall go on to show that DMF's with a small number of quantisation levels also have good properties in impulsive interference. These properties may be improved further by adding a device in front of the DMF which measures the total power going into the DMF and sets to zero all signals above the range from which the DMF can extract useful information. A block diagram of this revised device is shown in Fig. 5. The clipping device changes the power measured by the second power measuring device under certain circumstances. It does not change the measured power for the worst case noise calculations, so they are still valid. It does change the measured power for impulsive noise distributions, and as we shall see it can provide large improvements in output signal to noise ratio. However, there are potential problems with stability of this new device, especially with respect to step changes in input signal to noise ratio, sudden changes in noise statistics etc. This has not been investigated fully as yet, but extreme care should be used when choosing the time constants of the two power measuring devices.

### 6. SIMULATION RESULTS

#### 6.1 Preliminaries

6.1.1 Noise models. We shall show our results for five noise cases.

##### 1. Worst case noise.

The worst case noise parameters obtained from the optimisation process, specific to each optimisation. Thus this noise distribution is different for different values of  $q$  and different if the device is constrained to having linear quantisation steps.

##### 2. Gaussian noise

3 and 4.  $\epsilon$  mixture impulsive noise [7].

An empirical model of impulsive noise used in some of the literature [4] to model class A impulsive interference [8]. This model is a sum of two Gaussian distributions, shown in equation 1.

$$f(x) = (1 - \epsilon)f_0(x) + \epsilon f_1(x) \quad (1)$$

$f_0$  is a Gaussian distribution with variance  $\sigma_0^2$  and  $f_1$  is a Gaussian distribution with variance  $\sigma_1^2$ . The ratio of the variances is given by  $\gamma^2 = \sigma_0^2/\sigma_1^2$ . We shall use this model with ( $\gamma^2 = 100$ ,  $\epsilon = 0.01$ ) as our case 3 and ( $\gamma^2=100$ ,  $\epsilon = 0.1$ ) as our case 4.

5. A new impulsive noise model.

This is a new empirical model which is designed to be a crude approximation to class B impulsive interference [ 8]. It is similar to the  $\epsilon$  mixture model, but instead of being the sum of two Gaussian distributions it is the sum of a Gaussian distribution and a step distribution, as shown in equation 2.

$$f(x) = P i(x) + (1 - P)g(x) \quad (2)$$

where  $i(x)$  a step distribution as follows:-

$$i(x) = \begin{cases} \frac{P}{F} \sigma^2 & x < F \\ 0 & x \geq F \end{cases} \quad (3)$$

$g(x)$  is a Gaussian distribution with variance  $\sigma^2$ . The particular case we shall use is with  $P=0.999$  and  $F=0.07$ .

Measured envelope distributions are shown for the noise cases 2-5 all with variance 1.00 in Fig. 6.

### 6.1.2. Simulation conditions

It is assumed that the first power measuring device is completely accurate.

In the simulations of the clip to zero algorithm, the second power measuring device is originally set to the same as the first power measuring device and evolves as an average over 50 samples. The graphs are composed of a measurement for each 2dB step in input signal to noise ratio. Each measurement is an average of 2000 independent runs, with each output signal to noise ratio given by:-

$$\frac{S}{N_{out}} = \frac{\text{correlation amplitude}}{\text{RMS with shifted signal}} \quad (4)$$

All the simulations are of a DMF with 511 taps (theoretical analogue processing gain 27.08dB). Perfect synchronisation between the transmitted and received code is assumed in all simulations. In the simulations where a PN code is not used, the code is random and re-chosen for each of the 2000 runs.

### 6.2 Simulation results and discussion

Fig. 7 shows the performance of Cahn's original four-level optimal DMF. It shows good correlation with table 1 for worst-case noise. The Gaussian noise case

is shown to be fairly close to worst case noise. The other three noise cases show significant improvements over worst case noise, and all exceed the theoretical performance of an analogue matched filter by a small amount.

Fig. 8 shows the effect of the improvements suggested in section 4. All the graphs are for worst case noise. The graph labeled "Basic" is for Cahn's DMF and is the same as the graph shown in Fig. 7, case 1. The graph labeled "M-sequence" is for the same conditions, but with the random code replaced with an m-sequence. This shows a small improvement at small signal to noise ratios, rising to a large improvement at large output signal to noise ratios. This is because at large output signal to noise ratios the denominator of the right hand side of equation (3) is dominated by the auto-correlation noise of the code. This noise is much reduced using a PN sequence. The graph labeled "Tri" uses the modified dither functions discussed in section 4. It does not show any improvement over Cahn's DMF under these conditions. Turin [2] also found that this modification did not produce an improvement under all circumstances. The graph labeled "Comb" shows that the combination of the two improvements produces a much more marked increase in performance. The exact explanation for this is unclear at present, but it is thought that the modified dithers are equivalent to sampling a uniform distribution without replacement and that therefore the overall variance in the system is reduced. Why this only produces an increase in performance when combined with the m-sequence is not known. The final graph, labeled "Linear" is a simulation of a four-level device with linear quantisation in its worst case noise. The worst case noise used to generate the linear performance graph is different from the worst case noise used on the other graphs on this diagram, as it is the result of a different optimisation process. It shows good correlation with the result predicted in table 2.

Fig. 9. shows simulations of the best device that can be constructed from this research. It is an eight-level optimal DMF with the two improvements discussed in section 4, and using the clip to zero algorithm discussed in section 5. The graphs for Gaussian and worst case noise show a slight loss (up to 1.0dB) over the predicted worst case noise, thought to be due to the inaccuracy of the second power measuring device. No attempt has yet been made to optimise the length of time over which this device averages, but from these results a longer time may be beneficial. However, a longer measuring time will degrade the devices performance under transient noise conditions. Thus an optimal balance point between these opposing considerations will have to be established. The three impulsive noise graphs are the most interesting however, they show a significant improvements over the theoretical performance of an analogue device. The improvement in case 5 is especially large. This noise distribution is particularly well suited to this type of processing.

It is possible to make an approximation to the theoretical performance in case 5. The clip to zero algorithm will not attempt to extract any information from the high amplitudes caused by  $i(x)$ . These occur 7% of the time, thus the processing gain is reduced to

(0.93).511 = 475 = 26.7dB. However, the noise power in the remaining samples is reduced to  $(1 - P) = 0.001$  times its previous value, a reduction of 30dB. Thus, the overall processing gain is  $26.7 + 30 = 56.7$ dB. Examination of Fig. 9 shows that this is a good approximation to the performance in case 5 at low input signal to noise ratios. The dip in case 5 starting at 0dB input signal to noise ratio is caused by the second power measuring device including the signal power.

7. CONCLUSIONS

The performance of the device simulated in Fig. 9 shows that it is possible to design a DMF with good performance in Gaussian noise, a guaranteed worst case performance (although highly transient noise conditions may render this untrue) and exceptional performance in impulsive interference. More work needs to be done on the mathematical explanations of this performance and investigation of the clip to zero algorithm under transient conditions.

References

1. C. R. Cahn, "Performance of Digital Matched Filter Correlator with Unknown Interference," *IEEE Transactions on Communications*, vol. 19, no. 6, pp. 1163-1172, December 1971.
2. G. L. Turin, "An Introduction to Digital Matched Filters," *Proceedings IEEE*, vol. 64, no. 7, pp. 1092-1112, July 1976.
3. M. Miyake, T. Kojima, N. Katoaka, and T. Fujino, "Design and performance of direct-sequence spread-spectrum Modem using soft decision digital matched filter," *Proceedings of the IEEE Symposium on Spread Spectrum Techniques and Applications*, King's College, London England, pp. 135-139, September 1990.
4. B. Aazhang and H. V. Poor, "Performance of DS/SSMA Communications in impulsive channels - Part II: Hard-Limiting Correlation Receivers," *IEEE Transactions on Communications*, vol. 36, no. 1, pp. 88-97, January 1988.
5. B. Aazhang and H. V. Poor, "Performance of DS/SSMA Communications in impulsive channels - Part I: Linear correlation receivers," *IEEE Transactions on Communications*, vol. 35, pp. 1179-1188, November 1987.
6. I. G. Stiglitz, "Coding for a class of Unknown Channels," *IEEE Transactions on Information Technology*, vol. 12, no. 2, pp. 189-195, April 1966.
7. K. S. Vastola, "Threshold Detection in Narrow-Band Non-Gaussian Noise," *IEEE Transactions on Communications*, vol. 32, no. 2, pp. 134-139, February 1984.
8. D. Middleton, "Statistical-Physical Models of Electromagnetic Interference," *IEEE Transactions on Electromagnetic Compatibility*, vol. 19, no. 3, pp. 106-126, August 1977.

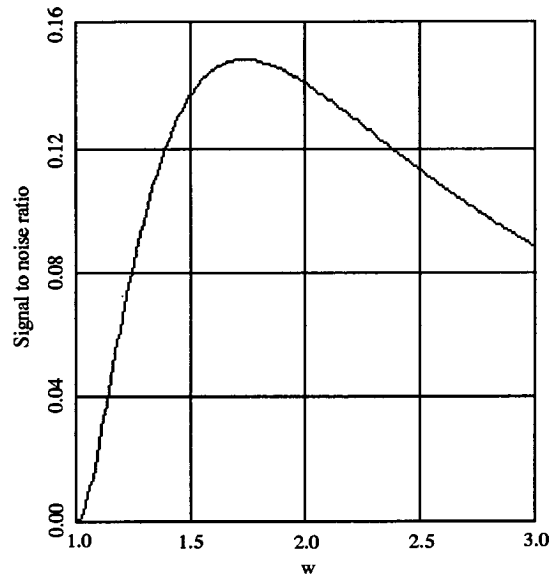


Fig. 1: Optimisation of binary quantisation DMF

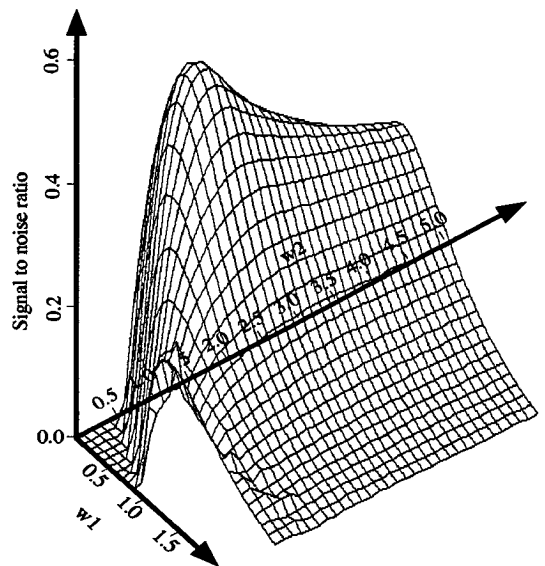


Fig. 2: Optimisation of a DMF with four-level quantisation

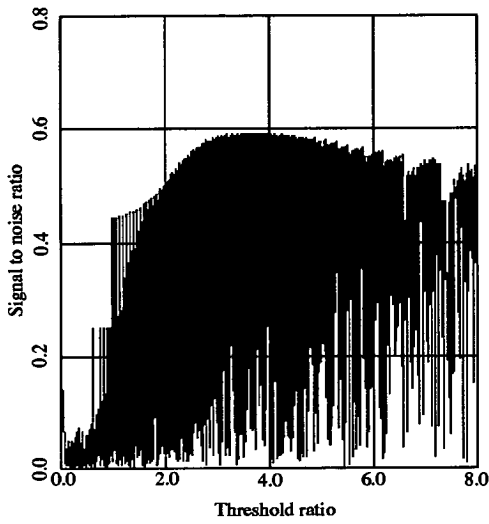


Fig. 3: Optimisation of a DMF with four-level linear quantisation

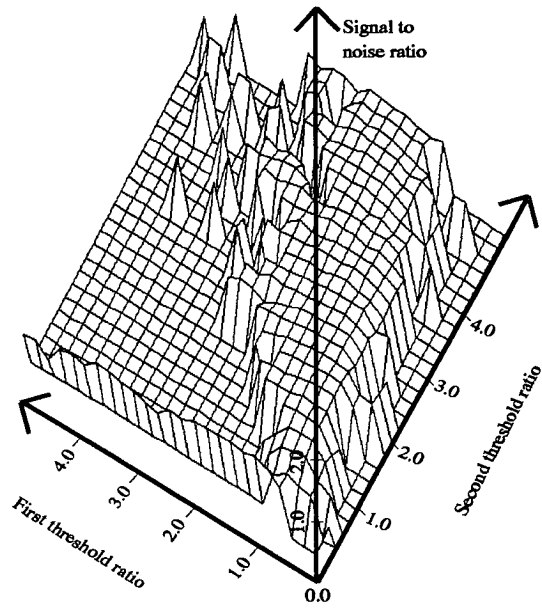


Fig. 4: Optimisation of a DMF with six-level linear quantisation

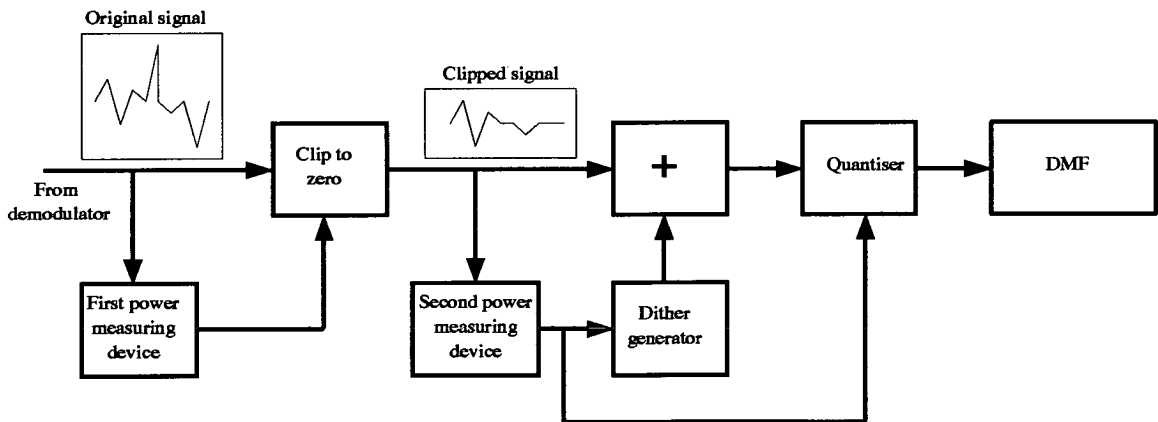


Fig. 5: Block diagram of clip to zero system



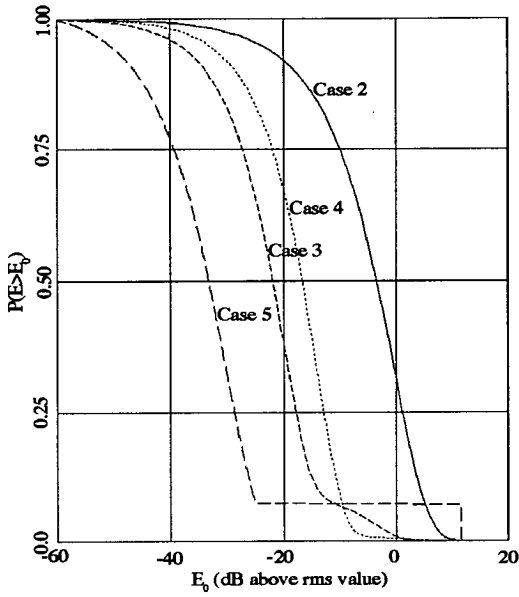


Fig. 6: Envelope distribution for noise cases 2-5.

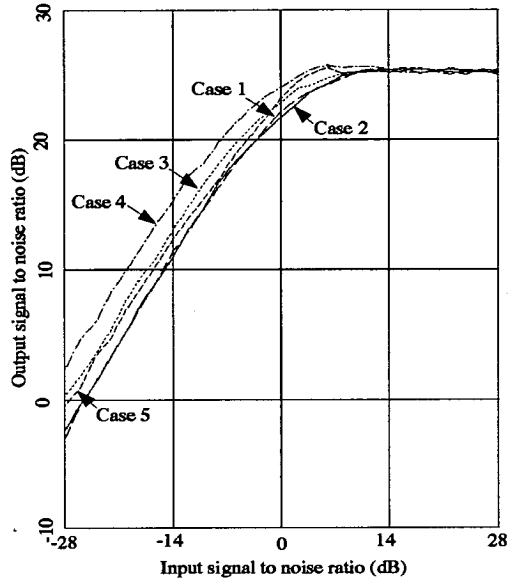


Fig. 7: Performance of Cahn's four-level optimal DMF

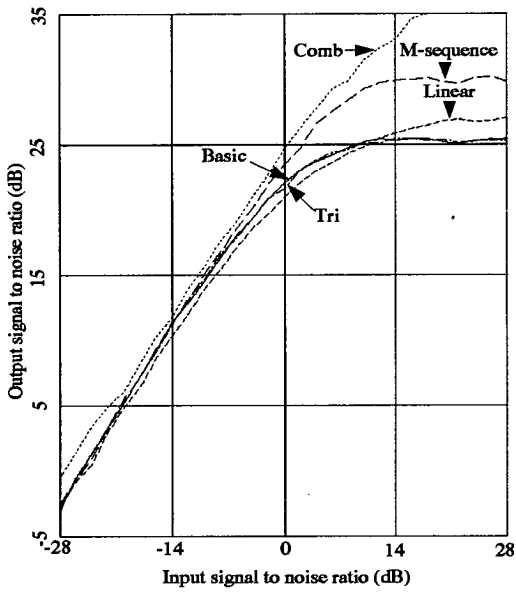


Fig. 8: Improvements to Cahn's DMF

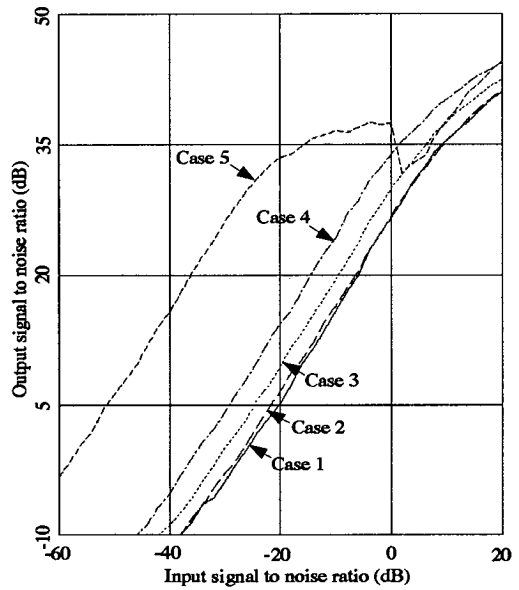


Fig. 9: Performance of an eight level DMF.

## Improved Matched Filter Performance in Impulsive Noise

David G. M. Cruickshank and James H. Dripps

Department of Electrical Engineering  
 University of Edinburgh  
 King's Buildings  
 Edinburgh EH9 3JL  
 Scotland UK  
 Telephone +44 31 650 5655 Fax +44 31 662 4358

### 1. Abstract

This paper examines the performance of matched filters in impulsive noise. It aims to show that by adding a non-linear clipping device to the front of a matched filter, the performance of the matched filter in impulsive noise will be improved. This is at the expense of a small degradation in Gaussian noise performance. Analysis is given for Gaussian and  $\epsilon$ -mixture impulsive noise.

### 2. Introduction

Impulsive interference occurs in many communication environments. The best known examples are in the HF radio bands and in and around high power electrical machinery such as motors and car ignition systems. The most commonly used model for impulsive interference is the  $\epsilon$ -mixture model [1], a simplification of the physically based Middleton [2] In conventional systems, impulsive noise severely degrades the system performance. It is the aim of this paper to show that in a spread spectrum system, it may be possible to design a system whose performance is better in impulsive noise than Gaussian noise. model.

The inspiration for this work comes from observations that limited precision digital matched filters can out perform analogue matched filters in impulsive interference environments [3]. The reason for this is that high amplitude pulses are clipped at the quantiser in a limited precision digital matched filter, and thus the power in such an impulse is reduced at the expense of losing any information it may have contained. The logical extreme of this clipping is to set to zero any input to the matched filter whose amplitude is greater than a given threshold. This pre-processor has become known as the clip to zero algorithm. A block diagram of the clip to zero pre-processor is shown in Fig. 1. The clip to zero algorithm may be thought of as discarding received chips of spread data whose signal to noise ratio is significantly worse than the average at the input to the matched filter in order to increase the average signal to noise ratio at the output.

### 3. The clip to zero algorithm in Gaussian noise

The clip to zero algorithm sets to zero all signals whose amplitudes are greater than a threshold  $a = A\sigma$ , as shown in Fig 1. If we normalise the signal amplitude to 1 and the noise power is  $\sigma^2$ , then the probability density function at the input to our system is:-

$$f_g(x) = \frac{1}{2} \frac{1}{\sqrt{2\pi\sigma^2}} \exp\left(-\frac{(x-1)^2}{2\sigma^2}\right) + \frac{1}{2} \frac{1}{\sqrt{2\pi\sigma^2}} \exp\left(-\frac{(x+1)^2}{2\sigma^2}\right) \quad -a < x < a$$

$$= 0 \quad \text{elsewhere} \quad (1)$$

We shall use the output signal to noise ratio from the matched filter as our performance measure. This is

defined as:-

$$\frac{S}{N_{out}} (dB) = 20 \log_{10} \left( \frac{\text{average correlation peak amplitude}}{\text{rms voltage with an uncorrelated input signal}} \right) \quad (2)$$

The average correlation peak amplitude is given by:-

$$E \left\{ \begin{array}{l} \frac{1}{\sqrt{2\pi}\sigma^2} \exp^{-\frac{(x-1)^2}{2\sigma^2}} \quad -a < x < a \\ 0 \quad \text{elsewhere} \end{array} \right\} \times \text{processing gain} \quad (3)$$

where:-

$$E \left\{ \begin{array}{l} \frac{1}{\sqrt{2\pi}\sigma^2} \exp^{-\frac{(x-1)^2}{2\sigma^2}} \quad -a < x < a \\ 0 \quad \text{elsewhere} \end{array} \right\} = \frac{\sigma}{\sqrt{2\pi}} \left( \exp\left\{-\frac{\left(\frac{-a-1}{\sigma}\right)^2}{2}\right\} - \exp\left\{-\frac{\left(\frac{a-1}{\sigma}\right)^2}{2}\right\} \right) + \text{erf}\left\{\frac{a-1}{\sigma}\right\} - \text{erf}\left\{\frac{-a-1}{\sigma}\right\} \quad (4)$$

The rms voltage with an uncorrelated input signal is given by:-

$$\sqrt{\text{Var}\{f_g(x)\}} \times \text{processing gain} \quad (5)$$

where:-

$$\begin{aligned} \text{Var}\{f_g(x)\} &= \frac{\sigma^2}{\sqrt{2\pi}} \left( -\left(\frac{a-1}{\sigma}\right) \exp\left\{-\frac{\left(\frac{a-1}{\sigma}\right)^2}{2}\right\} + \left(\frac{-a-1}{\sigma}\right) \exp\left\{-\frac{\left(\frac{-a-1}{\sigma}\right)^2}{2}\right\} \right) + \sigma^2 \left( \text{erf}\left\{\frac{a-1}{\sigma}\right\} - \text{erf}\left\{\frac{-a-1}{\sigma}\right\} \right) \\ &+ \frac{\sigma\sqrt{2}}{\sqrt{\pi}} \left( \exp\left\{-\frac{\left(\frac{a-1}{\sigma}\right)^2}{2}\right\} - \exp\left\{-\frac{\left(\frac{-a-1}{\sigma}\right)^2}{2}\right\} \right) + \text{erf}\left\{\frac{a-1}{\sigma}\right\} - \text{erf}\left\{\frac{-a-1}{\sigma}\right\} \end{aligned} \quad (6)$$

If we substitute equations (3) and (5) into equation (2), we can obtain the loss in Gaussian noise performance due to clipping, given by:-

$$\text{Loss (dB)} = 10 \log_{10}(\text{processing gain}) - \left( \frac{S}{N_{out}} (dB) - 10 \log_{10} \left( \frac{1}{\sigma^2} \right) \right) \quad (7)$$

Note that if we make  $a = A\sigma$ , as in fig 1, and  $a$  is much greater than 1, the loss is approximately independent of the input signal to noise ratio. In spread spectrum systems,  $\sigma$  is usually large compared with one, thus the loss will be independent of the input signal to noise ratio provided  $A$  is not much less than one.

#### 4. The clip to zero algorithm in $\epsilon$ -mixture noise

The  $\epsilon$ -mixture noise model is an empirical model for impulsive noise based on Middleton's physically based model[2]. The distribution for  $\epsilon$ -mixture noise is:-

$$f_\epsilon(x) = (1 - \epsilon)f_0(x) + \epsilon f_1(x) \quad (8)$$

where  $f_0(x)$  and  $f_1(x)$  are Gaussian distributions with variance  $\sigma_0$  and  $\sigma_1$  respectively. The ratio of  $\sigma_0/\sigma_1$  is  $\gamma^2$ . It is possible to derive the performance of the clip to zero algorithm in  $\epsilon$ -mixture noise from the Gaussian case. The average correlation peak amplitude is given by:-

$$\left( (1 - \varepsilon)E \left\{ \frac{1}{\sqrt{2\pi\sigma_0^2}} \exp \frac{-(x-1)^2}{2\sigma_0^2} \right\} + \varepsilon E \left\{ \frac{1}{\sqrt{2\pi\sigma_1^2}} \exp \frac{-(x-1)^2}{2\sigma_1^2} \right\} \right) \times \text{processing gain} \quad (9)$$

The expected values can be calculated from equation (4), with the appropriate substitution for  $\sigma$ . The rms voltage with an uncorrelated input signal is given by:-

$$\sqrt{(\text{Var}\{f_0(x)\} + \text{Var}\{f_1(x)\}) \times \text{processing gain}} \quad (10)$$

The variances can be calculated using equation (6), again with the appropriate substitutions for  $\sigma$ . Thus, substituting equations (9) and (10) into equation (2), we can obtain the output signal to noise from our matched filter in  $\varepsilon$ -mixture noise.

## 5. Simulation results

All graphs are for a 511 tap matched filter (processing gain 27.1 dB). Perfect synchronisation between the input signal and the reference signal is assumed. Each point on the simulation results is the average of 400 independent trials.

Fig. 2 shows the loss in signal to noise ratio caused by the clip to zero algorithm in Gaussian noise. The reference case is low input signal to noise ratio with no clipping. The theoretical graphs are from equations (2-7). Fig. 2 shows that the clip to zero algorithm causes a loss in performance in Gaussian noise which increases as the amount of clipping is increased.

Fig. 3 shows output signal to noise ratio vs input signal to noise ratio for the clip to zero algorithm in two  $\varepsilon$ -mixture impulsive noise distributions taken from [1]. The clipping factor A was set to 1.85. The theoretical graphs are taken from equations (2), (3), (9) and (10). Fig. 3 shows that the performance of the clip to zero algorithm is typically independent of the input signal to noise ratio, especially at low input signal to noise ratios where a spread spectrum system operates.

The most interesting results from this study are shown in Fig. 4. It shows the loss in output signal to noise ratio caused by the clip to zero algorithm as a function of the clipping factor A in the two  $\varepsilon$ -mixture impulsive noise distributions. The input signal to noise ratio was set to -15 dB. Fig. 4 shows that by clipping to zero with the correct clipping factor A, it is possible to obtain large gains (up to 13 dB in Fig. 4) over the unclipped case in  $\varepsilon$ -mixture noise.

## 6. Conclusions

We have demonstrated that it is possible to design a matched filter pre-processor that will give the matched filter enhanced performance in impulsive noise at the expense of some loss in Gaussian noise performance. Future work in this area will concentrate on finding the optimal clipping factor A for each  $\varepsilon$ -mixture distribution with a view to implementing adaptive clipping.

## References

1. K. S. Vastola, "Threshold Detection in Narrow-Band Non-Gaussian Noise," *IEEE Transactions on Communications*, 32, 2, pp. 134-139 (February 1984).
2. D. Middleton, "Statistical-Physical Models of Electromagnetic Interference," *IEEE Transactions on Electromagnetic Compatibility*, 19, 3, pp. 106-126 (August 1977).
3. B. Aazhang and H. V. Poor, "Performance of DS/SSMA Communications in impulsive channels - Part II: Hard-Limiting Correlation Receivers," *IEEE Transactions on Communications*, 36, 1, pp. 88-97 (January 1988).

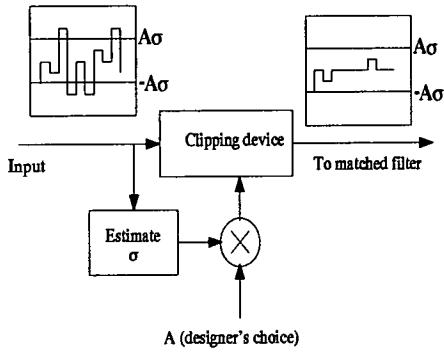


Fig. 1: Block diagram of the clip to zero algorithm.

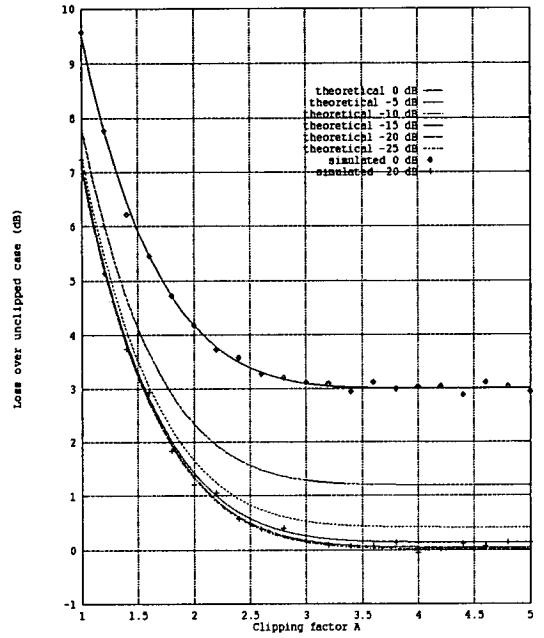


Fig. 2: Performance of the clip to zero algorithm in Gaussian noise.

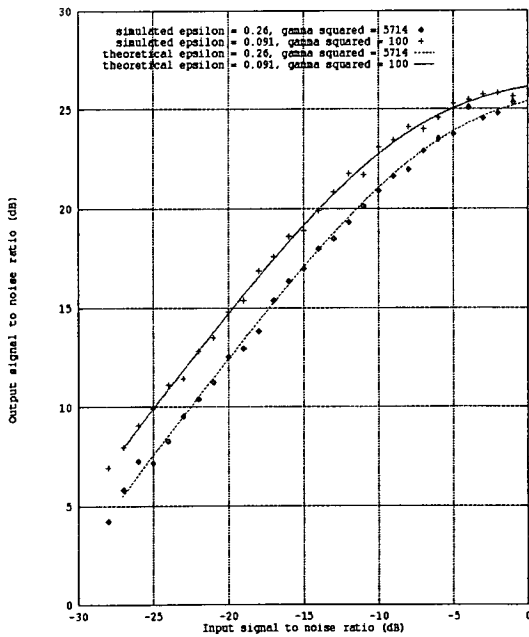


Fig. 3: Performance of the clip to zero algorithm in  $\epsilon$ -mixture noise (varying signal to noise ratio).

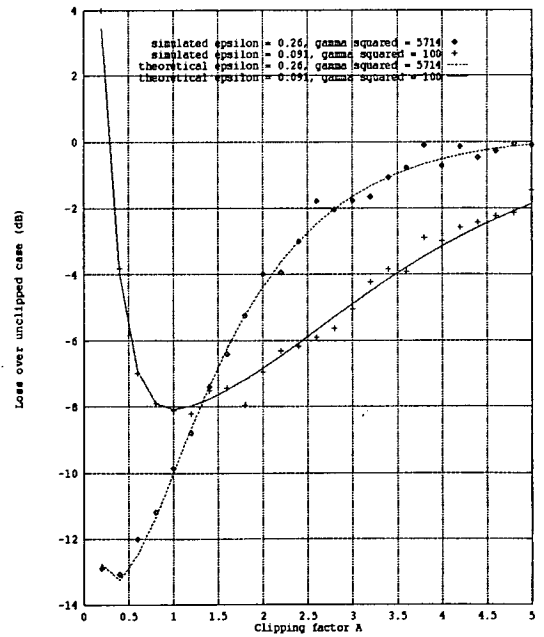


Fig. 4: Performance of the clip to zero algorithm in  $\epsilon$ -mixture noise (varying clipping factor).

DESIGN OF A SPREAD SPECTRUM SYSTEM FOR USE IN IMPULSIVE NOISE

David G. M. Cruickshank and James H. Dripps

University of Edinburgh, Department of Electrical Engineering, King's Buildings,  
Mayfield Road, Edinburgh, EH9 3JL

**1. Introduction**

Impulsive noise occurs in many communication environments. It is the result of electrical discharges from motors, vehicle ignition systems, high power electrical machinery and natural phenomenon such as lightning and other atmospheric disturbances. An impulsive noise distribution may be defined as a distribution that has significantly higher probability of a large amplitude than a Gaussian distribution with the same power. The effect on a conventional communication system can be described as dramatic and unpredictable. Attempts have been made to quantify the degradation caused by impulsive noise distributions (see for example the work of Jain and Gupta), but the degradation is dependent on the transmission format and the exact distribution of the noise. The exact distribution of the noise is almost certainly unknown to the system designer.

In the current work, we aim to show that spread spectrum systems have inherent advantages in impulsive noise and that these advantages can be further enhanced by a non-linear clipping device. The inspiration for this work comes from several sources. In [1] it is demonstrated that a hard-limiting correlation receiver can out-perform a linear receiver in impulsive noise, although the hard-limiting receiver is not as good as the linear receiver in Gaussian noise. Secondly, the central limit theorem dictates that the output of a matched filter used in direct sequence spread spectrum has a Gaussian noise distribution if the filter has enough taps. Thus it can be argued that at worst, a spread spectrum system should be unaffected by the input noise distribution. Finally, Viterbi [2] has already stated that Shannon's theorem implies that the worst case noise for a communications system is Gaussian noise. Viterbi also states that if the noise is not Gaussian, signal processing should be able to make the performance at least as good as in Gaussian noise with the same power level.

In our analysis, we shall use a direct sequence spread spectrum system with assumed perfect demodulation and matched filter de-spreading, ie. we shall concentrate on the matched filter de-spreading rather than the demodulation. The strategies that are developed using this conceptual system may be realised more practically by an architecture such as the one shown in ([3] Fig. 1) with few modifications. All the simulation results and theoretical predictions in this paper are for a 511 tap matched filter. Any power measuring devices are assumed to be perfectly accurate. Losses are expressed as the loss in dB over a matched filter with analogue word storage operating in Gaussian noise with the same power, ie. relative to a processing gain of 27.1 dB.

## 2. Limited precision matched filters

Work by C. R. Cahn [3] has shown that it is possible to design a digital matched filter (DMF) with a guaranteed minimum performance for any given quantisation precision. The minimum performance of these filters applies to all interference distributions, including impulsive noise. This work has been extended to larger numbers of quantisation levels by the authors [4]. However, for demonstration purposes, we shall use the four-level system as proposed by Cahn. Fig. 1 shows simulation results for Cahn's four-level DMF in different noise environments. The worst case loss of this device was calculated to be 2.3dB. The impulsive noise distributions are two of the  $\epsilon$ -mixture distributions shown in [5] used because they are simplifications of the physically based model proposed by Middleton for measured distributions [6], [7]. Each point on these graphs is the average of 400 independent trials. These simulations show that the worst-case performance is a loss of 2.3dB (except at high input signal to noise) and that in  $\epsilon$ -mixture noise the performance is significantly better than this minimum. This minimum performance is better than the performances reported in the literature for conventional systems in impulsive noise.

## 3. The clip to zero algorithm

The inspiration for this study comes from the observations that the limited precision matched filters discussed above can out-perform analogue matched filters in impulsive noise. This is due to the clipping of high amplitude samples during the quantisation process. This clipping removes the information content of a sample, but it also reduces

the contribution that the sample makes to the noise. If an individual sample contains a disproportionately large amount of noise, then clipping it can enhance the signal to noise ratio at the output of a matched filter. The logical extreme of this is to set to zero any signals whose amplitudes exceed a threshold  $a = A\sigma$  as shown in Fig. 2.

In Gaussian noise, this clipping action causes a loss in signal to noise ratio. If we normalise our clipping threshold using  $a = A\sigma$ , then we can quantify this loss. Fig. 3 shows this loss as a function of  $A$  for a 511 tap DMF. The figures on the key are input signal to noise ratio. The theoretical predictions can be found in [8].

In  $\varepsilon$ -mixture noise however, this clipping action can produce large gains in performance. Fig. 4 shows this loss as a function of the clipping factor  $A$  for two  $\varepsilon$ -mixture distributions. The input signal to noise ratio was set to -15 dB. Again, the theoretical predictions shown in Fig. 4 can be found in [8].

#### 4. Combining Limited Precision Matched Filters With The Clip To Zero Algorithm

The two techniques discussed in the previous two sections can be successfully combined. If we simply place the clip to zero algorithm before the limited precision matched filter, the net effect is to take the loss or gain from the clip to zero algorithm and add it to the guaranteed maximum loss of the limited precision matched filter. Fig. 5 shows simulation results obtained from doing this for Gaussian noise and one of our  $\varepsilon$ -mixture distributions.

#### 5. Conclusions

In a conventional system, impulsive noise causes an unpredictable degradation. We have shown that a direct sequence spread spectrum system may be designed such that the degradation has a known maximum bound. We have also shown that by employing a non-linear clipping device to the front of a matched filter, we may be able to obtain a gain rather than a loss when the noise statistics change from Gaussian to impulsive.



References

1. B. Aazhang and H. V. Poor, "Performance of DS/SSMA Communications in impulsive channels - Part II: Hard-Limiting Correlation Receivers," *IEEE Transactions on Communications*, 36, 1, pp. 88-97 (January 1988).
2. A. J. Viterbi, "Wireless digital communication: a view based on three lessons learned," *IEEE communications magazine*, 29, 9 (September 1991).
3. C. R. Cahn, "Performance of Digital Matched Filter Correlator with Unknown Interference," *IEEE Transactions on Communications*, 19, 6, pp. 1163-1172 (December 1971).
4. D. G. M. Cruickshank and J. H. Dripps, "Digital matched filters in unknown interference," *Proceedings of the IEE sixth international conference on the Digital Processing of Signals in Communications*, IEE conference publication 340, pp. 16-21 (September 1991).
5. K. S. Vastola, "Threshold Detection in Narrow-Band Non-Gaussian Noise," *IEEE Transactions on Communications*, 32, 2, pp. 134-139 (February 1984).
6. D. Middleton, "Statistical-Physical Models of Electromagnetic Interference," *IEEE Transactions on Electromagnetic Compatibility*, 19, 3, pp. 106-126 (August 1977).
7. D. Middleton, "Procedures for Determining the Parameters of the First-Order Canonical Models of Class A and Class B Electromagnetic Interference," *IEEE Transactions on Electromagnetic Compatibility*, 21, 3, pp. 190-208 (August 1979).
8. D. G. M. Cruickshank and J. A. Dripps, "Improved matched filter performance in impulsive noise," *IEE 4th Bangor Communications Symposium* (May 1992).

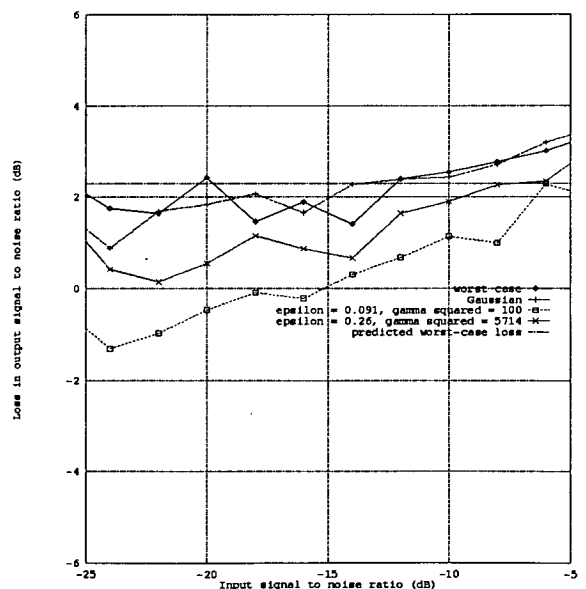


Fig. 1: Simulation results for Cahn's four-level DMF.

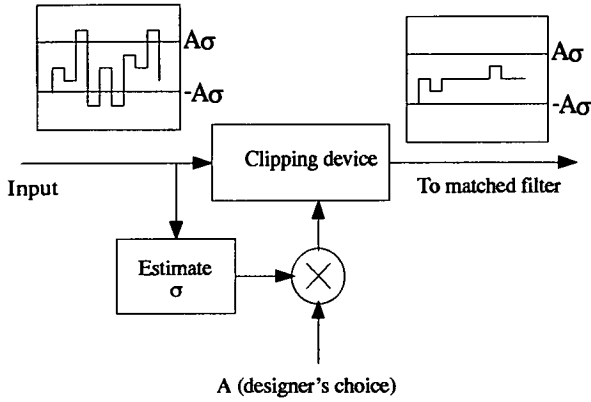


Fig. 2: Block diagram of the clip to zero algorithm.

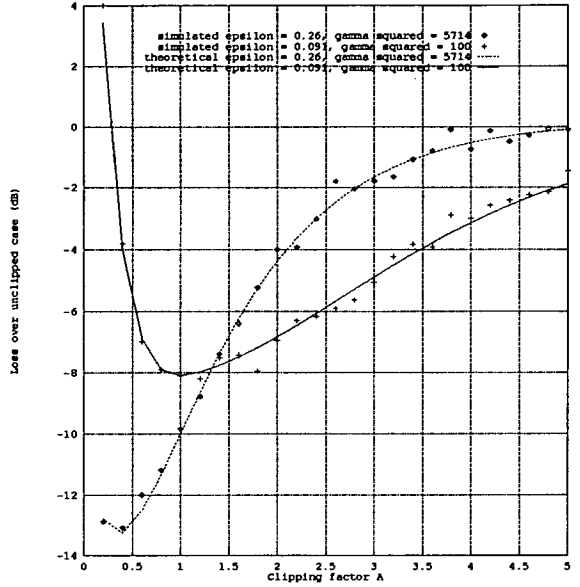


Fig. 4: Results for the clip to zero algorithm in impulsive noise.

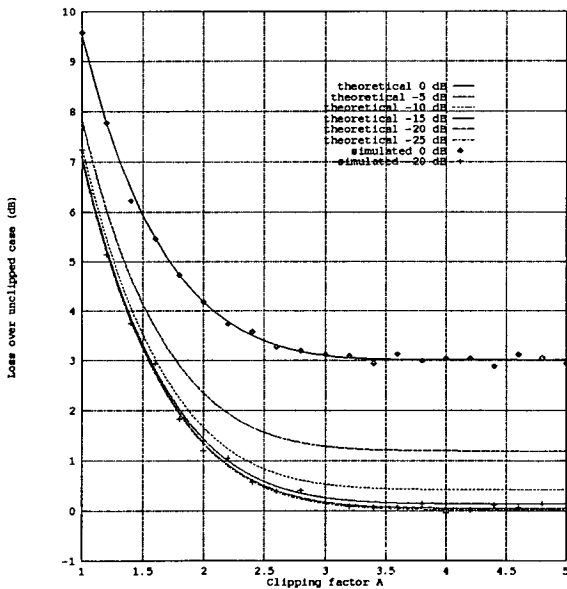


Fig. 3: Results for the clip to zero algorithm in Gaussian noise.

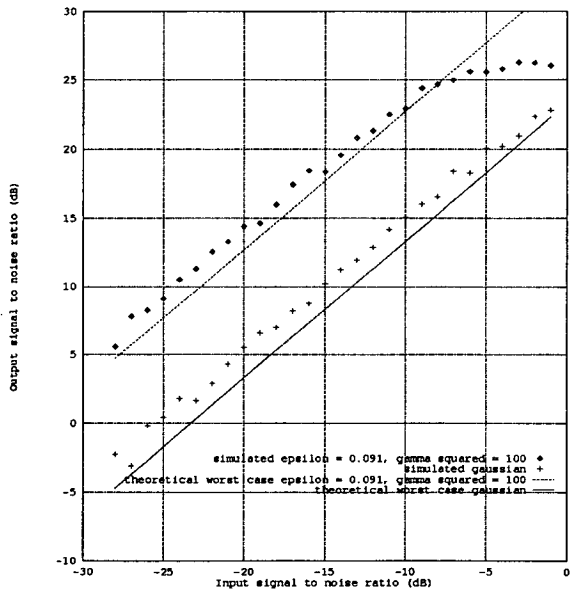


Fig. 5: Results for the clip to zero algorithm in combination with Cahn's four-level DMF.

---

## Appendix C: Software

---

This appendix describes some of the software written during the course of this project. The programs and data described below are contained on the high density 5 1/4 inch disk at the back of this thesis. The disk is formatted for an IBM† PC and compatibles. All programs are written in the 'C' programming language. The 'C' programs are entirely self contained, with input parameters specified in *#define* statements at the start of the programs. These programs should compile with any generic 'C' compiler. The paragraph titles correspond to the file names on the disk.

### **modtwotricahn.c**

This programme is included as an example of the simulation programs used to verify the performance of the matched filters and the clip to zero algorithm in chapters 3-5. This particular programme is the one used to generate the simulation results in fig. 5.12, for a limited precision digital matched filter in combination with the clip to zero algorithm. The input parameters are the length of the PN sequence, the number of samples to be used per output point and the noise distribution. The file to be used for impulsive noise samples is contained in the only *fopen* command within the programme. The PN sequence used is specified by setting the tap values at the beginning of the function *pn*.

---

† IBM is a trademark of International Business Machines

**esample1.c**

This programme generates samples from impulsive noise distributions. The input parameters are the distribution parameters from Middleton's model and the number of samples to be generated.

**pncodes.c**

This is the programme used to find and verify the m-sequences contained in appendix A. This programme has no input parameters.

**case1.dat, case2.dat, case3.dat**

These are data files containing the first 1000 samples for the impulse noise cases 1, 2 and 3 respectively (see fig. 5.3).